Tampere University

MARI SALMIVUORI

# New Options for Non-invasive Imaging and Non-invasive Treatment of Skin Cancers

Tampere University Dissertations 245

Tampere University Dissertations 245

MARI SALMIVUORI

# New Options for Non-invasive Imaging and Non-invasive Treatment of Skin Cancers

ACADEMIC DISSERTATION
To be presented, with the permission of
the Faculty of Medicine and Health Technology of Tampere University,
for public discussion in Auditorium F114,
of the Arvo building, Arvo Ylpön katu 24, Tampere,
on 20 November 2020, at 12 o'clock

ACADEMIC DISSERTATION

Tampere University, Faculty of Medicine and Health Technology
In collaboration with Päijät-Häme Social and Heath Care group, University of Jyväskylä and University of Helsinki

| | | |
|---|---|---|
| *Responsible supervisor and Custos* | Professor Emerita<br>Erna Snellman<br>Tampere University<br>Finland | |
| *Supervisor* | Docent Mari Grönroos<br>Tampere University<br>Finland | |
| *Pre-examiners* | Docent Sirkku Peltonen<br>University of Turku<br>Finland | Docent Raimo Suhonen<br>University of Eastern Finland<br>Finland |
| *Opponent* | Associate Professor John Paoli<br>University of Gothenburg<br>Sweden | |

The originality of this thesis has been checked using the Turnitin OriginalityCheck service.



Kannen suunnittelu: Roihu Inc.

ISBN 978-952-03-1540-5 (painettu)
ISBN 978-952-03-1541-2 (verkkojulkaisu)
ISSN 2489-9860 (painettu)
ISSN 2490-0028 (verkkojulkaisu)
http://urn.fi/URN:ISBN:978-952-03-1541-2

PunaMusta Oy – Yliopistopaino
Tampere 2020

To our two shines and to the spectrum of life with them – that's what truly matters – though research provides a nice counterbalance.

# ACKNOWLEDGEMENTS

The work for this dissertation was started in 2014 and completed in 2019. It was carried out at the Department of Dermatology and Allergology at Päijät-Häme Social and Health Care Group, Lahti, Finland. This work was supported by Tampere University and the Skin and Allergy Hospital, Helsinki University Hospital. I have received funding for this work from the Tampere University, the Competitive Research Financing of the Expert Responsibility Area of Tampere University Hospital, the Cancer Foundation Finland, the Instrumentarium Science Foundation, the Finnish Dermatological Society, the Foundation for Clinical Chemistry Research, the Finnish-Norwegian Medical Foundation, the Cancer Foundation of Irja Karvonen, and the Ida Montini Foundation. Our collaborators in this dissertation have been University of Jyväskylä, University of Helsinki, Yliopiston Apteekki and VTT Technical Research Centre of Finland.

I want to express my deepest gratitude to all those, who have participated and supported this work. I especially want to thank:

My supervisors Erna Snellman and Mari Grönroos for their understanding, advices, support and guidance. Combining family life with small children, dissertation and specialization isn't an easy task. My supervisors kept all the time clear that family comes first and all the other things will solve out. So in the end, it's about organising and right kind of atmosphere making positive things happen and the available time for research effective.

My co-researcher and member of follow-up group Noora Neittaanmäki for enthusiasm, support, advices and great collaboration. Noora, Mari and Erna I want to thank for ideas and enthusiasm which grasped me and showed that making science is interesting and fun.

The pre-examiners Sirkku Peltonen and Raimo Suhonen for reviewing my work and for their valuable comments on this dissertation.

The member of follow-up group Leea Ylitalo for advices during this work.

My co-researcher Ilkka Pölönen for helping and teaching me in technical details of hyperspectral imaging system, for development work of mathematical models, and for great collaboration.

The professor and chief physician Annamari Ranki and head physician Hannele Heikkilä from the Skin and Allergy Hospital, Helsinki Central University Hospital, for being flexible and enabling time for research during my residency at the Skin and Allergy Hospital.

All my fellow researchers and co-authors for their input, efforts and valuable comments in completing the studies and articles of this dissertation.

Our irreplaceable assistant nurse Ulla Oesch-Lääveri for everything. Without her I would have not completed recruiting the patients and collecting the materials for the studies. I want to thank her for organising all the practical issues and being an amazing co-worker and friend.

The research coordinator Marjo Soini for her help and advice during this work.

The statistician Mika Helminen from Tampere University Hospital for performing the statistical calculations for the studies.

Marc Baumann and Teija Inkinen from Biomedicum, University of Helsinki, for performing the quality control analysis of the Hexvix cream for the study III.

Maarit Bäckman from Yliopiston Apteekki for manufacturing the Hexvix cream for the study III.

Matthew James and Ada MacKeith for language editing, and thus making my articles and dissertation fluent.

My colleagues and staff from the Department of Dermatology and Allergology at Päijät-Häme Social and Health Care Group for supporting and helping attitude, and recruiting patients for my studies.

My friends, sisters and fellow residents for offering me counterbalance of work and for being a source of positive energy.

My parents-in-law, Kaisu and Pekka, for enabling the schedules. They were irreplaceable. They have fed and take care of our babies, they have travelled to Lahti to push baby carriage in the forests around the hospital, and later on have picked up kids from daycare.

My parents, Paula and Harri, for supporting me in my ambitions and believing in me. They have never said that I couldn't do something, if I had good arguments for my plans. If I have needed help, and ask for it, they have drove 500 km to help me.

My husband Jussi for understanding, supporting and loving me the way I am.

With this project I feel that I have been able to co-work with intelligent people and got new friends.

# ABSTRACT

**Background** Basal cell carcinoma is the most common cancer in the world. The incidence of superficial basal cell carcinoma, a subtype of basal cell carcinoma, is rising at a far steeper rate than the other subtypes, and as a non-aggressive subtype, it can be treated non-invasively. Aggressive subtypes of basal cell carcinoma are often ill-defined, which poses a clinical problem in preoperative margin assessment. Another ill-defined skin cancer type is lentigo maligna. Lentigo maligna is an *in situ* melanoma, and a precursor of lentigo maligna melanoma. These two forms are clinically challenging to distinguish from each other, which is crucial as melanoma has the worst prognosis of all skin cancers. Non-invasive imaging is an option for increasing the accuracy of preoperative diagnosis and the assessment. Hyperspectral imaging is a novel, fast, and computer-aided imaging modality with a wide field of view. In non-invasive treatment of non-aggressive basal cell carcinomas, photodynamic therapy has many advantages: an excellent cosmetic outcome as well as a shorter application time and recovery period. Notwithstanding these advantages, the efficacy of photodynamic therapy is lower when compared to topical pharmacological options such as imiquimod and 5-fluorouracil.

**Objectives** This dissertation focuses on non-invasive imaging and non-invasive treatment. In non-invasive imaging, the aim is to study the performance of a hyperspectral imaging system in separating lentigo maligna melanoma from lentigo maligna and assessing the preoperative margins of ill-defined basal cell carcinomas compared to clinical delineation assessments performed with a dermoscope. In non-invasive treatment, the aim is to compare the efficacy of three different photosensitisers in photodynamic therapy of non-aggressive basal cell carcinomas.

**Methods** There are two pilot studies with hyperspectral imaging: one on lentigo maligna and lentigo maligna melanoma, and another one on ill-defined basal cell carcinoma. Tumours were preoperatively visually inspected utilising a dermoscope, and thereafter imaged with the hyperspectral imaging system. Next, surgical excision was performed. Hyperspectral images were created with computer-aided mathematical models. Additional mathematical models were subsequently

developed. In the results analysis, the findings of the hyperspectral imaging and clinically assessed margins were compared to the histopathology results, where assessment was performed blind to the hyperspectral imaging findings.

A non-sponsored, prospective, randomised, controlled and double-blinded trial focused on non-invasive treatment. In this trial, two novel photosensitisers, 5-aminolevulinic acid nanoemulsion and low-concentration hexylaminolevulinate, were compared to the commonly used methylaminolevulinate in photodynamic therapy of non-aggressive basal cell carcinomas, i.e. thin nodular or superficial subtypes. The primary outcome was histological clearance at three months. Secondary outcomes included adverse events such as pain associated with the treatment while using a long-lasting local anaesthetic as pain management, post-treatment reaction, as well as cosmetic outcome, and fluorescence and photobleaching during the illumination. We used an experimental fluorescence imaging system. Punch biopsies were performed prior to treatment and during follow-up. Both patient and observers of outcomes were blind to the photosensitiser that was used.

**Results** Hyperspectral imaging exhibited a unique hyperspectral graph for lentigo maligna melanoma, lentigo maligna, and healthy skin. Based on these results, hyperspectral images were created where hyperspectral data was represented in several abundance maps. The maps showed differing abundances for lentigo maligna melanoma and lentigo maligna, and it was possible to localise the invasion site inside the lesion. For ill-defined basal cell carcinoma, the margins of the tumour were delineated more accurately than by clinical assessment, and the results were confirmed with histopathology.

The results of the clinical trial in photodynamic therapy showed that the histological clearance of hexylaminolevulinate was similar compared to 5-aminolevulinic acid nanoemulsion and methylaminolevulinate, with no differences in cosmetic outcome, pain or post-treatment reaction between the arms. In our fluorescence and photobleaching analyses the results were widely spread.

**Conclusions** In conclusion, hyperspectral imaging seems to be a promising and useful new imaging modality with a wide field of view: it is fast, easy to use and it seems to be capable of visualising subclinical findings. In non-invasive treatment, hexylaminolevulinate is an interesting option for photodynamic therapy of non-aggressive basal cell carcinomas. Hexylaminolevulinate at low concentrations achieves a comparable efficacy to 5-aminolevulinic acid nanoemulsion and methylaminolevulinate at higher concentrations. No differences were observed in adverse events or cosmetic outcome between the arms.

# TIIVISTELMÄ

**Tausta** Tyvisolusyöpä on maailman yleisin syöpä. Tyvisolusyövällä on eri alatyyppejä, joista pinnallinen tyvisolusyöpä ja ohut nodulaarinen tyvisolusyöpä ovat vähäisen riskin tyyppejä, jotka on mahdollista hoitaa muutoin kuin leikkaamalla. Pinnallinen tyvisolusyöpä on lisääntynyt muita alatyyppejä nopeammin, ja näin ollen myös ei-kirurgisten hoitovaihtoehtojen käyttö todennäköisesti lisääntyy. Valoaktivaatiohoito ja voidehoidot, joita ovat imikimodi ja 5-fluorourasiili, ovat vaihtoehtoja kirurgialle. Valoaktivaatiohoidon etuja ovat erinomainen kosmeettinen lopputulos sekä lyhytkestoisempi hoitoaika ja paikallisreaktion kesto verrattuna voidehoitoihin. Imikimodin teho on kuitenkin parempi kuin valoaktivaatiohoidon. Suuren riskin tyvisolusyöpiä ovat aggressiiviset alatyypit, joille tyypillisiä ovat kasvaimen epätarkkarajaisuus ja kliinisesti näkymättömät kasvainalueet. Lentigo maligna -melanooma on ihomelanooman alamuoto, jolle tyypillisiä ovat myös nämä piirteet. Lentigo maligna on lentigo maligna -melanooman esiastemuoto. Näitä kahta on vaikea erottaa toisistaan silmin ja dermatoskoopilla arvioiden. Epätarkkarajaiset ihosyövät ovat siis kliininen haaste. Kajoamattomilla kuvantamismenetelmillä on mahdollista parantaa ihokasvainten diagnostiikkaa ja arviota. Hyperspektrikuvantaminen on uusi, nopea ja tietokoneavusteinen kuvantamismenetelmä, jolla on laaja kuvausalue.

**Tavoitteet** Väitöskirjassa tutkitaan hyperspektrikuvantamista ja vähäisen riskin tyvisolusyövän valoaktivaatiohoitoa kliinisessä lääketutkimuksessa. Tavoitteena on tutkia hyperspektrikameran kykyä erottaa lentigo maligna -melanooma ja lentigo maligna toisistaan, sekä arvioida hyperspektrikameran kykyä määrittää epätarkkarajaisen tyvisolusyövän rajat ennen leikkausta verrattuna kliiniseen arvioon dermatoskoopin kanssa. Kliinisen lääketutkimuksen tavoitteena on verrata kolmen eri valoherkistäjävoiteen tehoa vähäisen riskin tyvisolusyövän valoaktivaatiohoidossa.

**Menetelmät** Hyperspektrikuvantamista tutkittiin kahdessa pilottitutkimuksessa. Näistä toisessa kuvattiin lentigo malignaa/lentigo maligna –melanoomaa, ja toisessa epätarkkarajaista tyvisolusyöpää. Molemmissa tutkimuksissa kasvaimet arvioitiin ennen kuvantamista kliinisesti dermatoskoopin avulla. Lopuksi kasvaimet leikattiin.

Hyperspektrikuvat tuotettiin matemaattisen mallinnuksen avulla tietokoneavusteisesti. Patologi, joka arvioi leikkeet, ei tiennyt, mitä hyperspektrilöydökset olivat. Kameran löydöksiä verrattiin histopatologiaan, ja epätarkkarajaisen tyvisolusyövän tapauksessa myös kliinisesti määritettyihin kasvaimen rajoihin.

Kliininen lääketutkimus oli tutkijalähtöinen, prospektiivinen, kontrolloitu, satunnaistettu ja kaksoissokkoutettu. Tutkimuksessa verrattiin kahden uudehkon valoherkistäjävoiteen eli 5-aminolevuliinihapon nanoemulsion ja matalapitoisen heksyyliaminolevulinaatin tehoa laajasti käytettyyn metyyliaminolevulinaattiin. Päätulos oli histologinen paraneminen kolme kuukautta valoaktivaatiohoidon jälkeen. Toissijaisia tuloksia olivat kosmeettinen lopputulos sekä hoidon haittavaikutukset eli kipu ja hoidonjälkeinen paikallisreaktio. Kivunhoitona käytettiin pitkävaikutteista paikallispuudutetta ennen kasvainten käsittelyä valoaktivaatiohoitoa varten. Tutkimuksessa arvioitiin myös valoherkistäjävoiteen fluoresenssia ja kulumista valotuksen aikana (ns. photobleaching) kokeellisella laitteistolla. Diagnoosi ja hoitotulos varmistettiin koepaloin. Tutkimuksessa potilaat ja tulosten arvioijat eivät tienneet, mitä valoherkistäjää oli käytetty.

**Tulokset** Lentigo maligna -melanooman, lentigo malignan ja terveen ihon hyperspektrikäyrät ovat erilaisia. Näin ollen lentigo maligna -melanooma ja lentigo maligna on mahdollista erottaa toisistaan hyperspektrikuvantamisen avulla. Hyperspektrikuvien perusteella oli myös mahdollista paikallistaa invaasioalue. Hyperspektrikamera määritti epätarkkarajaisen tyvisolusyövän rajat tarkemmin kuin kliinisesti oli määritetty, ja histopatologia tuki tätä löydöstä.

Valoaktivaatiohoidossa tyvisolusyöpä parani lähes yhtä hyvin matalapitoisella heksyyliaminolevulinaatilla kuin korkeapitoisemmilla 5-aminolevuliinihapon nanoemulsiolla ja metyyliaminolevulinaatilla. Valoherkistäjävoiteiden välillä ei ollut eroja haittavaikutuksissa tai kosmeettisessa lopputuloksessa. Fluoresenssin ja valoherkistäjän kulumisen tuloksissa oli laaja hajonta.

**Johtopäätökset** Hyperspektrikuvantaminen vaikuttaa lupaavalta uudelta menetelmältä, jolla on laaja kuvausalue, ja joka on nopea ja helppokäyttöinen. Lisäksi hyperspektrikamera näyttää pystyvän visualisoimaan silmälle näkymättömiä muutoksia. Heksyyliaminolevulinaatti on mielenkiintoinen uusi vaihtoehto vähäisen riskin tyvisolusyövän valoaktivaatiohoitoon, sillä jo matalalla pitoisuudella saavutetaan vastaava hoitotulos kuin korkeammilla pitoisuuksilla 5-aminolevuliinihapon nanoemulsiota tai metyyliaminolevulinaattia. Kuitenkaan hoidon kosmeettisessa lopputuloksessa tai haittavaikutuksissa ei ole eroja valoherkistäjien välillä.

# TABLE OF CONTENTS

## *List of Figures*

## *List of Tables*

# ABBREVIATIONS

| | |
|---|---|
| AJCC | American Joint Committee for Cancer |
| AK | Actinic keratosis |
| 5-ALA | 5-aminolevulinic acid |
| BCC | Basal cell carcinoma |
| nBCC | Nodular basal cell carcinoma |
| sBCC | Superficial basal cell carcinoma |
| BF-200 ALA | 5-aminolevulinic acid nanoemulsion |
| CMOS | Complementary metal-oxide semiconductor |
| FOV | Field of view |
| 5-FU | 5-Fluorouracil |
| FPI | Fabry-Perot interferometer |
| ENVI | Environment for visualising images (i.e. image processing software) |
| HAL | Hexylaminolevulinate |
| HIS | Hyperspectral imaging system |
| HSI | Hyperspectral imaging |
| KC | Keratinocyte carcinoma |
| LDH | Serum lactate dehydrogenase |
| LM | Lentigo maligna |
| LMM | Lentigo maligna melanoma |
| MAL | Methylaminolevulinate |
| MAPK | Mitogen-activated protein kinase |
| MM | Cutaneous malignant melanoma |
| MMS | Mohs micrographic surgery |
| NMSC | Non-melanoma skin cancer |
| NSAID | Non-steroidal anti-inflammatory drug |
| OCT | Optical coherence tomography |
| PDT | Photodynamic therapy |
| PUVA | Psoralens and ultraviolet A |

| | |
|---|---|
| PpIX | Protoporphyrin IX |
| RCM | Reflectance confocal microscopy |
| RGB | Red-Green-Blue |
| SCC | Squamous cell carcinoma |
| SLN | Sentinel lymph node |
| SSM | Superficial spreading melanoma |
| TNM | Tumour-Nodules-Metastasis |
| USB | Unified S-band |
| UVA | Ultraviolet radiation of relatively long wavelengths |
| UVB | Ultraviolet radiation of relatively short wavelengths |
| UVR | Ultraviolet radiation |
| VAS | Visual analogue scale |
| WHO | World Health Organization |

# ORIGINAL PUBLICATIONS

Publication I Neittaanmäki N, Salmivuori M, Pölönen I, Jeskanen L, Ranki A, Saksela O, Snellman E, Grönroos M: Hyperspectral imaging in detecting dermal invasion in lentigo maligna melanoma. Br J Dermatol. 177(6):1742-1744, 2017 Dec.

Publication II Salmivuori M, Neittaanmäki N, Pölönen I, Jeskanen L, Snellman E, Grönroos M. Hyperspectral Imaging System in the Delineation of Ill-defined Basal Cell Carcinomas: a pilot study. J Eur Acad Dermatol Venereol. 33(1):71-78, 2019 Jan.

Publication III Salmivuori M, Grönroos M, Tani T, Pölönen I, Räsänen J, Annala L, Snellman E, Neittaanmäki N. Hexyl aminolevulinate, 5-aminolevulinic acid nanoemulsion, and methyl aminolevulinate in photodynamic therapy of non-aggressive basal cell carcinomas: A non-sponsored, randomized, prospective and double-blinded trial. ACCEPTED MANUSCRIPT: doi:10.1111/jdv.16357

# 1 INTRODUCTION

This dissertation consists of three original communications, which are concerned with the diagnosis and treatment of skin cancer. With an aging population and a consistently increasing incidence of skin cancers, there is a pressing need for new technologies and treatments to improve the use of available resources.

Skin cancers are divided into three main groups: the melanocytic cancers, i.e. cutaneous malignant melanoma (MM), keratinocyte skin cancers (KC), which are further divided into squamous cell carcinoma (SCC) and basal cell carcinoma (BCC), and other skin cancers such as Merkel cell carcinoma and adnexal tumours. 80% of KCs are BCCs, and KCs are the most common cancers in the world. Thus, BCC is the most common cancer of all.

BCC is not regarded as a lethal cancer. It is extremely rare that BCC metastasises or advances locally, but it is a versatile cancer with different subtypes, each with a different level of aggressiveness. It is also common that one individual has several BCCs: multiple primaries and sometimes multiple recurrences. Thus, BCC causes remarkable costs in diagnosis and care, and significant morbidity, especially among individuals with multiple lesions (Chen, Bertenthal et al. 2007, Chren, Sahay et al. 2007, Holm, Nissen et al. 2016). The gold standard for the treatment of BCC is surgery, but for patients with high morbidity or low-risk BCC, an alternate, non-surgical option could be the best choice for treatment.

Clinically, BCCs are classified into morpheaphorm, i.e. ill-delineated, and well-delineated by the visualisation of the lesion border.

The well-delineated BCCs are often indolent and thus low-risk tumours when located at low-risk sites. The indolent subtypes of BCC are nodular (nBCC) and superficial (sBCC) BCC. sBCC, which typically is not a thick, but is a potentially wide tumour, is a particular subtype that can be treated with non-surgical options, of which there are several. One elegant, tumour-selective topical treatment is photodynamic therapy (PDT). The components involved in the mode of action for PDT include a photosensitiser acting as the source and precursor of photoactive protophorphyrin IX (PpIX), a light-source, and the oxygen level of the target tissue. In the PDT reaction, radical oxygen species are created, which leads to cell apoptosis and necrosis. Due to differences in the permeability of the stratum

corneum, and in the metabolic activity and cell proliferation rate of healthy and malignant cells, the photosensitiser accumulates in the tumour tissue. Thus, malignant tissue is destroyed, and healthy skin is preserved. The disadvantages of PDT are its varying effectiveness, and intensive pain that often occurs during illumination. The main advantages of PDT are an excellent cosmetic outcome, and a short application time. Healthcare professionals deliver the treatment. The treatment outcome may vary due to differing treatment protocols that use different photosensitisers. Therefore, to enhance the effectiveness of PDT, it is crucial to search for new and more efficient photosensitisers in PDT of sBCC.

Ill-defined BCCs are often of the aggressive subtypes; morpheaphorm, infiltrative and micronodular, which are often located in the head and neck area and can instigate a perineural invasion. Ill-defined BCCs challenge the surgeon, as preserving the function and cosmetic appearance is essential in this area. The aggressive subtypes of BCCs often lead to re-excisions, because the margins appear insufficient post-surgery. The need to re-excise increases the treatment costs. Additionally, repeated treatment is overtly stressful for patients. Thus, ill-defined BCCs are a true clinical challenge, and often it is these subtypes that are the most aggressive.

Lentigo maligna melanoma (LMM) is one subtype of melanoma, and lentigo maligna (LM) is graded as a melanoma *in situ*, i.e. a precursor to LMM. LMM is a tumour that has already invaded through the basal membrane of the skin. Both LM and LMM are also clinical challenges, since the tumour is often located in the head and neck area. Approximately 50% of invasive head and neck melanomas are LMM in subtype. In addition, the margins may be ill-defined with subclinical extensions, the lesions can be wide, and the invasion may not be recognisable. In distinguishing LM and LMM the correct diagnosis is crucial, as LMM requires wider margins and regular follow-up of the patient compared to LM.

There are special operation techniques, such as Mohs micrographic surgery (MMS), which is designed to preserve a maximal amount of healthy tissue while minimising the risk of recurrence. MMS is often used and recommended in the treatment of challenging and high-risk tumours. MMS is time-consuming and requires a highly trained team, but it can be cost-effective when tumour selection is performed correctly (Mosterd, Krekels et al. 2008, Tolkachjov, Brodland et al. 2017).

Non-invasive imaging diagnostic methods are increasingly under investigation. Bio-optical imaging systems could provide one solution to improve and speed up the pre-operative diagnosis and assessment of skin cancers (Tkaczyk 2017). When

the diagnosis is achieved non-invasively, precisely and quickly, it is possible to properly plan the treatment and accomplish it in one session. Bio-optical diagnosis and imaging provide several advantages: the possibility to make a bedside diagnosis non-invasively, to select for optimal sample sites for histopathology, and to make a more precise tumour dimension assessment compared to current methods in tumour delineation. Non-invasive imaging is not intended to replace the histopathological examination of the excised tumours. Optimally, it would speed up and improve the preoperative diagnosis and assessment of skin cancers.

Hyperspectral imaging is another novel, non-invasive bio-optical imaging method in the diagnosis of skin cancer. The advantages of hyperspectral imaging are a wide imaging area, a rapid imaging process and the possibility of obtaining spectral data from digital images, thus possibly obtaining information that is invisible to the human eye.

In this dissertation, two original communications focus on studying the feasibility of hyperspectral imaging in clinically challenging situations, such as in recognising the invasion in LMM and in the delineation of ill-defined BCCs. The third communication, a prospective, randomised, double-blinded and non-sponsored clinical trial focuses on the effectiveness and adverse events of PDT, and also assesses the photobleaching effect of three photosensitisers during the treatment of non-aggressive BCCs.

# 2 REVIEW OF THE LITERATURE

## 2.1 Skin cancers

### 2.1.1 Classification

Epidermal skin cancers are divided into keratinocyte, melanocyte and Merkel cell carcinoma. KC, which is often referred to as non-melanoma skin cancer (NMSC), is further divided into BCC and SCC. The embryological origins of both BCC and SCC are in ectodermal cells (Lai, Cranwell et al. 2018). Melanocyte carcinoma, i.e. malignant melanoma, and Merkel cell carcinoma are their own entities, and both are derived from the neural crest mesenchymal cells (Lai 2018). KCs and MM share common aetiological factors, such as ultraviolet (UV) radiation (Armstrong, Kricker 2001).

### 2.1.2 Epidemiology

A report from the World Health Organization (WHO) on the global burden of ultraviolet radiation (UVR) (Lucas, McMichael et al. 2006) presents worldwide epidemiological data and estimates from the year 2000. Table 1 summarises epidemiological data on the incidence and mortality from a one-year time period to emphasise the impact of skin cancers.

**Table 1.** Worldwide number of skin cancers during the year 2000, information acquired and modified from the WHO report on Global burden of disease from solar UVR (Lucas, McMichael et al. 2006)

| Skin cancer | Incidence | Mortality | Mortality/ Incidence | Burden of disease in DALYs |
|---|---|---|---|---|
| MM | 211 921 | 65 161 | 0.30 | 690.248 |
| SCC | 2 883 037 | 13 534 | 0.06 | 161.892 |
| BCC | 10 532 711 | 3245 | 0.0003 | 57.983 |

According to the 2004 update on the Global burden of disease report by WHO, melanoma and other skin cancers are the 12th leading cause of death worldwide for males and 15th for females during the year 2004 (World Health Organization 2008).

The disability-adjusted life year (DALY) is a measurement used by the WHO to assess the burden of disease. One DALY is equal to the loss of one year of life spent in full health. The DALY also takes into account premature death caused by the disease and life lived disabled by the disease (World Health Organization 2008).

In Finland, the latest report from the Finnish Cancer Registry is from the year 2017. According to this report, SCC is the 6th and MM the 7th most common cancer in Finland for males. The situation is reversed for females: MM is the 6th and SCC the 7th most common cancer (Finnish Cancer Registry 2017). Regarding the mortality of cancer deaths, MM ranks 11th for males and 9th for females (Finnish Cancer Registry 2017). The Finnish Cancer Registry excludes BCC in the statistics mentioned before. Regarding LM, the statistics are not published in the yearly cancer report, as they are considered unreliable. LM is reported to the Finnish Cancer Registry in the class of benign tumours, as it is only a local pathological change in *in situ* form, and thus the reliability of reporting is questionable. Table 2 presents the incidence and mortality rates in Finland from the year 2017 including BCC. Regarding the BCC data from the Finnish Cancer Registry, it should be mentioned that only one BCC per person is registered yearly, and only one BCC per anatomic area per person per lifetime is registered.

**Table 2.** Number of skin cancers during the year 2017 in Finland, information acquired and modified from the Cancer 2017 report (Finnish Cancer Registry 2017)

| Skin cancer | Incidence | | Mortality | | Mortality/ Incidence | |
|---|---|---|---|---|---|---|
| | MALE | FEMALE | MALE | FEMALE | MALE | FEMALE |
| MM | 917 | 802 | 150 | 71 | 0.16 | 0.09 |
| SCC | 944 | 734 | 25 | 16 | 0.03 | 0.02 |
| BCC | 4194 | 4573 | 0 | 0 | 0 | 0 |

### 2.1.3 Basal cell carcinoma

#### 2.1.3.1 Basal cell carcinoma subtypes

BCC can be classified clinically and histopathologically, with a partial overlap in the two classification methods (Trakatelli, Morton et al. 2014). Clinically, BCCs are divided into nodular, superficial and morpheaform, where nBCCs have well-defined borders, morpheaform BCC is ill-defined, and sBCCs can be either, but usually this is not a problem in the case of sBCC (Trakatelli, Morton et al. 2014). Sometimes fibroepithelioma of Pinkus is classified as a rare form of BCC, but it is distinct in both anatomical and clinical form (Trakatelli, Morton et al. 2014).

In histopathology, BCCs have previously been classified in relation to structures of the skin, for example apocrine, eccrine and sebaceous, as well as differentiated BCC versus solid, i.e. undifferentiated BCC (Crowson 2006). However, the most useful histopathological classification is the architectural growth pattern, which has been proven to correlate with prognosis (Crowson 2006) (Table 3). The risk of recurrence is not only influenced by the BCC subtype, but also the location, which is crucial (Figure 1).

**Table 3.** BCC classification by architectural growth pattern and risk for recurrence. Table information acquired and modified from (Trakatelli, Morton et al. 2014), (Crowson 2006), (NCCN Clinical Practice Guidelines In Oncology, NCCN Guidelines®).

| | Indolent growth pattern | | Intermediate step to aggressive growth pattern | Aggressive growth pattern | | |
|---|---|---|---|---|---|---|
| Clinical type | Superficial | Nodular | Morpheaphorm | | | Other |
| Borders | Often well-defined | Well-defined | Ill-defined | | | Either |
| Clinical appearance | Pinkish flat scaly patch/plaque | Pinkish nodule/ papule with overlying telangiectasia, also can be pearly or translucent | Whitish indurated scar-like plaque | | | Features of BCC and SCC |
| Ulceration | Can be present | Can be present | Can be present (rarely in sclerosing) | | | Can be present |
| Pigmentation | Can be present | Can be present | Can be present | | | Can be present |
| Histological type by architecture | Superficial | Nodular (sometimes referred as nodulo-cystic) | Micronodular | Infiltrating | Morpheaform= sclerosing | Basosquamous i.e. Metatypical |
| Features | Proliferation of basaloid cells parallel to the longitudinal axis of epidermis with slit-like stromal reaction, and with apposition of band-like lymphoid infiltrate, sBCC can be multifocal | Discrete small or large nests of basaloid cells in papillary or reticular dermis with palisading interface to the stroma | Resemble nBCC but nests are smaller and widely dispersed with asymmetrical distribution with stromal proliferation, and also extending deeper to dermis and even subcutis | Irregular sized and shaped basaloid nests with jagged contour and with elongated tumor cell strands of 5-8 cells in thickness in fibrotic stroma reaching to subcutis and even adjacent structures | Columns of basaloid cells in wideness of one to two cells with dense collagenized stroma with widespread invasion to reticular dermis and penetration to subcutis and even adjacent structures | Tumor with infiltrating and jagged tongues of cells with palisade and basaloid morphology, and other areas with intracellular bridge formation or cytoplasmic keratinisation, which can be confused with SCC |
| Mitoses | Low | Low | High | High | High | High |
| Perineural invasion | - | - | - | Can be present | Can be present | Can be present |
| Mixed histology | Combination of different growth patterns -> should be treated by the most aggressive component | | | | | |

| | | |
|---|---|---|
| **Risk for recurrence** | Low, when size < 2 cm in L, or size < 1cm in M | High in any size |
| | High, when size > 2cm in L, or size > 1cm in M, or any size in H is high risk | |
| Patient-related factor | History of immunosuppression or radiotherapy (on site of the tumour) highly increase risk | |
| Tumour-related factors | Recurrence, perineural invasion and ill-defined borders highly increase risk | |

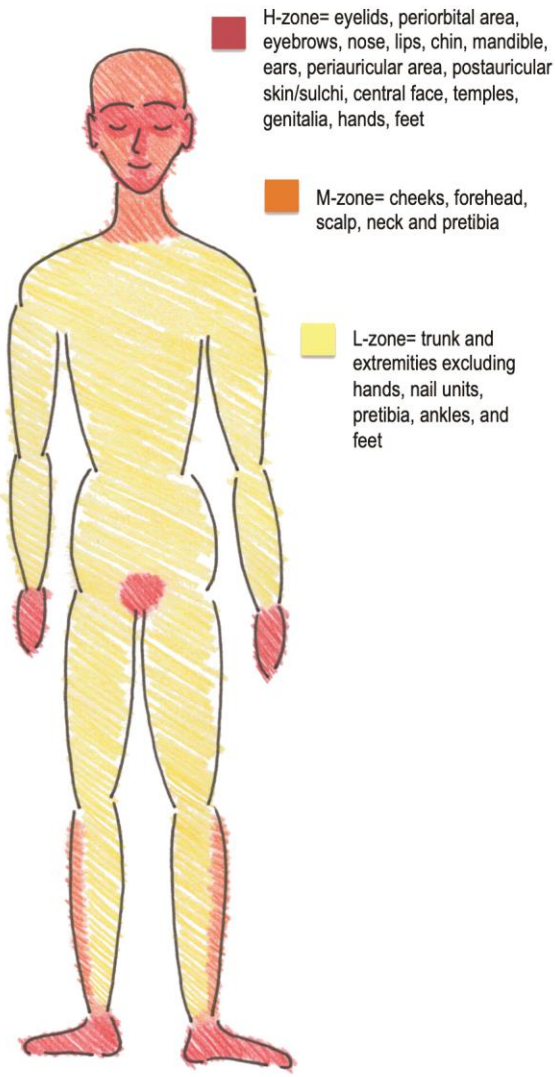


**Figure 1.** Risk areas in BCC, information for illustration acquired and modified from (NCCN Clinical Practice Guidelines In Oncology, NCCN Guidelines®) (H-zone= high risk areas, M-zone= intermediate risk areas, L-zone= low risk areas).

#### 2.1.3.2 Epidemiology of basal cell carcinoma in detail

BCC is the most common cancer in the world, though it should be noted that it mainly affects populations of Caucasian ancestry (Lucas, McMichael et al. 2006). A rough estimation based on the WHO report on the global burden of UVR and non-communicable diseases (Lucas, McMichael et al. 2006, World Health Organization 2008) approximated that 40% of all cancers in the world are KCs. A similar estimate was also found by Cakir et al. (Cakir, Adamson et al. 2012). Based on calculations from the data presented in Table 5, about 80% of new KCs are BCCs.

BCC is the most common skin cancer of the fair, Caucasian skin phototype, and it is also the most common skin cancer of the intermediately dark skin phototypes. Accordingly, BCC is also the most common skin cancer in Hispanic, Chinese Asian and Japanese populations with a predominance of the pigmented subtype (Gloster, Neal 2006). For Blacks and Asian Indians, BCC is the second most common skin cancer after SCC (Gloster, Neal 2006). In dark skin, skin cancer tends to have greater morbidity and mortality when compared to fair skin types (Gloster, Neal 2006). A Singaporean register study from 1968 to 1997 showed a trend of increasing incidence for BCC, and the degree of increase was higher for lighter skin types compared to darker ones (Koh, Wang et al. 2003).

Regarding reported numbers of BCC, the registration of KCs varies and this applies especially for BCC (Verkouteren, Ramdas et al. 2017). Vries et al. estimated that the stated number of BCCs in registries should be multiplied by 1.3 to correspond to the actual number of BCCs in four European territories, including Finland (de Vries, Micallef et al. 2012). In low-risk cases, BCCs are often treated without histological confirmation. For example, in four European territories including Finland, up to 24.1% of the BCCs were treated without histological confirmation in a given time frame (Flohil, Proby et al. 2012). Thus, when the multiplicity and treatment based on clinical and/or dermoscopic diagnosis is acknowledged, the actual number of BCCs is even higher than reported in national cancer or hospital pathology registries (de Vries, Micallef et al. 2012, Flohil, Proby et al. 2012).

Worldwide, the incidence of BCC is constantly increasing, but the rate of increase is also affected by latitude and the skin type of the population (Lomas, Leonardi-Bee et al. 2012). KC incidence varies in such a way that in lower latitudes, where the daily ambient UVR dose is higher, the incidence of KCs is higher. However, personal sun exposure habits can also have an effect (Xiang, Lucas et al.

2014). This applies to both SCC and BCC, but more strongly to SCC (Xiang, Lucas et al. 2014). Traditionally an outdoor profession, like farming, has been a risk factor for BCCs (Apalla, Lallas et al. 2016, Szewczyk, Pazdrowski et al. 2016), but recently a shift has been observed in the BCC risk for indoor workers. This could be due to outdoor activities during leisure time and on vacations (Deady, Sharp et al. 2014, Lindelof, Lapins et al. 2017). In Europe, an annual increase of 5.5% in the incidence of BCC has taken place during the past decades, and in the USA the annual increase rate is 2%. In Australia, the increase seems to have reached a plateau, yet Australia still has the highest incidence of BCC in the world at 884/100 000 person-years for both genders, based on a 2002 estimation (Lomas, Leonardi-Bee et al. 2012).

The average age of BCC onset is around 65 to 69 years (Betti, Radaelli et al. 2010, Scrivener, Grosshans et al. 2002). In some subgroups, such as younger adults under 40 years of age, females, individuals of high socio-economic status and urban populations, the increase in incidence has been even sharper during recent decades (Deady, Sharp et al. 2014, Raasch, Buettner et al. 2006). Furthermore, there has been a proportional shift towards the superficial subtype of BCC (Arits, A H M M., Schlangen et al. 2011). In young females, the solid superficial subtype is more common than a mixed-type histology on the trunk or extremities (Pyne, Myint et al. 2017). Therefore, with a shift towards an ever greater proportion of sBCC, non-surgical options could be the treatment of choice more often (Arits, A H M M., Schlangen et al. 2011). BCC is 1.5 times more common in males than in females (Xiang, Lucas et al. 2014), but in some countries, this ratio has reversed in younger populations (Verkouteren, Ramdas et al. 2017). Additionally, the incidence of BCC is still high and increasing in the very elderly (over 80 years), with the most common subtype for this group being nBCC in the head and neck region (Lubeek, van Vugt et al. 2017). In this age group, it is especially important to weigh the pros and cons of treatment (Lubeek, van Vugt et al. 2017). The risk of recurrence compared to the burden and adverse events of the treatment should be carefully considered.

The most common subtype of BCC is the nodular type, and thereafter the superficial and aggressive types (Raasch, Buettner et al. 2006, Scrivener, Grosshans et al. 2002). It is possible that the aggressive types are more common in countries with high daily UVR doses (Scrivener, Grosshans et al. 2002, Raasch, Buettner et al. 2006, Burdon-Jones, Thomas 2006). Nodular and aggressive subtypes are most commonly seen in the head and neck area, and sBCC on the trunk (Scrivener,

Grosshans et al. 2002, Raasch, Buettner et al. 2006, Betti, Radaelli et al. 2010) (Figure 2).

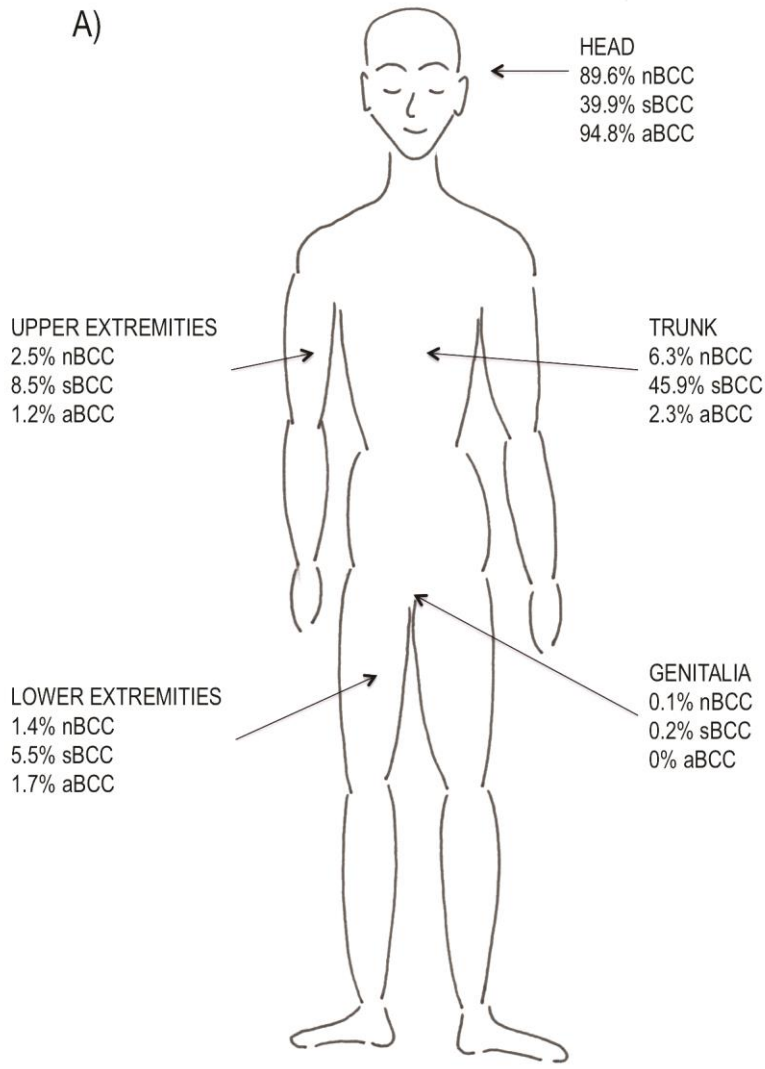


**Figure 2.** Anatomic distribution of BCC by subtype. Information for illustrations acquired and modified from (Scrivener, Grosshans et al. 2002) A) Distribution of different subtypes on different body areas (percentages are calculated in each subtype) B) Distribution of different subtypes on the head (percentages in colours are proportionate to each site)

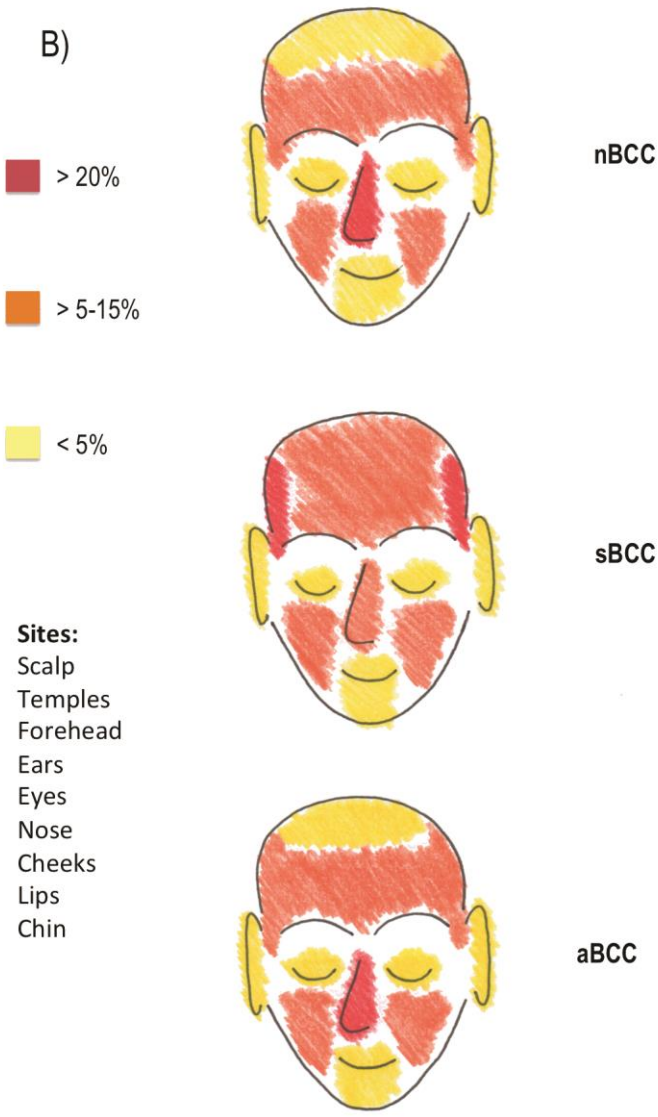


Most BCCs are located in the head and neck area, which poses a challenge for treatment as preserving the function and cosmetic outcome in this delicate location is essential. There is also a difference seen by age group with regard to the prevalence of certain subtypes (Betti, Radaelli et al. 2010, Raasch, Buettner et al. 2006) (Figure 3). In a study where tumour density was calculated by the site-specific body surface area, the highest BCC densities were found in the following order: nose, cheeks/perioral area, eyes, forehead/temples, ears, chin/jaw, neck, back, upper arm (including shoulder), lower arm, chest/abdomen), lower leg,

hands, scalp, and lastly feet and hip/upper leg which had the same body-surface-standardized incidence. Unfortunately, the density was not reported by subtypes (Richmond-Sinclair, Pandeya et al. 2009).

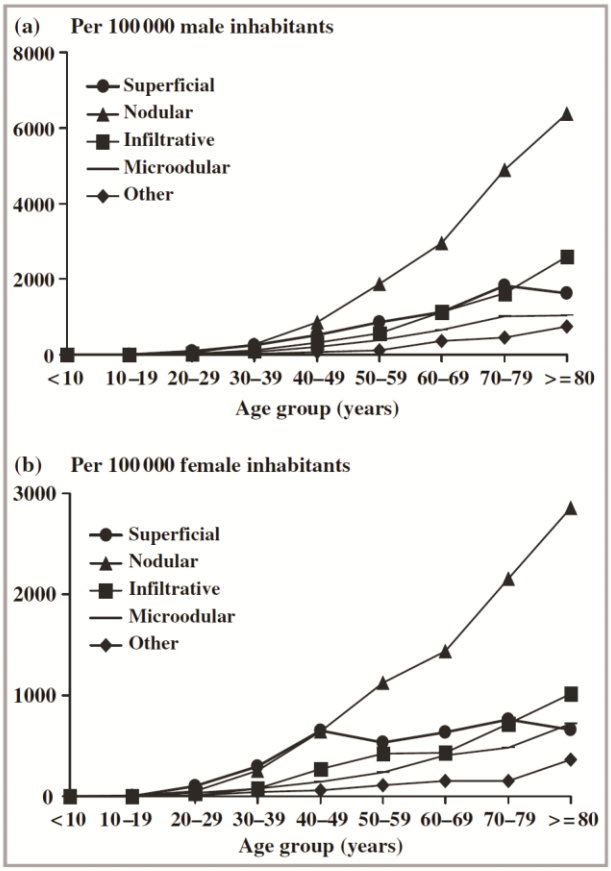


Fig 1. Age-specific incidence rates for histological subtypes of basal cell carcinoma in male (a) and female (b) Australian patients. The data were recorded in Townsville, Queensland, Australia, between 1997 and 1999.

**Figure 3.** BCC subtypes by age group. Figure borrowed from (Raasch, Buettner et al. 2006), courtesy of the British Journal of Dermatology.

Some studies have speculated that the rise in global temperature might enhance the effective UVR dose. Thus, climate change could also play a role in the increasing incidence of KC (van der Leun, Jan C., Piacentini et al. 2008, Piacentini, Della Ceca et al. 2018). More commonly postulated reasons for the increasing incidence include improved registration, aging populations, increased awareness, better

availability of surgery and changed UVR exposure habits (Verkouteren, Ramdas et al. 2017, Deady, Sharp et al. 2014).

The use of sunscreens in the prevention of KCs is widespread and often recommended based on the idea of UVR as an aetiological factor. However, good quality evidence is sparse. There is more evidence for actinic keratosis (AK) and SCC, but it is more unclear for BCC (Sanchez, Nova et al. 2016, Waldman, Grant-Kels 2019). Screening has some impact on KC incidence (Eisemann, Waldmann et al. 2014), and some preventive interventions like oral acitretin (Bath-Hextall, Leonardi-Bee et al. 2007) or oral nicotinamide (Chen, Martin et al. 2015) in high-risk groups have shown evidence for the prevention of KCs. Risk factors for developing KC or subsequent BCC as well as risk factors in high-risk groups have been studied, and clinical tools and predictors based on these have been developed (Lowenstein, Garrett et al. 2017, Whiteman, Thompson et al. 2016, Verkouteren, Smedinga et al. 2015).

#### 2.1.3.3 Basal cell carcinoma: burden of disease and economical impact

In BCC, it is typical that a single patient can have multiple BCCs, either at the same time or as multiple primaries, or at the time passing as new primaries or recurrences. In Australia, during a ten-year follow-up 46% of patients with BCC were diagnosed with multiple lesions, and 54% with a single lesion (Richmond-Sinclair, Pandeya et al. 2009), thus roughly half of the patients with BCC will develop multiple lesions. From those patients who have multiple BCCs, 56% will have over three lesions, 26% over four and 17% over five (Richmond-Sinclair, Pandeya et al. 2009). The incidence for patients with a single BCC was 935/100 000 person-years, whereas for patients with multiple BCCs it was 705/100 000 person-years (Richmond-Sinclair, Pandeya et al. 2009). The risk of lesion multiplicity is greater for older individuals (Flohil, van der Leest, Robert J T et al. 2013).

In a systematic review and meta-analysis from patients with BCC, 29% will develop a subsequent BCC, 4.3% a SCC and 0.5% a MM, and correspondingly the risks were 17.4-fold for BCC, 3.2-fold for SCC and 2.4-fold for MM, when compared to the general population (Flohil, van der Leest, Robert J T et al. 2013). The risk for subsequent skin cancer was highest in Australia, thereafter in the USA and lowest in Europe (Flohil, van der Leest, Robert J T et al. 2013).

A sharper rise in the incidence of sBCC and of aggressive BCC in general has been observed in younger populations (Arits, A H M M., Schlangen et al. 2011). It

is possible that there are some undiscovered biological differences between early-onset BCC, having the first BCC at an average age of 40 years, and late-onset BCC, at an average age of about 60 years (Barton, Zens et al. 2016). Early-onset BCC is more likely to be an aggressive subtype (Barton, Zens et al. 2016). When looking at the proportion of patients with early-onset BCC, 34% of them will develop a subsequent skin cancer, and 31% of early-onset BCC patients will develop a new BCC with a median development time of 1.1 years for the subsequent skin cancer (Berlin, Ferrucci et al. 2015). Thus, a remarkable proportion of early-onset BCC patients will develop a new BCC much faster compared to the 36.2% five-year cumulative risk generally observed in BCC (Flohil, van der Leest, Robert J T et al. 2013).

There seems to be an association between mortality in other cancers and having a KC, as the association is stronger for SCC than BCC (Barton, Armeson et al. 2017). Thus, the idea of KCs being a marker for a cancer-prone phenotype has been proposed (Barton, Armeson et al. 2017, Jensen, Bautz et al. 2008).

In extremely rare cases, BCC can be locally advanced or metastatic. In these cases oncological and costly treatments are required (Puig, Berrocal 2015, Mohan, Chang 2014). In a Danish registry study, the incidence of metastatic BCC was 0.0039% among patients with a history of BCC, compared to 0.0001% in the general population (Nguyen-Nielsen, Wang et al. 2015). A registry study from the USA found the incidence for locally advanced disease to be 0.8% (Goldenberg, Karagiannis et al. 2016). About 1–10% of BCCs are locally advanced (Mohan, Chang 2014).

KCs have a small but remarkable impact on quality of life of affected individuals, and this should be noted in the treatment of these patients (Gaulin, Sebaratnam et al. 2015). Quality of life should be included more often as an outcome in the research of KCs, not least due to the fact that KCs are commonly a chronic condition (Gaulin, Sebaratnam et al. 2015).

BCC diagnosis and treatment costs are generally low for individual cases, but due to BCC being so common, the expenses are the fifth highest when taking all cancers into account, with only prostate, lung, colon and breast cancers having higher costs (Cakir, Adamson et al. 2012). When comparing skin cancers, the total cost of illness for BCC in a three-year period was as high as for melanoma, but naturally melanoma had a higher cost per case (Bentzen, Kjellberg et al. 2013).

### 2.1.3.4 Risk factors of basal cell carcinoma

There are several risk factors for developing a BCC, and the relationships between them are complex (Verkouteren, Ramdas et al. 2017). There is a predisposing genotype as well as several environmental risk factors interacting in the development of BCC (Verkouteren, Ramdas et al. 2017) (Table 4).

**Table 4.** Risk factors of BCC, information acquired and modified from (Dessinioti, Antoniou et al. 2010, Kraft, Granter 2014, Verkouteren, Ramdas et al. 2017).

| Genotype | Phenotype | Risks in environment | Protective factors in environment |
|---|---|---|---|
| Somatic mutations (sporadic PTCH1 and p53) | Age | UVR (solar, therapeutic, tanning beds) | Coffee (caffeine or marker of lifestyle and life habits??) |
| Germline polymorphism (MC1R variants, CYP family, GST family) | Male sex | Photosensitising agents (PUVA) | Selenium?? |
| Germline mutations ** (genodermatoses: *PTCH1* and nucleotide excision repair genes, some unknown genes) | Personal history of skin cancer | Ionising radiation (therapeutic, environmental) | Carotenoids?? |
| ? Epigenetic factors, something else | Family history of skin cancer | Chemicals (arsenic) | Vitamins?? |
| | Sensitivity to UVR and poor ability to tan | Immunosuppression | |
| | Fair complexion, light hair and eye colour | | |
| | Signs of excessive UVR exposure and signs of photodamage * | | |

* melanocytic nevi, freckles, solar elastosis, solar lentigines and actinic keratoses

** *PTCH1* mutation in nevoid basal cell carcinoma syndrome, nucleotide excision repair genes in xeroderma pigmentosum, unknown gene in Xq24-27 region in Bazex-Dupré-Christol syndrome, unknown mutation in Rombo syndrome.

? Possible aetiological factor

?? Inconsistent and insufficient evidence

The above-presented risk factors often associate with primary BCCs. The risk factors that predict a high risk for a second BCC include being 60-75 years of age at the moment of the first BCC, male sex, less than three cups of coffee per day, the first BCC being of a superficial subtype and more than one BCC at first diagnosis (Verkouteren, Smedinga et al. 2015). Additionally, if a patient has more than one BCC at first diagnosis the multiple BCCs are more likely to occur on the

trunk. Furthermore, multiple BCCs are also more likely to be of the superficial subtype (Kuo, Batra et al. 2017).

There is a strong UVR signature in mutations leading to BCC (Kraft, Granter 2014, Verkouteren, Ramdas et al. 2017, Armstrong, Kricker 2001, Dessinioti, Antoniou et al. 2010), but the relationship of the pattern of exposure to a specific subtype, site and the multiplicity of BCC is under discussion (Verkouteren, Ramdas et al. 2017). The association of UVR to BCC is based on epidemiological data, such as the linkage of latitude and incidence, and high incidence on sun-exposed anatomic locations (Xiang, Lucas et al. 2014, Richmond-Sinclair, Pandeya et al. 2009, Armstrong, Kricker 2001). It is clear that cumulative UVR dose is a risk for SCC and AK, but in BCC, the pattern of exposure and interaction with other causative factors play a major role (Xiang, Lucas et al. 2014, Dessinioti, Antoniou et al. 2010, Verkouteren, Ramdas et al. 2017, Armstrong, Kricker 2001).

Intense intermittent UVR exposure, especially in childhood, increases the risk for BCC (Verkouteren, Ramdas et al. 2017, Pelucchi, Di Landro et al. 2007). Intense intermittent exposure has also been associated with a location on the trunk. sBCC is reported to be more common on the trunk (Verkouteren, Ramdas et al. 2017), but in a study from Australia, a country with high UVR exposure, the distribution of all subtypes on different anatomic locations was more equal compared to the data from low UVR exposure countries, thus blurring the possible association of intense intermittent exposure and superficial subtype (Raasch, Buettner et al. 2006). Nodular and aggressive BCCs are more common in the head and neck area. For nBCC, the cumulative UVR dose could be an independent risk factor in the head and neck area, whereas in sBCC on the trunk, the capability of DNA repair or other molecular factors could play a bigger role (Raasch, Buettner et al. 2006, Pelucchi, Di Landro et al. 2007). Early-onset BCC associates with an aggressive subtype, high solar sensitivity and the number of blistering sunburns experienced in childhood (Kuo, Batra et al. 2017). Early-onset BCC is more common in women and in the head and neck area (Kuo, Batra et al. 2017). Interestingly, solid sBCC with no mixed histology is also more common in women, but in young women it is often located on the extremities and trunk (Pyne, Myint et al. 2017). The biology of BCC is diverse.

UVR of relatively short wavelengths (UVB) is capable of causing direct DNA damage, via the DNA acting as a chromophore and absorbing the energy of UVB. In the case of UVR of relatively long wavelengths (UVA), the effect on DNA is indirect, as other structures absorbing UVA create radical oxygen species, which can cause DNA damage (Dessinioti, Antoniou et al. 2010). In addition to DNA

damage, UVR causes immunosuppression (Dessinioti, Antoniou et al. 2010), and it is also being proposed that differences in apoptosis and local immune response could affect the type of the tumour and the site-specific incidence of KCs (Manestar-Blazic, Batinac et al. 2007).

#### 2.1.3.5 Tumour cell origin and pathophysiology of basal cell carcinoma

BCC probably arises from stem cells in hair follicles or in the interfollicular epidermis (Wang, Wang et al. 2011, Verkouteren, Ramdas et al. 2017). In the pathophysiology of BCC, the Hedgehog signalling pathway is essential (Wang, Wang et al. 2011, Kraft, Granter 2014). This pathway controls cell proliferation, differentiation and apoptosis (Kraft, Granter 2014). PTCH and SMO are proteins in association with the cell membrane and are part of the Hedgehog pathway, and when Hedgehog proteins bind to PTCH, the SMO is released and activates the pathway (Kraft, Granter 2014). *PTCH1* is the gene encoding the PTCH protein, and mutations in this gene, such as those found in basal cell nevus syndrome patients and often in sporadic BCC, lead to decreased suppression of SMO by PTCH (Kraft, Granter 2014). Activating mutations in *SMO* will also lead to activation of the Hedgehog pathway (Kraft, Granter 2014). In sporadic BCC, 67–90% have mutations in *PTCH1* and 10–20% in *SMO* (Kraft, Granter 2014).

In sporadic BCC, mutations on the tumour suppressor gene *TP53* are also common, with some 40-65% carrying these mutations, which lead to the overexpression of *p53* (Kraft, Granter 2014). A polymorphism of melanocortin 1 receptor (MC1R) leads to different kinds of photo-protective qualities of eumelanin, which lies over keratinocytes' nuclei (Kraft, Granter 2014). In Xeroderma Pigmentosum, a syndrome with multiple BCCs, DNA repair is impaired. In sporadic BCC, the role of mutations in DNA repair genes is unclear, but they may affect the aggressiveness of different subtypes (Kraft, Granter 2014).

### 2.1.4 Lentigo maligna and lentigo maligna melanoma

#### 2.1.4.1 Cutaneous melanoma subtypes

Melanoma has four main histopathological subtypes: LMM, acral lentigious melanoma, superficial spreading melanoma (SSM) and nodular melanoma (Su

1997) (Table 5). Additionally, there are rare variants, which can also be classified by their clinicopathological features (Perniciaro 1997) (Table 5).

**Table 5.** Subtypes of primary cutaneous melanomas, information acquired and modified from (Su 1997), (Perniciaro 1997) and (Gershenwald, Scolyer et al. 2017)

| | Common melanoma subtypes: 95% of cases | | | | | Rare variants: 5% of cases | | | | |
|---|---|---|---|---|---|---|---|---|---|---|
| Clinical type | LM | LMM | Acral lentiginous melanoma | SSM | Nodular melanoma | Desmoplastic melanoma | Amelanotic melanoma | MM in benign nevi | Balloon cell malignant melanoma | Spindle cell melanoma |
| Precursor | Solar lentigo | LM (in situ melanoma) | In situ | In situ | - | - | - | ? | - | - |
| Timeline | Years from LM (radial growth phase) to LMM (vertical growth phase and invasion to basal membrane) | | Fast from radial to vertical | After some period from radial to vertical | Very fast from radial to vertical | ? | ? | ? | ? | ? |
| Borders | Irregular and Ill-defined | | Irregular and often well-defined | Irregular and often well-defined | Often well-defined | Irregular | Ill-defined | Sometimes irregular or ill-defined | - | - |
| Clinical appearance | Occurs as irregular spot on sun-exposed areas in the elderly with different shades of colour brown/black/grey/blue (in LMM deeper and more blue colour, possible a nodule) | | Brown/dark spots in feet, hands, digits or subungual areas (most often soles), more common in darker skin types | Irregular spots with varying colour, regression areas, expansions of margins, and in vertical phase with papules, nodules and diffuse induration, more typical in light skin types, in young adults or adults, in trunk or extremities | Deeply pigmented and rapidly enlarging nodule, often ulcerating | Irregular, sclerotic plaque with little or no pigmentation, may occur in common MM types (in LM in head and neck area) or de novo | May be metastases on skin or arise de novo especially in LM, depigmented patch or nodules, often with pink colour | MM suspect areas in ordinary compound nevi, congenital nevi or atypical nevi | Metastases or primary, resembles benign balloon cell nevus | - |

| Histological subtype | LM (radial) | LMM (vertical) | Acral lentiginous melanoma | SSM | Nodular melanoma | Desmoplastic melanoma | Amelanotic melanoma | MM in benign nevi | Balloon cell malignant melanoma | Spindle cell melanoma |
|---|---|---|---|---|---|---|---|---|---|---|
| Features | Atypical melanocytes singly or in nests within epidermis. | Like LM but additionally atypical melanocytes focally in the papillary dermis. In deeper invasion to the dermis, spindle shaped cells and sometimes epithelioid cells are detected. | Radial: atypical melanocytes in epidermis and irregular lentiginous hyperplasia, some times dendritic melanocytes and pagetoid cells may be seen in epidermis. Vertical: irregular nests and masses of atypical melanocytes in junctional area, superficial dermis and reticular dermis, often infiltration to eccrine ducts. | Radial: large melanocytes with dark atypical nuclei and abundant pale cytoplasm, similar changes in the epidermis as in Paget's disease. Vertical: epithelioid cells in the dermis, nesting at junctional area, and in the epidermis anaplastic melanocytes may be present as scattered in all layers of the epidermis. Tumour cells invaded the papillary and reticular dermis. | Radial/Vertical: Atypical melanocytes in nests or pagetoid pattern in the epidermis and pleomorphic tumour cells in the dermis/subcutis as aggregates, fascicles or sheets. Nuclei are large and mitoses are common, minimal epidermal spreading lateral to the dermal mass. | Dermal fibrosis, spindle cells within the dermis, lentiginous hyperplasia of atypical melanocytes at the junction area. Tendency for neurotropism, and neurogenic differentiation. 97% are positive in S-100 immunohistochemical staining. | Cords or nests of atypical melanocytes in the dermis. Immunohistochemical staining is helpful. | Features of MM in benign nevi, and 35% are remnants of benign nevi. | Melanocytes with clear cytoplasm admixed with nests of conventional melanoma cells. | Undifferentiated melanoma: nests of atypical cells at junction area or intraepidermal spread or both. Immunohistochemical staining is helpful, may have pleomorphic pattern resembling atypical fibroxanthoma. |
| Depth correlates with prognosis | Breslow thickness: tumour thickness in mm from granular layer of epidermis to deepest invasion on tumour cells (less than 0.76mm doesn't usually metastasise) | | | | | | | | | |
| Ulceration correlates with prognosis | Ulceration: full thickness absence of an intact epidermis above any portion of the primary tumour with a host reaction on the site, where fibrinous and acute inflammatory exudate is detected. | | | | | | | | | |
| Regression | Regression may occur in all types -> "invisible melanoma" -> only melanophages, mild fibroplasia and telangiectasia present | | | | | | | | | |

Rare forms of melanoma that are also reported include angiotropic, myxoid, pedunculated and verrucous variants (Perniciaro 1997), and rare forms of the vertical growth phase include minimal deviation melanoma, nevoid melanoma, infantile/childhood melanoma, pigment-synthesising melanoma and metastatic melanoma (Liu, Mihm 2003). Melanoma can also be discovered based on the appearance of tumour metastases on the skin or elsewhere, and in this case the primary tumour may be of unknown origin (Perniciaro 1997, Gershenwald, Scolyer et al. 2017). In the histopathology of melanoma metastases in the skin, there are usually clusters of atypical spindle-shaped or cuboidal melanocytes in the dermis or subcutaneous fat, but the histology can vary widely (Perniciaro 1997).

For prognosis, the tumour-nodules-metastases (TNM) -classification is used, where the different categories correlate with survival (Gershenwald, Scolyer et al. 2017). The latest, 8th edition of melanoma staging with TNM-classes was recently released by the American Joint Committee for Cancer (AJCC) (Gershenwald, Scolyer et al. 2017) (Table 6).

**Table 6.** Factors defining the TNM-categories, information acquired and modified from (Gershenwald, Scolyer et al. 2017).

| | |
|---|---|
| **T** | Tumour thickness |
| | Ulceration |
| **N** | Lymph nodes: clinically occult (SLN positive)/clinically detected |
| | Number of involved lymph nodes |
| | Presence of in-transit satellites and/or micro-satellite metastases |
| **M** | Evidence of distant metastasis |
| | Anatomic site of metastasis |
| | If metastasis present, LDH level elevated or not |

In the AJCC staging, there is only one non-microscopic or non-anatomic prognostic factor, which is the serum lactate dehydrogenase (LDH) level. However, there are reports of several biomarkers which can already affect the treatment of melanoma. These factors may potentially have an impact on the staging systems in the future, or even make them obsolete (Gershenwald, Scolyer 2018) (Table 7). It has been suggested that melanoma could have four genomic classes based on the underlying driver mutation: *BRAF*, *RAS*, *NF1* and triple-wild type (Cancer Genome Atlas Network 2015). Classification could also be based on a UV-exposure pattern: melanomas of chronically sun-exposed skin (LMM and

desmoplastic melanoma) and intermittently exposed sun-protected skin (Armstrong, Cust 2017, DeWane, Kelsey et al. 2019).

When considering the prognosis of a LM/LMM patient, it is crucial that these two conditions are distinguished, as the prognosis of LMM is similar to other melanoma types of the same Breslow thickness (Gershenwald, Scolyer et al. 2017). LM is an *in situ* melanoma, and has a different prognosis, treatment, and follow-up compared to invasive melanoma (Gershenwald, Scolyer et al. 2017, Wright, Souter et al. 2019).

**Table 7.** Potential biomarkers in melanoma, information acquired and modified from (Axelrod, Johnson et al. 2018) and (Weiss, Hanniford et al. 2015).

<table>
<tr><th colspan="2" rowspan="2">Biomarkers</th><th colspan="2">Predictive: outcome of therapy</th><th>Prognostic:</th></tr>
<tr><th>Targeted therapy</th><th>Immune checkpoint inhibitors</th><th>Diagnostic tools</th></tr>
<tr><td rowspan="2">Tumour genome</td><td>Driver mutations</td><td>BRAF-inhibitors/ MEK-inhibitors</td><td rowspan="15">CTLA-4/ PD-1 -response</td><td rowspan="15">Potential tools for diagnosis and prognosis</td></tr>
<tr><td>Gene expression: messengerRNA and microRNA</td><td rowspan="14">Potential new therapies</td></tr>
<tr><td rowspan="6">Antitumor immune response/ Tumour-infiltrating lymphocytes</td><td>Tumour microenvironment</td></tr>
<tr><td>Tumour cell signalling</td></tr>
<tr><td>Mutation burden and neoantigens</td></tr>
<tr><td>Antigen presentation</td></tr>
<tr><td>Recognition of antigens by T cell receptors</td></tr>
<tr><td>Cytotoxic T cell response</td></tr>
<tr><td rowspan="3">Circulating blood/ Serum markers</td><td>Proteins (like LDH)</td></tr>
<tr><td>microRNA</td></tr>
<tr><td>tumourDNA</td></tr>
<tr><td rowspan="3">Clinical signs</td><td>Immune-related adverse events</td></tr>
<tr><td>Site of metastases</td></tr>
<tr><td>Tumour burden</td></tr>
<tr><td>Microbiome</td><td>Pretreatment microbiome in gut/ modification of gut microbiome</td></tr>
</table>

### 2.1.4.2 Epidemiology of lentigo maligna and lentigo maligna melanoma in detail

The overall incidence of melanoma has risen globally for the past few decades, and the increase has been from 3–7% to 100% (=2-fold) for every 10–20 years in populations with Caucasian ancestry (Nikolaou, Stratigos 2014, Lai, Cranwell et al. 2018). Interestingly, in younger age groups in Australia, the USA and Europe the incidence has begun to stabilise, but the increase has been even more dramatic in age groups over 60 years, especially among males. In the USA, a peak in the incidence rate has also been observed in young adults aged 20 to 24 years (Nikolaou, Stratigos 2014). In Scandinavia, the increase in melanoma incidence has been 10-fold from 1953 to 1997 (Nikolaou, Stratigos 2014). In Europe, there are variations in the increase rate in Northern, Southern, Western and Eastern regions, perhaps due to different registration systems or shortages in them. The male to female ratio and age also vary between the geographic regions (Nikolaou, Stratigos 2014).

Melanoma is rare in darker skin phototypes, with 1-8% of skin cancers being melanoma in Blacks, 10-15% in Asian Indians, and 19% in Japanese (Gloster, Neal 2006).

Even though the incidence of melanoma has increased dramatically, the mortality of melanoma has stabilised in Europe, Australia and the USA (Nikolaou, Stratigos 2014, Lai, Cranwell et al. 2018). This reflects the early detection of thin melanomas at a stage with a better prognosis. However, the increasing mortality rate in elderly men over the age of 60 with thick melanomas often of the nodular type in the head and area, is an exception (Lai, Cranwell et al. 2018, Nikolaou, Stratigos 2014). The increased mortality rate in this age group has been associated with a poorer prognosis at the moment of diagnosis, as the melanomas are thick and late in stage at the time of detection (Lasithiotakis, Petrakis et al. 2010). The survival rate is generally better for females compared to males. The reason for this is unknown, and unrelated to sex hormones (Nikolaou, Stratigos 2014).

The anatomic location of melanoma associates with age, as young patients' melanomas are typically located on the trunk or extremities, and in the elderly they are more often located in the head and neck area (Nikolaou, Stratigos 2014). The distribution is different in dark skin phototypes, as melanomas in dark skin types are often located in non-exposed sites such as the palms, soles and mucosa. Accordingly, acral lentiginous melanoma is the most common subtype in Blacks (Gloster, Neal 2006).

Approximately 50% of invasive head and neck melanomas are LMM, compared to only 2% of all melanomas (Cox, Aitchison et al. 1996, Linos, Li et al. 2017). Regarding the body distribution in LMM, 18% are reported to be extra-facial (Cox, Aitchison et al. 1998). However, it seems that extra-facial LMM is more common in low latitudes such as Australia and Hawaii, where extra-facial LMMs make up to 57% of LMMs (Inskip, Rosendahl 2016). The most common sites for LMM are presented in Figure 4. There are differences in location between the sexes, as females more commonly have LM on the cheeks, and males more commonly on the scalp and cartilaginous area of the ears (Tiodorovic-Zivkovic, Argenziano et al. 2015).

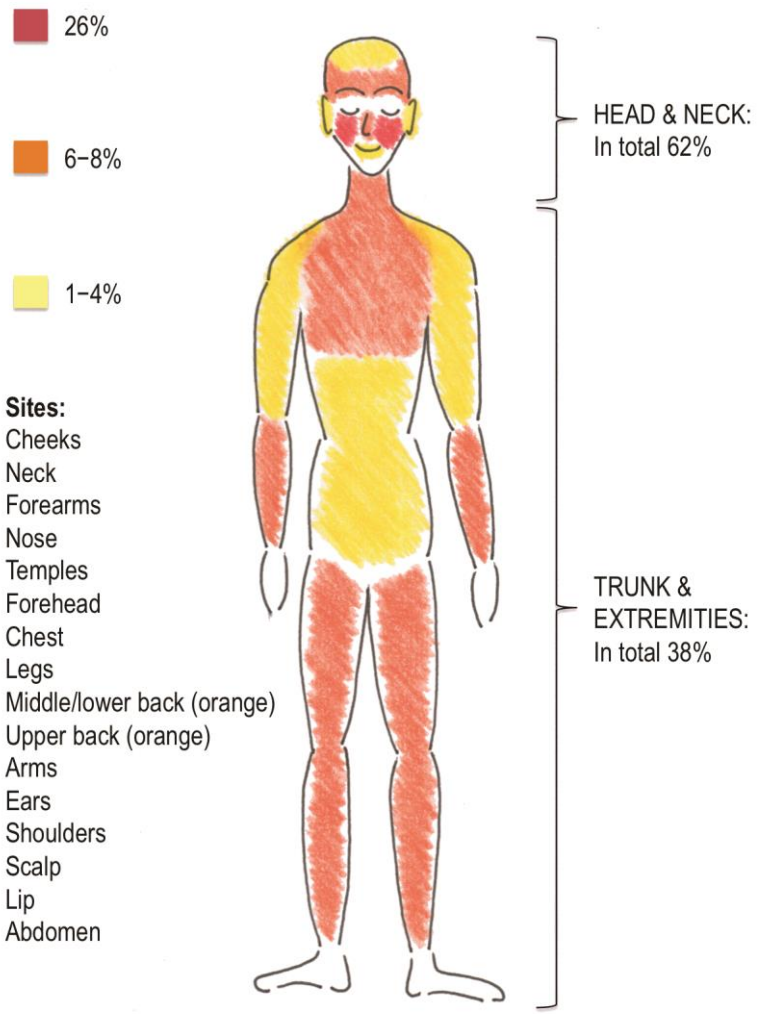


**Figure 4.** LM incidence by body area (percentages announced in colours are proportionate to each site), information acquired and modified for illustration from (Mirzoyev, Knudson et al. 2014).

About 10% of melanomas are LMM (Kraft, Granter 2014), but this proportion might be changing, as the incidence of LM/LMM is increasing in studies performed in Europe and the USA (Toender, Kjaer et al. 2014, Swetter, Boldrick et al. 2005, Greveling, Wakkee et al. 2016, Mirzoyev, Knudson et al. 2014).

Additionally, the overall incidence for melanoma *in situ* has increased in Europe, the USA and Australia (Coory, Baade et al. 2006, Toender, Kjaer et al. 2014, Helvind, Holmich et al. 2015) (Table 8). This increase is mainly due to LM, as 79–83% of melanomas *in situ* are LM (Swetter, Boldrick et al. 2005). A change has also been observed in the location of melanomas, as more melanomas and LM are located in the head and neck area (Helvind, Holmich et al. 2015, Mirzoyev, Knudson et al. 2014).

**Table 8.** Increasing incidence of LM/LMM in the USA and Europe, information acquired and modified from (Toender, Kjaer et al. 2014, Swetter, Boldrick et al. 2005, Mirzoyev, Knudson et al. 2014, Greveling, Wakkee et al. 2016 and Higgins, Lee et al. 2015).

| | | Incidence per 100 000 person-years | | Annual percentage change (timeline) | |
|---|---|---|---|---|---|
| | | Female | Male | Female | Male |
| Minnesota 1970-2007 | LM | 0.8 -> 10.0 | 4.0 -> 19.2 | - | |
| | LMM | - | | - | |
| California 1990-2000 | LM | both sexes 5.4 -> 10.0 * | | both sexes 4.2% (1999-2000) | |
| | LMM | both sexes 1.6 -> 3.2 * | | both sexes 3.7% (1999-2000) | |
| Denmark LM 1997-2011 LMM 1985-2011 | LM | 0.6 -> 1.5 | 0.5 -> 1.4 | 7.53% (1997-2011) | 7.17% (1997-2011) |
| | LMM | 0.23 -> 0.54 | 0.23 -> 0.71 | 4.7% (1985-2011) | 5.2% (1985-2011) |
| Netherlands 1989-2013 | LM | 0.76 -> 4.16 | 0.68 -> 3.76 | 8.7% (2007-2013) | 7.4% (2002-2013) |
| | LMM | 0.22 -> 1.18 | 0.26 -> 1.25 | 14.4% (2009-2013) | 14.1% (2007-2013) |

* Calculated as an average of the different age groups given in the reference and greater proportion for male was reported

The annual percentage change in incidence for LM/LMM has been greater than for any other cancer in the USA (Higgins, Lee et al. 2015). Interestingly, the LM and LMM incidence is higher for males in the USA, especially in the 65 years and over-age group (Swetter, Boldrick et al. 2005, Mirzoyev, Knudson et al. 2014), whereas in Europe it seems that the incidence of LM is higher in females, but the incidence of LMM is higher in males (Toender, Kjaer et al. 2014, Greveling, Wakkee et al. 2016, Helvind, Holmich et al. 2015). Furthermore, in Europe the increasing incidence of melanomas *in situ* has been sharpest for males over 60 years of age (Helvind, Holmich et al. 2015). In the most recent epidemiological study of LM/LMM by Grevling et al. from the Netherlands, the differences between females and males were slight, and for both sexes the increased incidence did not have an impact on mortality or the 5-year survival rate, which was 104% for LM and 99% for LMM (Greveling, Wakkee et al. 2016). The risk for developing LMM after being diagnosed with LM is 2–3% (Greveling, Wakkee et al. 2016), whereas earlier it had been reported to be 5% (Higgins, Lee et al. 2015). It should be noted

that the prognosis of melanoma is similar for LMM as it is for other subtypes of similar Breslow thicknesses (Gershenwald, Scolyer et al. 2017).

It has been speculated that the observed increased incidence of melanomas *in situ* could partially be due to improved registration and diagnosing melanomas at an earlier stage (Helvind, Holmich et al. 2015). Regarding the epidemiology of melanomas *in situ*, the registries are not as complete as for invasive melanoma (Higgins, Lee et al. 2015). However, it seems that there is a true increase in the incidence of LM and LMM, which poses a challenge for treatment, as LM/LMM is often located in the head and neck area, where preserving the function and cosmetic appearance is essential.

The median age for developing LM/LMM has increased from >60 years to >70 years, when comparing data before and after the year 2000 (Greveling, Wakkee et al. 2016, Mirzoyev, Knudson et al. 2014). Younger patients (mean age 68 years) tend to have smaller (diameter <10mm) and solitary LM lesions compared to older patients (mean age 71 years) who typically have larger (diameter >10mm) LM lesions with multiple surrounding freckles (Tiodorovic-Zivkovic, Argenziano et al. 2015).

*BRAF* mutations are less common than *KIT* and *NRAS* mutations in melanomas of chronically sun-exposed skin. It is also likely that there are common mutations yet to be discovered (Whiteman, Pavan et al. 2011, DeWane, Kelsey et al. 2019). Interestingly, melanomas with *KIT* mutations typically have ill-defined borders, akin to LM/LMM, mucosal and acral lentiginous melanomas (Whiteman, Pavan et al. 2011).

Melanoma *in situ* patients are under increased risk of developing a recurrence, a new primary malignant melanoma, which is likely to occur in the same anatomic location as the preceding one, and other malignancies (Higgins, Lee et al. 2015, Youlden, Youl et al. 2014). The 5-year life expectancy is the same for melanoma *in situ* patients as it is for the general population (Higgins, Lee et al. 2015).

There is evidence for the screening and prevention of all subtypes of melanoma, especially in high-risk groups, although with higher costs in the case of melanoma *in situ* (Higgins, Lee et al. 2015, Brunssen, Waldmann et al. 2017, Whiteman, Bray et al. 2008). The good-quality evidence on sunscreen's preventative effect on melanoma is sparse, but there is some evidence that regular sunscreen use could have a decreasing effect on MM incidence. However, the evidence for melanoma *in situ* is indeterminate (Higgins, Lee et al. 2015). A systematic review and meta-analysis concluded that the use of sunscreen is not a risk factor for skin cancer

(MM or KCs), but that in the general population the protective effect cannot be confirmed (Silva, Tavares et al. 2018).

#### 2.1.4.3 Risk factors for melanoma, lentigo maligna and lentigo maligna melanoma

There are several genetic and environmental risk factors for melanoma, which are presented in Table 9.

**Table 9.** Risk factors for melanoma, information acquired and modified from (Nikolaou, Stratigos 2014).

| Genotype | Phenotype | Risks in environment | Protective factors in environment |
|---|---|---|---|
| Hereditary mutation in *CDKN2A*, *CDK4* or *BAP1* (familial melanoma) | Fair complexion, light hair and eye colour | UVR (solar, therapeutic, tanning beds) | Smoking/nicotine (anti-inflammatory) |
| Hereditary polymorphism/mutation in genes associating with pigment phenotype (*MC1R, ASIP, TYR*) | Sensitivity to UVR and poor ability to tan (especially skin types I-II) | Painful sunburns | Use of NSAIDs?? |
| Hereditary polymorphism/mutation in genes associating with nevi proliferation (PLA2G6, MTAP, IRF4) | Freckling | HIV/AIDS | |
| Hereditary polymorphism/mutation in genes associating with DNA repair pathways and apoptosis (*TERT/CLPTM1L, TIPARP* (formerly *PARP-1*), *ATM*, *CASP8*) | Multiple nevi (melanoma of trunk and extremities) | Use of TNFα | |
| Hereditary polymorphism/mutations in genes associating with gene's transcription activity (*MITF**) | Dysplastic/ atypical nevi (correlation of number and risk level) | Immunosuppression related to organ transplantation | |
| | Family history of melanoma | Recent stressful life event??? | |
| | Personal history of KC | Insecticides??? | |
| | Personal history of childhood cancer | Heavy metals??? | |
| | Lymphoproliferative disease | | |
| | Parkinson's disease** | | |
| | Heavy birth weight? | | |

* MITF, which is also associated with nevus count, non-blue eyes and renal cancer

** Additionally melanoma patients have an increased risk for Parkinson's disease

? Result of one study, and the design should be repeated

?? Evidence contradictory

??? Observational design

There is discussion that melanomas should not be regarded as a single entity, as all subtypes do not share exactly the same risk factors, and differences in aetiology could have an impact on prognosis (Whiteman, Pavan et al. 2011). Risk factors for

LM/LMM compared to SSM, the most common subtype, are presented in Table 10.

**Table 10.** Comparing risk factors for LMM and SSM, information acquired and modified from (Kvaskoff, Siskind et al. 2012).

| LMM | SSM |
|---|---|
| Presence of solar lentigines | Number of nevi |
| Personal history skin cancer | Multiple lifetime sunburns |
| Fair complexion | Fair complexion |
| Freckling | Freckling |
| Sensitivity to UVR | Sensitivity to UVR |
| Number of AK | Number of AK |

In a study from France, where risk factors of LM were compared to other melanomas including superficial, nodular, acral lentiginous and unclassified, sunburns were also associated with LM (Gaudy-Marqueste, Madjlessi et al. 2009). Kvaskoff et al. (information in Table 9) performed their study in Australia with higher ambient UVR doses, as did Gaudy-Marqueste et al. in France. The French compared the LM with all other subtypes, while the Australians only with SSM, which can influence the results.

The relationship of UVR and melanoma is complex. The epidemiological evidence of the causal role of UVR in melanoma is strong, as melanoma is more common in populations living in lower latitudes closer to the equator, in fair-skinned populations that have migrated to low latitudes, and in fair skin phototypes when compared to dark ones (Nikolaou, Stratigos 2014). The role of UVR in melanoma is particularly complex when looking at melanomas among indoor and outdoor workers, and the anatomic distribution of the melanoma. Chronic sun-exposure is associated with head and neck melanoma only in low-latitude populations, but melanoma on the trunk is associated with intermittent exposure to sunburns in all latitudes. Additionally, there are differences in the anatomical distribution of different subtypes (Nikolaou, Stratigos 2014).

There is much discussion on the role of UVR as an aetiological factor, and it seems that it is not clearly understood (Nikolaou, Stratigos 2014). In molecular and genetic studies, it seems that the role of UVR varies for different subtypes (Whiteman, Pavan et al. 2011, DeWane, Kelsey et al. 2019). The fact is that melanoma cannot be regarded as a single entity in the future (Nikolaou, Stratigos 2014, Whiteman, Pavan et al. 2011, DeWane, Kelsey et al. 2019).

In addition to LMM, the desmoplastic subtype seems to associate strongly with chronic sun-exposure, and interestingly LMM and a desmoplastic subtype occur together quite often (DeWane, Kelsey et al. 2019).

#### 2.1.4.4 Tumour cell origin and pathophysiology of melanoma, lentigo maligna and lentigo maligna melanoma

Melanoma originates from melanocytes, but the precursors of melanocytes and their developmental origin could influence the cancerous potential of the melanocytes (Whiteman, Pavan et al. 2011). Melanocytes derive from the neural crest and migrate to the outermost layer of the fetus, the epidermal layer. Later in life, melanocytes can differentiate from multipotent precursor cells, which are preserved along nerve projections. In melanoma, the inhibiting pathways of these precursor cells are altered (Whiteman, Pavan et al. 2011). The variety of other cell types in the neural crest along the cranio-caudal axis can also affect the precursors via epigenetic factors. Thus, the origin of melanocytes is not uniform throughout the body (Whiteman, Pavan et al. 2011).

The potential of melanocytes to develop into a melanoma also depends on the interactions and gene expression of the surrounding cells: keratinocytes, Langerhans cells and fibroblasts (Whiteman, Pavan et al. 2011). The density of melanocytes also varies throughout the body. This is probably related to melanocyte dispersal due to the varying growth periods of different body parts during childhood (Whiteman, Pavan et al. 2011). In an embryo there is a similar amount of melanocytes migrated to the different parts of the embryo, but during childhood the density of melanocytes changes with growing body parts. The morphology and functional properties of the melanocytes varies in different anatomical sites, and they also vary even between skin structures like hair follicles, the interfollicular epidermis, sebaceous glands and the dermis (Whiteman, Pavan et al. 2011). These morphological and functional differences can have an effect on the amount of pigment formed, on the amount of melanocytes and on nevus formation (Whiteman, Pavan et al. 2011).

About 70% of melanomas arise *de novo* (Pampena, Kyrgidis et al. 2017). Family history is a well-known risk factor for melanoma, and part of this can be attributed to genetics, especially with regard to high penetration mutations. However, some of the risk can also be due to common life habits (Olsen, Carroll et al. 2010), as approximately only 7% of melanomas arise due to genetic familial risk (Olsen, Carroll et al. 2010).

High penetration gene mutations that incur a risk to develop melanoma are involved in cell cycle control, melanocyte senescence, melanocyte differentiation, DNA repair, and telomerase maintenance (Aoude, Wadt et al. 2015, Cust, Mishra et al. 2018). Many high penetration gene mutations also increase the risk to other cancers (Aoude, Wadt et al. 2015). Low to medium penetration gene mutations and variants that incur a risk to develop melanoma are involved in pigment phenotypes, melanocyte differentiation, melanocyte development and cell cycle control (Cust, Mishra et al. 2018, Aoude, Wadt et al. 2015). Environmental factors can lead to the development of driver mutations, especially in individuals carrying risk mutations or variants for melanoma (Cust, Mishra et al. 2018).

The main, currently recognised signalling pathways involved in melanoma development are the mitogen-activated protein kinase (MAPK), cell cycle, DNA damage response and cell death, PI3K/Akt and telomerase pathways (Cancer Genome Atlas Network 2015). Epigenetic factors are also recognised as being involved (Cancer Genome Atlas Network 2015). In molecular melanoma classes, *BRAF*, *NRAS* and *NF1* mutations affect the MAPK pathway, either upstream or downstream (Cancer Genome Atlas Network 2015). Activated MAPK pathway leads to mitogenic activity, and thus affects cell survival and proliferation (Romano, Schwartz et al. 2011). In triple-wild-type melanoma, *KIT* mutations are currently the most common recognised mutation (Cancer Genome Atlas Network 2015). KIT is a type III transmembrane receptor tyrosine kinase which is activated by stem cell factors, and when activated, affects the MAPK (cell proliferation), PI3K/Akt (cell proliferation) and JAK-STAT (transcription signal transducer and activator) pathways (Cancer Genome Atlas Network 2015, Romano, Schwartz et al. 2011). Certain driver mutations are associated with typical histopathology, such as the association of *BRAF* with SSM (Kraft, Granter 2014). For LMM, no such associations have been found yet. It is likely that there are still many major oncogenes to discover (Kraft, Granter 2014, Whiteman, Pavan et al. 2011, Cust, Mishra et al. 2018).

In sporadic melanoma, 80% of mutations in genes encoding proteins of the MAPK signalling pathway are *BRAF* or *NRAS* mutations, and interestingly these mutations also associate with nevi (Kraft, Granter 2014). In melanomas of chronically sun-exposed skin, some LMMs carry mutations in *KIT* (25–28%), and some desmoplastic melanomas in *NF1* (up to 93%) (Kraft, Granter 2014). Interestingly, melanomas with *KIT*-mutations typically have ill-defined borders akin to LM/LMM, mucosal and acral lentiginous melanomas (Whiteman, Pavan et al. 2011). In UV-damaged skin, alterations in genes for the serine phosphatase PPP6C,

and for the Ras-related Rho family GTPase RAC1, could be the driver mutations (Kraft, Granter 2014). In melanomas of chronically sun-exposed skin there is often a UVR signature in the alterations (Kraft, Granter 2014, DeWane, Kelsey et al. 2019).

Histopathologically, there are two phases in melanoma development: the radial and vertical growth phase (Kraft, Granter 2014). In the radial phase, the tumour is limited to the epidermis as *in situ* melanoma or to the superficial dermis without mitotic activity. In the vertical phase, the tumour invades deeper structures, or there is mitotic activity in the invasive component (Kraft, Granter 2014). In the case of LMM, the timeline between the *in situ* and invasive form can be long, even years, thus allowing a possibility for early diagnosis in the radial phase, which is crucial to the prognosis, treatment and follow-up.

## 2.2 Sectioning of the tissue specimens and tumour margin assessment

The traditional histopathological technique to examine samples is called "bread-loafing", i.e. serial sectioning. Only about 1% of the slice margins are examined with this method (Boehringer, Adam et al. 2015, Trakatelli, Morton et al. 2014). Usually the sections are cut into 1–5 mm in length (Boehringer, Adam et al. 2015), and the slices are a few micrometers in thickness.

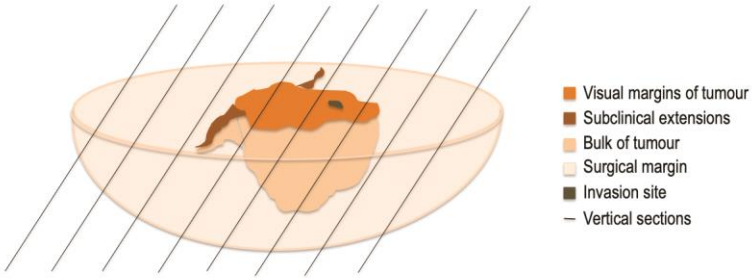


**Figure 5.** Serial sectioning of the elliptical excision specimen and the possible error in the method, where subclinical extensions or invasive parts might exist between the vertical sections and thus are not examined.

In 21.9% of BCC specimens, a positive surgical margin was found when the tissue processing was performed with serial sections, whereas a three-dimensional microscopy method resembling MMS with 100% margin control found a positive margin in 42.6% of BCC specimens (Boehringer, Adam et al. 2015). Thus, with a method of 100% margin control, subclinical extensions i.e. tumour extensions not visible to the human eye in clinical examination, are discovered twice as often when compared to traditional serial sectioning, and this applies especially for aggressive BCCs (Boehringer, Adam et al. 2015).

The existence of subclinical extensions is also nicely emphasised by the relation of the surgical margin and the recurrence rate of BCC. For example, with a 2-mm surgical margin the risk for recurrence is 10 times as high when compared to a 5-mm surgical margin (Gulleth, Goldberg et al. 2010).

The probability of detecting positive surgical margins in melanoma *in situ* with serial sectioning of 1, 2, 4 or 10 mm intervals was correspondingly 58, 37, 19 or 7 % (Kimyai-Asadi, Katz et al. 2007). To gain a 100 % margin control in melanoma *in situ*, the serial section would need to be cut with 0.1 mm intervals (Kimyai-Asadi, Katz et al. 2007).

## 2.3 Non-invasive optical imaging

Non-invasive imaging technologies can reduce the burden of care for the patient and ease the treatment process of skin neoplasms and inflammatory skin diseases (Tkaczyk 2017). These techniques are based on the optical features of biological tissue. Developing these non-invasive optical imaging methods requires the collaboration of both engineers and clinicians (Tkaczyk 2017).

In optical imaging, the escape of illuminated light from tissue is used for diagnostic purposes, in contrast to the therapeutic use of light, where the emitted light is absorbed into the tissue and the absorption energy plays a major role in the desired therapeutic effect (Jacques 2013). Biological tissue has optical scattering, refractive, absorption and anisotropic properties, and these properties are due to tissue chromophores. Coefficients and indices can be calculated for these optical parameters, which can then be used in optical imaging (Jacques 2013). The main chromophores in biological tissue are melanin, blood (hemoglobin), water, fat and yellow pigments (bilirubin and beta-carotene) (Jacques 2013). The proportions of the chromophores affect the average optical parameters of the tissue, such as the average scattering coefficient (Jacques 2013). The average optical tissue parameters can also vary depending on the wavelength of the imaging device (Jacques 2013). It should also be noted that in *in vivo* imaging, the tissue parameters vary between subjects, anatomical sites, the time of imaging, and all these even within the same individual (Jacques 2013).

The most widely used technologies in optical imaging are dermoscopy, optical coherence tomography (OCT) and reflectance confocal microscopy (RCM). Out of these methods, RCM can replace the biopsy procedure in the diagnosis of skin lesions in certain situations (Tkaczyk 2017). Optical diagnosis can remarkably reduce biopsies of benign lesions (Tkaczyk 2017). Non-invasive imaging methods can also make a difference in distinguishing LM and LMM from each other.

According to a recent review, there are currently eleven different optical technologies for dermatological optical imaging (Tkaczyk 2017). The research in the field is active. From the optical non-invasive techniques, dermoscopy is the only one which is familiar to most dermatologists (Tkaczyk 2017). RCM is familiar to few dermatologists at the moment, but could be used by all dermatologists who are able to invest in the training (Tkaczyk 2017). At the moment OCT is familiar for few academic dermatologists (Tkaczyk 2017). All optical imaging methods demand training for their interpretation, but RCM may be the method that requires the most extensive training when compared to dermoscopy and OCT. For all three

aforementioned technologies, there are commercial products available (Tkaczyk 2017). Thus in theory, they are available to everyone, although the price of an RCM device is 100-times more expensive than a dermoscope, and OCT even more (Tkaczyk 2017).

Any other optical technology is not yet as easy to apply in practice as dermoscopy, which is a hand-held, pocket-sized device. Thus, dermoscope is like the stethoscope of a dermatologist. RCM and OCT are large devices, which move on wheels, and the optical probe is attached to the machine. RCM and OCT can have a hand-held probe, but the large machine still needs to be attached to it. In dermoscopy, the processing and interpretation of the image is performed while using the device. In RCM and OCT, the images need to be processed with the technology before interpretation. In practice the imaging process is similar for non-invasive imaging devices: an optical probe is attached to the skin, light is emitted, information is detected, the image is processed, and finally the image is interpreted. Figure 6 presents a schematic illustration of the devices.

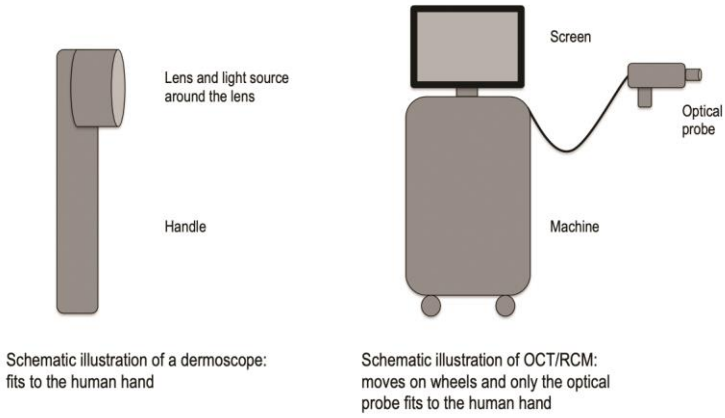


**Figure 6.** Non-invasive imaging devices: dermoscope, OCT/RCM

Hyperspectral imaging is a more novel imaging method, when compared to the dermoscope, RCM and OCT. Hyperspectral imaging is one form of spectral imaging, and as of yet there are no commercial devices available. In the field of spectral imaging, there are two commercial products for triaging pigmented lesions,

i.e. to recognize melanoma from other pigmented lesions. If the device gives reason to suspect melanoma, the diagnosis would be confirmed with a biopsy. These two devices are Melafind and SiaScope, which are multispectral imaging devices (Tkaczyk 2017). The sensitivity is 98.3% for Melafind, but the specificity is only 9.9% (Tkaczyk 2017). For SiaScope, the sensitivity is 80% with a specificity of 76% (Tkaczyk 2017). With these accuracies, the multispectral devices have not gained wide popularity in clinical practice. Multispectral imaging utilises about ten different wavelengths of light for the imaging (Tkaczyk 2017). Our HIS device uses 70 different wavelengths, and thus there is much more data from the different levels of the skin, when compared to multispectral imaging.

Different modalities have differing strengths and limitations. Table 11 presents the advantages and disadvantages of dermoscopy, RCM, OCT and hyperspectral imaging.

**Table 11.** Comparison of features of dermoscopy, RCM, OCT and hyperspectral imaging. Information aquired and modified from (Tkaczyk 2017).

| Modality | Strengths | Limitations | Prospects for future |
|---|---|---|---|
| Dermoscopy | Rapid skin cancer screening<br>Good evidence for improving the sensitivity and specificity of the user | Highly user- and training-dependent<br>Only horizontal images | Mobile apps<br>Possibility to computational analyses |
| RCM | Cellular level images<br>Able to visualise dendrites on melanocytes<br>Highest accuracy | Only horizontal images<br>Time consuming<br>Depth penetration only to the papillary dermis i.e. 0.25 mm in depth | Intraoperative use<br>Combining to fluorescence techniques |
| OCT | Penetration depth to around 1 mm<br>Possibility to image flow with Doppler or speckle variance<br>Provides vertical images | Diagnostic accuracy limited by lateral resolution - though fourier-domain OCT overcomes this, but with limited penetration depth to 0.2 mm | Intraoperative use<br>Possibilities to improve the lateral resolution of the technology |
| Spectral imaging | Mapping of chemical compounds throughout the imaging depth<br>Penetration depth to around 2 mm | Dependent on the used algorithm<br>Only horizontal images | Research needed to study the correlation of spectral properties to different diseases<br>Possibility to development of hand-held cameras and connection to tablets |

### 2.3.1 Dermoscopy in basal cell carcinoma

Dermoscopy has previously been called epiluminescence microscopy. The fundamental technology in dermoscopy is the use of polarised and unpolarised light (Tkaczyk 2017). When the scattering of light from the skin surface is reduced by immersion oils or with polarisation of the light, the morphology of the skin and subsurface components of the epidermis and papillary dermis can be visualised (Que 2016). Dermoscopes have about a 10-time magnification of the image, which is obtained when the user views the light-source illuminated target tissue through a lens. Nowadays, the light source is often light emitting diodes (LEDs).

Dermoscopy is an important aid to the clinical diagnosis by improving the accuracy compared to naked eye, and also enhancing clinical diagnosis on histopathological subtyping and aiding follow-up after non-surgical treatment of sBCC (Trakatelli, Morton et al. 2014, Lallas, Apalla et al. 2014, Lallas, Tzellos et al. 2014, Apalla, Lallas et al. 2014, Reiter, Mimouni et al. 2019) (Table 12).

**Table 12.** Dermoscopic findings in BCC subtypes by architectural pattern. Table information acquired and modified from (Lallas, Apalla et al. 2014) and (Lallas, Tzellos et al. 2014).

| | Indolent growth pattern | | Intermediate step to aggressive growth pattern | Aggressive growth pattern | | |
|---|---|---|---|---|---|---|
| Clinical type | Superficial | Nodular | Morpheaform | | | Other |
| Histopathological type by architecture | Superficial | Nodular (sometimes referred as nodulo-cystic) | Micronodular | Infiltrating | Morpheaform= sclerosing | Basosquamous i.e. Metatypical |
| Mixed histology | Combination of different growth pattern -> should be treated by the most aggressive component | | | | | |
| Dermoscopy findings | Superficial fine telangiectasia<br>Multiple small erosions<br>Shiny white-red structureless areas<br>Maple leaf-like areas<br>Spoke wheel areas<br>Concentric structures<br>Multiple blue-grey dots<br>In-focus dots!<br>Detection of blue-grey ovoid nests excludes the diagnosis of superficial BCC | Arborising vessels<br>Ulceration<br>Short white streaks (seen only with polarized dermoscopy)<br>Blue-grey ovoid nests<br>Multiple blue-grey dots<br>In-focus dots<br>Maple leaf-like areas*<br>Spoke wheel areas*<br>Concentric structures*<br>* typically detected at the peripheral, superficial parts of the lesion | Features of nodular BCC with some dermoscopic findings of aggressive patterns | Arborising vessels (usually finer, more scattered and with fewer branches comparing to the vessels of nodular BCC)<br>Ulceration<br>White-red structureless areas<br>Blue-grey ovoid nests<br>Multiple blue-grey dots<br>In-focus dots | Arborising vessels (usually finer, more scattered and with fewer branches comparing to the vessels of nodular BCC)<br>Ulceration<br>Whitish background<br>Blue-grey ovoid nests<br>Multiple blue-grey dots<br>In-focus dots | Arborising vessels<br>Keratin masses<br>White structureless areas<br>Superficial scale<br>Ulceration/blood crusts<br>Blood spots in keratin masses<br>Blue-grey ovoid nests<br>Multiple blue-grey dots |

### 2.3.2 Reflectance confocal microscopy in basal cell carcinoma

In confocal microscopy, the light source is a near-infrared laser light at 830 nm. The light is refracted to the target tissue through a lens with a dichroid mirror. The light is reflected back from the target tissue and emitted as fluorescence of the target tissue to the detector of the microscope through a pinhole filter. With the pinhole filter the light outside of the desired focal plane is blocked and thus a good lateral resolution is obtained. (Que2016)

RCM provides a cellular level image on the horizontal plane that is comparable to histology. The main limitation of RCM is its limited imaging depth of only 200 μm (Que 2016) and field of view (FOV) of 1x1mm, where mosaicking makes it possible to obtain 14 $mm^2$ per minute (Kose, Cordova et al. 2014). With video-mosaicking the FOV can be enlarged to 240–360 $mm^2$ per minute (Kose, Cordova et al. 2014).

In diagnosis of BCC *in vivo*, a Cochrane review concluded that RCM could be used to avoid diagnostic biopsies in lesions which clinically appear highly suspicious for BCC (Dinnes, Deeks et al. 2018b). The Cochrane review included studies where RCM was compared to traditional clinical diagnosis by visual inspection with or without a dermoscope. Meta-analyses of equivocal lesions pooled data from three studies, and found a 94% sensitivity and 95% specificity in detecting BCC for RCM, compared to 85% sensitivity and 92% specificity for dermoscopy (Dinnes, Deeks et al. 2018b). In meta-analyses of any suspicious lesion, data was pooled from four studies, and found a 76% sensitivity and 95% specificity in detecting BCC for RCM (Dinnes, Deeks et al. 2018b). In equivocal lesions, RCM was more sensitive but less specific than clinical diagnosis. In equivocal lesions, utilising RCM could risk the misdiagnosis of melanoma as BCC (Dinnes, Deeks et al. 2018b).

RCM seems to be useful and have good correlation with histopathology in the subtyping of BCC *in vivo* and *ex vivo*. The accuracy of the subtyping could be improved by combining RCM pre- and intraoperatively (Villarreal-Martinez, Bennassar et al. 2018). *In vivo* subtyping of BCC with RCM has a lower specificity than punch biopsy (38% *vs* 79%) (Kadouch, Leeflang et al. 2017).

In intraoperative *ex vivo* diagnosis of BCC between the MMS stages, RCM has an overall sensitivity of 88–99% and a specificity of 89–99% in the detection of BCC (Que 2016). In *ex vivo* RCM, dyeing with acridine orange improves the

accuracy. Furthermore, this dye does not disturb hematoxylin and eosin staining later on (Que 2016). The advantages of *ex vivo* diagnosis with RCM include saved time (RCM 5–7 min vs. frozen sections 20–45 min) and thus increased surgical efficiency compared to traditional frozen sections in MMS (Que 2016).

RCM seems to be useful in the non-invasive follow-up after cryosurgery (Ahlgrimm-Siess, Horn et al. 2009), PDT (Venturini, Sala et al. 2013) and after or during vismodegib treatment (Couzan, Cinotti et al. 2018). In assessing methylaminolevulinate (MAL) -PDT outcome at three months, RCM recognised 5/20 residual lesions compared to 2/20 by visual inspection and 3/20 by dermoscopy, where 1/3 were shown to be false positives by RCM (Venturini, Sala et al. 2013).

### 2.3.3 Optical coherence tomography in basal cell carcinoma

Conventional OCT provides vertical images and has an analogue with ultrasound, but instead of sound, a 1310 nm light wave is used. In OCT, the emitted light from the light source is divided in two with a beam splitter, where one is heading to the target tissue, and the other to a mirror. When the target tissue reflects the light back, only those bands which are coherent with the light reflecting back from the mirror are recorded with the detector. (Que 2016)

With OCT, a better resolution is gained when compared to ultrasound (Que 2016). The resolution of conventional OCT does not correlate with histology, but its imaging depth is up to 1.5 mm. In high-definition OCT, a resolution comparable to histology is possible to achieve, although at the cost of imaging depth: high-definition OCT reaches up to 570 μm in depth (Que 2016). In newer OCT devices, the properties of conventional and high-definition OCT are combined, and these devices are called frequency or Fourier-domain OCT (Reddy, Nguyen 2019). The frequency or Fourier-domain OCT also provides a horizontal plane in addition to the vertical image, which can offer more diagnostic information (von Braunmuhl, Hartmann et al. 2016). Dynamic OCT imaging also makes it possible to obtain en face images, especially of the vasculature of BCC, and this can help in the non-invasive subtyping of BCC (Themstrup, De Carvalho et al. 2018). It is also possible to discriminate the subtype of BCC with moderate accuracy from vertical slices of OCT (Holmes, von Braunmuhl et al. 2018). 3D visualisation is also possible with mathematical modeling in OCT with an image area sized 6x6x2mm (Verne, Magno et al. 2018).

In the diagnosis of BCC *in vivo*, a Cochrane review concluded that OCT could have a diagnostic role in clinically challenging lesions, but larger, more qualified and prospective trials are required. Additionally, the different imaging methods should be compared head-to-head (Ferrante di Ruffano, Dinnes et al. 2018). The meta-analysis of the Cochrane review included two studies where OCT was compared to clinical evaluation by visual inspection with or without dermoscopy. In meta-analyses the pooled sensitivity was 95% and specificity was 77% for conventional OCT compared to visual inspection alone, with sensitivity of 80% and specificity of 37%. The sensitivity rose to 86% and the specificity to 55% when visual inspection was aided with a dermoscope (Ferrante di Ruffano, Dinnes et al. 2018). In another systematic review on the *in vivo* performance of OCT in the diagnosis of BCC, conventional OCT had a sensitivity of 77.3% and a specificity of 57.5% compared to Fourier-domain OCT, which had a sensitivity of 93.7% and a specificity of 61.4% (Reddy, Nguyen 2019).

Intraoperatively, in MMS conventional OCT does not perform well in *ex vivo* diagnosis, with a sensitivity of only 19% and a specificity of 56% (Que 2016). With newer frequency/Fourier-domain OCT, the performance in *ex vivo* diagnosis of BCC on MMS slices improves, reaching a 81.2% sensitivity and a 94.3% specificity (Rashed, Shah et al. 2017).

OCT seems to be useful in the follow-up of non-invasively treated BCCs. In MAL-PDT-treated BCCs, OCT revealed a residual lesion in 7/18 cases, when residual lesions were clinically suspected in 5/18 cases three months after treatment (Themstrup, Banzhaf et al. 2014).

### 2.3.4 Impact of non-invasive technologies on delineation of basal cell carcinoma

Subclinical extensions in BCC can be a clinical problem, as 32–39% conventional excisions are re-excised (Cakir, Adamson et al. 2012), and in MMS, the subclinical extension can lead to additional stages (Que 2016).

In the preoperative delineation of aggressive BCCs, dermoscopy has not reduced the stages of MMS (Que 2016). In MMS, the preoperative delineation of BCC by RCM reveals a subclinical extension outside of the dermoscopic margin in 3/10 BCCs (Venturini, Gualdi et al. 2016). OCT delineates the margin as 1.4 +/- 1.3 mm smaller than by clinical assessment in cases where one MMS stage was needed. In 100% of cases where more than one stage was needed, OCT recognised

the subclinical extension (Wang, Meekings et al. 2013). In another study, where OCT-delineated margins were compared to the margins assessed by the MMS surgeon, OCT recognised the subclinical extension in all cases where more than one MMS stage was required. However, there were 2/13 false positive cases by OCT (Tankam, Soh et al. 2019).

In the assessment of the margin depth in combined RCM and OCT, a good correlation was found compared to the depth measurements in histopathology when dividing the lesions to shallow (depth<500 μm) and deep (depth>500 μm) (Sahu, Yelamos et al. 2018). In the evaluation of the depth in BCC, high-frequency ultrasound had a moderate correlation with histopathology, but low correlation with the width of the diameter (Nassiri-Kashani, Sadr et al. 2013). MMS stages were not reduced compared to the clinical evaluation when preoperatively assessing tumour margins with high-frequency ultrasound (Marmur, Berkowitz et al. 2010).

### 2.3.5 Wood's light in lentigo maligna and lentigo maligna melanoma

The Wood lamp uses light with relatively short wavelengths from 320 to 400 nm. With these wavelengths, mainly dermal collagen and porphyrins absorb the energy and emit fluorescence, which can be detected. The Wood lamp is an old diagnostic tool used in several indications like pigmented lesions, porphyrias, bacterial infections and fungal infections. (Ponka and Badder 2012)

Dermoscopy outperforms the Wood lamp in the delineation of LM (Robinson 2004), as does hyperspectral imaging (Neittaanmaki-Perttu, Gronroos et al. 2015).

### 2.3.6 Dermoscopy in lentigo maligna and lentigo maligna melanoma

In the diagnosis of skin cancers, especially of pigmented lesions, dermoscopy improves the sensitivity and decreases the number of biopsies of benign lesions (Yelamos, Braun et al. 2019). In a Cochrane review and meta-analysis on the accuracy of dermoscopy in the diagnosis of MM in adults, the in-person sensitivity was 16 % better for dermoscopy with visual inspection versus visual inspection alone, and specificity was 20% better in a corresponding comparison (Dinnes, Deeks et al. 2018a). There are well-known features typical for melanoma in the dermoscopic criteria, and certain features associate with chronically sun-exposed skin, typically in the head and neck area (Jaimes, Marghoob 2013). These criteria for sun-exposed skin are typical for LM/LMM, and dermoscopy is particularly

useful in distinguishing LM/LMM from other macular lesions (Jaimes, Marghoob 2013, Tschandl, Kittler et al. 2015) (Table 13). Extrafacial LM/LMM can differ from LM/LMM with a facial location, but they do share some common features (Gamo-Villegas, Pampin-Franco et al. 2019). In extrafacial LM, the most common features are erased areas, blue-grey regression and geometrical structures (Gamo-Villegas, Pampin-Franco et al. 2019)

**Table 13.** Dermoscopic criteria in the distinction of facial solar lentigo/ thin seborrheic keratoses versus LM/LMM, information acquired and modified from (Lallas, Argenziano et al. 2014).

| Solar lentigo/thin seborrheic keratoses | LM/LMM |
|---|---|
| Light brown fingerprint areas | Asymmetric pigmented follicular opening |
| Yellow opaque areas | Dark rhomboidal structures |
| Milia-like cysts | Slate-grey globules |
| Moth-eaten border | Slate-grey dots |
| Sharp demarcation | |
| Elongated brown circles | |

When all criteria from Table 13 for LM/LMM on the face are present, the sensitivity is 89% and specificity 96% in predicting the lesion to be LM/LMM (Lallas, Argenziano et al. 2014). In flat, pigmented facial lesions, a pattern of circles heightens the suspicion for LM/LMM. Furthermore, any grey color, regardless of the pattern, is suspicious for a malignancy (Tschandl, Kittler et al. 2015). Certain dermoscopic criteria associate with a facial location. For example, asymmetrical pigmented follicular openings are more common on the nose and lower part of the face, and rhomboidal structures are more common on the upper part of the face than in other locations. Grey colouration is associated with all parts of the face (Tiodorovic-Zivkovic, Argenziano et al. 2015). In dermoscopy, a target-like pattern and a circle within a circle are more commonly seen in males than in females (Tiodorovic-Zivkovic, Argenziano et al. 2015).

The deeper the dark brown, grey or blue colors, and the more structureless areas between follicles are present with scar-like and milky-red areas, the more probable it is that LM has progressed into LMM (Lallas, Argenziano et al. 2014). However, there are no dermoscopic criteria for a reliable distinction. Dermoscopy does offer a valuable tool for choosing a representative biopsy site for a histopathological LM/LMM diagnosis (Mataca, Migaldi et al. 2018).

### 2.3.7 Reflectance confocal microscopy in melanoma, lentigo maligna and lentigo maligna melanoma

A Cochrane review found that if a Pellicani's RCM was used in the diagnosis of MM, the pooled sensitivity was 92% and specificity 72% (Dinnes, Deeks et al. 2018c). In the recognition of MM in any suspicious lesion, if sensitivity would assumed to be fixed at 90%, the specificity would be 82% for RCM compared to the 42% of dermoscopy, and in the recognition of MM in equivocal lesions sensitivity and specificity would be 86% and 49% correspondingly (Dinnes, Deeks et al. 2018c). However, in a head-to-head trial comparing RCM and dermoscopy in the diagnosis of LM/LMM, RCM had a sensitivity of 80% and a specificity of 81% compared to dermoscopy, which had a 61% sensitivity and a 92% specificity (Cinotti, Labeille et al. 2018). RCM is especially useful in the diagnosis of hypomelanotic and recurrent LM/LMM (Cinotti, Labeille et al. 2018). The clinical indication for using RCM in the recognition of melanoma is a lesion on chronically sun-damaged skin in the head and neck area, which shows regression in dermoscopy (Borsari, Pampena et al. 2016). RCM should be considered as an add-on examination to dermoscopy in the diagnosis of MM, thus improving the accuracy in the diagnosis of MM (Edwards, Osei-Assibey et al. 2017). RCM is especially useful in the differential diagnosis of flat and pigmented macules on the face (Farnetani, Manfredini et al. 2019). There are also some RCM features, which could help distinguish desmoplastic MM, the other melanoma type of chronically sun-exposed skin, from melanoma *in situ* (Maher, Solinas et al. 2017).

In the *in vivo* delineation of LM/LMM, RCM recognised a positive margin in 55/60 cases compared to 21/60 cases for dermoscopy, and the dermoscopic dimensions of the lesion were 60% smaller than those defined by RCM (Edwards, Osei-Assibey et al. 2017). The dimensions defined by video-mosaic-RCM correlated well with the surgical defect of LM/LMM (Farnetani, Manfredini et al. 2019). When comparing dermoscopically assisted clinical margin assessment of LM/LMM to hand-held RCM technology, the accuracy of clinical assessment was 26%, and 91% for hand-held RCM, when the true margins were confirmed in histopathology (Farnetani, Manfredini et al. 2019).

In *ex vivo* use, RCM seems to have good correlation with histopathology in measuring the thickness of MM when the larger area is first scanned, and measurements performed thereafter (Hartmann, Krammer et al. 2016).

Both dermoscopy and RCM can guide the clinician in obtaining a representative, presurgical biopsy of LM/LMM to confirm the diagnosis, and help

in planning the surgery. However, RCM has better sensitivity for more robust histopathological criteria for the diagnosis (Mataca, Migaldi et al. 2018).

RCM could also be useful in the follow-up of non-surgical treatment of LM. After treating LM with imiquimod, RCM recognised 70% of the responders, with no false negative cases compared to histopathological clearance (Alarcon, Carrera et al. 2014).

### 2.3.8 Optical coherence tomography in melanoma, lentigo maligna and lentigo maligna melanoma

A Cochrane review concluded that the data is too limited to make pooled analyses and conclusions on the performance of OCT in detecting MM (Ruffano 2018). A descriptive review on OCT in melanoma concluded that the performance of newer OCT devices is better than conventional OCT, and that OCT seems to be useful in the visualisation of MM (Rajabi-Estarabadi 2019). For high-definition OCT, a sensitivity of 74.1% and a specificity of 92.4% was reported (Rajabi-Estarabadi 2019). In another systematic review for high-definition OCT, the pooled sensitivity was 81% and specificity 93.8%, although only two studies were included in the meta-analysis. Thus, some melanomas can be missed with OCT (Yi-Quan 2018). Interestingly, in a small study OCT showed potential in separating invasive melanomas from *in situ* ones and from benign nevi, when only pigmented lesions were compared to each other (Moares Pinto Blumetti 2015).

In *ex vivo* use, the performance of frequency-domain OCT was lower for melanocytic lesions compared to KCs (Jerjes, Hamdoon et al. 2019). In detecting LM *ex vivo* with frequency-domain OCT, the sensitivity was 55% and specificity 89.5%, and correspondingly for MM 43.8% and 76.2% (Jerjes, Hamdoon et al. 2019). The diagnostic accuracy of OCT for BCC is good, but in detecting melanoma the performance of OCT is insufficient. Thus OCT should be used with caution especially in pink, equivocal amelanotic or hypomelanotic lesions (Maher, Blumetti et al. 2017).

In assessing the thickness of melanocytic skin lesions, conventional OCT had a stronger correlation with histopathology than high-frequency ultrasound, although both techniques seemed to overestimate the depth (Hinz, Ehler et al. 2011).

### 2.3.9 Hyperspectral imaging in melanoma, lentigo maligna and lentigo maligna melanoma

Hyperspectral imaging is a form of spectral imaging and is based on the wide range of electromagnetic radiation. In hyperspectral imaging, wavelengths from UVR from visible light to near infrared can be used. In hyperspectral imaging, the light is emitted, and the diffuse reflectance spectra is recorded. The diffuse reflectance spectra include the back-reflected light, as well as fluorescent and scattered light from the light source when it has interfered with the target tissue. The composition of tissue chromophores varies in different tissues, and between the healthy and diseased tissues. Thus, the diffuse reflectance spectra also differ similarly. For example, haemoglobin is a main tissue chromophore, and in neoplastic tissue, angiogenesis and hypermetabolism are hallmarks of a cancer, and thus the composition of oxygenated, and deoxygenated haemoglobin differs between healthy and neoplastic tissue. Thus, hyperspectral imaging makes it possible to non-invasively obtain information about the tissue composition. There is a third dimension in hyperspectral imaging which contains the information from the diffuse reflectance spectra when compared to ordinary two-dimensional photographs obtained with visible light. Thus, hyperspectral imaging combines the spatial information of ordinary photography with spectroscopy. (Lu and Fei 2014)

The procedure of imaging is similar to the aforementioned non-invasive optical imaging techniques.

Nagaoka et al. introduced a discrimination index to distinguish melanoma from other pigmented skin lesions based on hyperspectral imaging (Nagaoka, Kiyohara et al. 2015). Their method achieved a 96% sensitivity and a 87% specificity in detecting melanoma (Nagaoka, Kiyohara et al. 2015).

In assessing the margins of LM/LMM, Neittaanmäki-Perttu et al. have shown that hyperspectrally defined borders corresponded to the histopathology in 94.7% of cases, and the hyperspectral imaging system (HIS) delineated the lesions more accurately in 52.6% of the cases compared to the clinical evaluation utilising a Wood's light (Neittaanmaki-Perttu, Gronroos et al. 2015).

Hyperspectral imaging has also been studied on pathological slices to enhance the diagnostics in histopathology (Gaudi, Meyer et al. 2014, Dicker, Lerner et al. 2006).

In one study by Dicker et al., hyperspectral imaging was studied in the follow-up of RAF inhibitor treatment, and it seemed that the hyperspectral graph from a

biopsy of proven melanomas differed before and after the RAF inhibitor treatment (Dicker, Kahn et al. 2011).

### 2.3.10 Comparison of non-invasive technologies in recognizing cutaneous malignant melanoma

There are few head-to-head trials that test different technologies for their ability to recognize MM. Most comparisons are made to dermoscopy and not to another new technology. In one cross-sectional study, the performance of a multispectral device (Melafind®) was compared to RCM (VivaScope 1500®) in detecting melanoma, and RCM outperformed multispectral imaging with a sensitivity of 85.7% *vs* 71.4% and a specificity of 66.7% *vs* 25% (Song, Grant-Kels et al. 2016).

The different technologies can also be divided into subgroups based on where they can be applied (Fink, Haenssle 2017). There are technologies for large-scale screening purposes (dermoscopy); for the assessment of a few preselected lesions, where some of the devices guide the user (multispectral imaging, electrical impedance spectroscopy, Raman spectroscopy); for the assessment of preselected lesions in specialised clinics with devices requiring expertise (RCM, multiphoton tomography) (Fink, Haenssle 2017). In addition to optical devices, there is a device called Nevisense®, which utilises electrical impedance to detect melanoma (Fink, Haenssle 2017). Table 14 compiles different technologies for detecting melanoma, but it should be noted that the information is gathered from different studies, and thus populations and study criteria vary. Table 14 should thus be considered as only indicative.

**Table 14.** Detecting MM with different non-invasive technologies.

| Non-invasive technologies for detecting melanoma | Device | Image area | Depth | Sensitivity** | Specificity ** | PPV ** | NPV** | Image | References |
|---|---|---|---|---|---|---|---|---|---|
| Epiluminescence microscopy | **Dermoscopy (multiple devices)** | - | - | 69.5-80 | 55.9 | 51.3 | - | Yes | (Hauschild, Chen et al. 2014, Wells, Gutkowicz-Krusin et al. 2012, Friedman, Gutkowicz-Krusin et al. 2008, Ahnlide, Bjellerup 2013) |
| RCM | **Vivascope 3000 Vivascope 1500 Vivascope 1000** | 1x1mm* or 0.5x0.5 mm* | 250-300 µm | 97.3-97.5 | 83-99 | 70.6-97.5 | 98.6-99 | Yes | (Kang, Bahadoran et al. 2010, Guitera, Pellacani et al. 2010, Langley, Walsh et al. 2007, Kose, Cordova et al. 2014) |
| High definition OCT | **Skintell®** | 1.8x1.5 mm | 570 µm | 74.1 | 92.4 | 80 | 89.7 | Yes | (Gambichler, Schmid-Wendtner et al. 2015) |
| Electrical impedance spectrometer | **SCIbase III** | d 5 mm | - | 99.4 | 24.5 | 31*** | 99.1*** | No | (Mohr, Birgersson et al. 2013) |
| Raman spectroscopy | **Raman Sp.** | d 3.5 mm | - | 90-99 | 15-68 | 15-30 | 98-99 | Yes | (Lui, Zhao et al. 2012) |
| Multispectral imaging | **SIAscope®** | 12/24 mm | 2 mm | 82.7-100 | 59-80.1 | - | - | Yes | (Moncrieff, Cotton et al. 2002, Glud, Gniadecki et al. 2009, Sgouros, Lallas et al. 2014) |
| Multispectral imaging | **MelaFind®** | 20x20 mm | 2.5 mm | 96-98.4 | 8-44 | 48.3*** | 75*** | No | (Hauschild, Chen et al. 2014, Wells, Gutkowicz-Krusin et al. 2012, Friedman, Gutkowicz-Krusin et al. 2008, Monheit, Cognetta et al. 2011) |
| Hyperspectral imaging system | **HIS (Mitaka, Japan)** | d 40 mm/ 16x20mm | - | 90-100 | 84-94.4 | - | - | Yes | (Nagaoka, Nakamura et al. 2012, Nagaoka, Nakamura et al. 2013, Nagaoka, Kiyohara et al. 2015) |
| Hyperspectral imaging system | **HIS (VTT, Finland)** | d 40 mm | 2 mm | 90 | 90.5 | 81.8 | 95 | Yes | Study I of this dissertation: Neittaanmäki et al. 2017 |

d = diameter, PPV = positive predictive value, NPV = negative predictive value

* Possible to combine images to form a mosaic image with field of view 8x8 mm

**The values are not directly comparable (the comparison group vary in different studies, including different pigmented skin lesions)

***The direct information was not provided in the references, but it was possible to calculate the values based on the information provided

An interesting option to improve non-invasive imaging technologies is the combination of different technologies. There are studies combining OCT with RCM (Sahu, Yelamos et al. 2018), OCT with Raman spectrometry (Mazurenka, Behrendt et al. 2017), OCT with photoacoustic tomography (Zhou, Chen et al. 2017), and even three technologies to multimodal systems (Varkentin, Mazurenka et al. 2018). It seems that it might be possible to overcome the shortcomings of one technology with another one.

## 2.4 Treatment with surgery

### 2.4.1 Surgery of basal cell carcinoma

Surgery is the treatment of choice for BCC, but in selected low-risk cases the non-surgical treatments could be the choice instead (Trakatelli, Morton et al. 2014). For surgical excision the five-year recurrence rate varies between 2-8% for primaries, but for recurrent lesions the five-year rate varies between 12-17% (Trakatelli, Morton et al. 2014). The location, size and histological type define the width of the surgical margin with the goal of minimising the removal of healthy tissue while not compromising the cure rate (Trakatelli, Morton et al. 2014).

With a 2, 3, 4 and 5 mm surgical margin in excision, negative histological margins were achieved in 82, 85, 85 and 85% of the cases, respectively, but having a different risk for recurrence respectively at 3.96, 2.56, 1.62 and 0.39 %, compared to a 27% rate of risk for recurrence with a positive surgical margin (Gulleth, Goldberg et al. 2010). However, the risk for recurrence is higher than 27% for aggressive types of BCC, and with recurrent lesions the risk for a new recurrence with a positive margin is over 50% (Trakatelli, Morton et al. 2014).

It should be noted that about 33% of recurrences appear during the first year, 50% between two and five years, and up to 18% even later (Trakatelli, Morton et al. 2014). In a study with a 10-year follow-up of aggressive high-risk BCCs treated with excision or MMS, the recurrence occurred in 56% of primaries after 5 years (van Loo, Mosterd et al. 2014).

For recurrent lesions and high-risk tumours, especially in the mid-face, MMS is recommended with 100% margin control and minimal removal of healthy tissue (Trakatelli, Morton et al. 2014). The 3–5 year cure rates for MMS vary between 97-99% for primaries, and between 93-98% for recurrent lesions (Trakatelli, Morton

et al. 2014). In selected cases, MMS could be a cost-effective option compared to traditional excision (Trakatelli, Morton et al. 2014, Mosterd, Krekels et al. 2008, Tolkachjov, Brodland et al. 2017). MMS is recommended for facial recurrent BCCs, and for primary BCCs with a diameter over 1 cm and a location in the H-zone. MMS could be used for SCC with similar indications (Murray, Sivajohanathan et al. 2019a). However, in complex situations like Gorlin syndrome, multiple KCs on the face, immunosuppressed patients and lesions in functionally and cosmetically important locations, MMS could only be used in tumours with a diameter less than 1 cm (Murray, Sivajohanathan et al. 2019a, Murray, Sivajohanathan et al. 2019b).

In a head-to-head trial on the treatment of aggressive high-risk BCCs with a 10-year follow-up, the cumulative recurrence rate for primaries was 4.4% for MMS and 12.2% for excision, and for recurrent ones 3.9% and 13.5% respectively (van Loo, Mosterd et al. 2014). In a study from Sweden, the five-year recurrence rate for aggressive and recurrent, i.e. high-risk, facial BCCs was 2.1% for primaries and 5.2% for recurrent ones, and the defect after MMS was approximately twice as large as the defect would have been if the lesion had been removed on the visible border with 2 or 3 mm surgical margins (Paoli, Daryoni et al. 2011). Thus, the subclinical extensions of aggressive BCCs are a true challenge in the treatment of high-risk BCCs.

### 2.4.2 Surgery of lentigo maligna and lentigo maligna melanoma

For the treatment of LMM, surgery is the treatment of choice with a 1 cm excision margin for Breslow thickness ≤ 1 mm, and with a 2 cm excision margin for Breslow thickness > 1mm (Garbe, Peris et al. 2016, Wright, Souter et al. 2019, Swetter, Tsao et al. 2019). Generally, the surgery is the treatment of choice also for LM with an excision margin of 0.5–1 cm (Garbe, Peris et al. 2016, Wright, Souter et al. 2019, Swetter, Tsao et al. 2019).

MMS is an option in the surgery of LM (Garbe, Peris et al. 2016, Swetter, Tsao et al. 2019), but in a recent Canadian systematic review and guideline on the indications for MMS, it was concluded that in the treatment of invasive melanoma or melanoma *in situ*, MMS does not show any survival or recurrence benefit over traditional surgical excision (Murray, Sivajohanathan et al. 2019b, Murray, Sivajohanathan et al. 2019a). However, MMS is capable of sparing tissue, if needed.

## 2.5 Topical and non-surgical treatment of basal cell carcinoma and lentigo maligna

Generally, all the non-surgical options in the treatment of BCC are recommended for low-risk BCCs, and in cases where surgery is contraindicated or impractical (Trakatelli, Morton et al. 2014, Work Group, Invited Reviewers et al. 2018).

The non-surgical options in the treatment of LM should be considered only in selected cases, but for LMM, the treatment is always surgery (Swetter, Tsao et al. 2019, Garbe, Peris et al. 2016).

### 2.5.1 Cryosurgery

In the treatment of BCC, the lesions may or may not be debulked with curettage prior to cryotherapy (Trakatelli, Morton et al. 2014). The lesion and margins are frozen with liquid nitrogen, with tissue temperature reaching -50 to -60 degrees Celsius, thus destroying the treated area. Usually, two freeze-thaw cycles are used in the case of BCC (Trakatelli, Morton et al. 2014). In the treatment of low risk BCC, the recurrence rates vary between 6.3% and 40%, but when performed by an expert, the recurrence rate may be as low as 1% (Trakatelli, Morton et al. 2014, Work Group, Invited Reviewers et al. 2018). Thus, the experience of the physician can have a remarkable impact on the treatment outcome.

A systematic review on cryosurgery concluded that the efficacy of cryosurgery for primary sBCCs or nBCCs is comparable to PDT, with the five-year recurrence rates being 19.6% for cryosurgery with curettage, 20% for cryosurgery alone, 22% for MAL-PDT, in comparison to 8.4% for surgical excision (Tchanque-Fossuo, Eisen 2018). In the systematic review the expertise of the physician was not reported, thus both cryosurgery and PDT could have better outcomes in experienced hands.

### 2.5.2 Imiquimod

Imiquimod is a pharmacological topical treatment option for sBCC (Trakatelli, Morton et al. 2014). Imiquimod is an immune modulator, and it is an agonist for toll-like-receptors 7 and 8. Furthermore, it induces proinflammatory cytokines, chemokines and other mediators, and thus activates innate immunity with the Th1-

weighted anti-tumoural cellular response. It also induces tumour suppression, and apoptosis at higher concentrations (Trakatelli, Morton et al. 2014).

Some 58 to 92 % of patients treated with imiquimod have side effects including erosion, ulceration, induration, itching, burning and pain, and the severity of the local reaction is associated to the treatment outcome (Trakatelli, Morton et al. 2014). In the treatment of sBCC, imiquimod is applied once a day for five days per week, from six to twelve weeks (Arits, Aimee H M M, Mosterd et al. 2013, Trakatelli, Morton et al. 2014). This regimen is approved in the EU and the USA for treating sBCC in adults with a normal immune response, a lesion diameter up to 2 cm and a location on the neck, trunk or extremities (excluding hands and feet) (Trakatelli, Morton et al. 2014). Imiquimod is a cost-effective option compared to surgery in the treatment of sBCC (Trakatelli, Morton et al. 2014) (Trakatelli 2014). However, patient compliance should be evaluated carefully in the choice of the treatment, as a majority of patients will get local adverse events, and this will continue for weeks. For PDT, the occurrence of serious local post-treatment reactions was lower compared to imiquimod, but pain was higher when compared to topical pharmacological treatments. However, in PDT the duration of the pain is shorter (Collier, Haylett et al. 2018).

The efficacy of imiquimod at three months is 81%, and the probability of overall treatment success at five years is 77.6% for low-risk sBCCs, and for nBCCs sized from 0.5 to 1.5 cm in diameter on low-risk locations the efficacy at six weeks was 76% with a regimen of daily applications for twelve weeks (Trakatelli, Morton et al. 2014). Most of the recurrences seem to occur during the first year after treatment (Trakatelli, Morton et al. 2014).

A single-blinded, non-inferiority, controlled, prospective and randomised trial by Jansen et al. compared MAL-PDT, 5-FU and imiquimod in the treatment of sBCC, where imiquimod achieved a 83.5% cumulative tumour-free probability at one year and 80.5% at five years (Jansen, Mosterd et al. 2018).

In selected cases of LM, topical imiquimod can be used instead of surgery with a 75–88% complete response rate, but as a treatment method without histological control, it requires close follow-up (Garbe, Peris et al. 2016, Swetter, Tsao et al. 2019) (Garbe 2016).

### 2.5.3 5-fluorouracil

5-fluorouracil (5-FU) is another pharmacological topical treatment option, but is poorly studied for treating sBCC (Trakatelli, Morton et al. 2014). In the treatment of sBCC, 5-FU is applied twice daily for four weeks with similar local reactions as imiquimod (Arits, Aimee H M M, Mosterd et al. 2013). Regarding the mode of action, 5-FU inhibits DNA synthesis, cell proliferation and thus causes tumour necrosis (Arits, Aimee H M M, Mosterd et al. 2013).

In the trial by Jansen et al. the cumulative tumour-free probability for 5-FU at one year was 80.1%, and at five years 70.0% (Jansen, Mosterd et al. 2018).

### 2.5.4 Photodynamic therapy

#### 2.5.4.1 Mode of action and photobleaching

A light source with a wavelength equal to the activation spectrum of protoporphyrin IX (PpIX), a photoactive compound, is required for the PDT reaction. In addition to the light source, PpIX and oxygen are needed. The PDT reaction generates radical oxygen species, which cause cell apoptosis and death (Morton, Szeimies et al. 2015, Ozog, Rkein et al. 2016, Fantini, Greco et al. 2008). PpIX is generated endogenously in the heme synthesis pathway (Ozog, Rkein et al. 2016). Administration of an exogenous photosensitiser leads to the accumulation of PpIX (Ozog, Rkein et al. 2016). Accumulation and the concentration of PpIX can be measured as fluorescence of PpIX, and during the illumination phase the accumulated PpIX is consumed in the PDT reaction (Tyrrell, Campbell et al. 2010b). Thus, photobleaching can be calculated as the difference of the measured fluorescence before and after illumination. Photobleaching does not take place in the reaction without oxygen (Ericson, Grapengiesser et al. 2003), and in order to increase efficacy, the amount of accumulated PpIX and especially the degree of photobleaching is essential (Tyrrell, Paterson et al. 2019). Validated fluorescence measurements correlate with the efficacy of PDT (Tyrrell, Campbell et al. 2010a, Tyrrell, Paterson et al. 2019). It has been suggested that the measurement of singlet oxygen luminescence could be a more precise predictor of PDT efficacy than measuring fluorescence alone, but fluorescence measurements are easier to implement in practice (Mallidi, Anbil et al. 2014).

PDT is selective for tumour tissue due to abnormal epithelium, which allows the photosensitiser to better penetrate into the tumour tissue than into healthy skin (Kennedy, Pottier et al. 1990). Additionally, the accumulation of PpIX or the generation of reactive oxygen species correlates positively with the cell's proliferation rate or metabolic activity (Wang, Shi et al. 2017). Often, tumour cells under treatment are more active in their proliferation and metabolism compared to the healthy surrounding skin.

In a study performed on normal rat skin, the rat skin with stratum corneum had lower PpIX levels when compared to mucosa. Removing the stratum corneum enhanced PpIX production, and increasing the concentration or lengthening the incubation time further enhanced PpIX production (van den Akker, J T., Iani et al. 2000). The accumulation of PpIX increases linearly with the length of the incubation time (Campbell, Brown et al. 2017). The location of the lesion affects PpIX production, but gender, lesion type or skin type do not (Campbell, Brown et al. 2017). However, PpIX production does decline with age (Nissen, Philipsen et al. 2015). Accumulation of PpIX happens faster in the face and head area compared to other body parts (Campbell, Brown et al. 2017). On acral skin, the accumulation and photobleaching is reduced when compared to non-acral skin, due to thicker stratum corneum on acral sites (Tyrrell, Morton et al. 2011). Additionally, the temperature affects PpIX production: in higher temperatures, PpIX production increases compared to lower ones (Moan, Berg et al. 1999).

#### 2.5.4.2 Photosensitisers and light sources

5-aminolevulinic acid (5-ALA) is a natural precursor of PpIX in the heme synthesis pathway, and when 5-ALA or another prodrug is administered exogenously, there is an oversupply of 5-ALA (Ozog, Rkein et al. 2016). In the heme synthesis pathway 5-ALA is converted through some steps to PpIX, but the cell's ability to turn PpIX into heme is exceeded when an exogenous source is provided (Ozog, Rkein et al. 2016). Thus PpIX is accumulated, and when light activates PpIX, radical oxygen species are released (Ozog, Rkein et al. 2016).

PpIX has a wide and strong absorption peak from 405 nm to 415 nm, and several smaller absorption peaks from 500 nm to 635 nm (Ozog, Rkein et al. 2016). Traditional light sources that are used in PDT include red (635 nm) and blue light (417 nm). Additionally, daylight is a widely used option (Ozog, Rkein et al. 2016). A daylight-imitating coherent white light source is an alternative for natural daylight, and it is practical in low latitudes with less daylight in the dark seasons

(Marra, LaRochelle et al. 2018). Different kinds of lasers can also be used as a light source (Ozog, Rkein et al. 2016). The official recommendation for the illumination of BCC is with red light, and blue light and daylight are indicated for AK. However, it seems that in sBCC daylight can also achieve a good efficacy (Wiegell, Skodt et al. 2014).

Long wavelengths penetrate deeper into the skin compared to shorter ones, thus blue light penetrates to about 2 mm in depth, but red light penetrates deeper (Ozog, Rkein et al. 2016). Blue light excites PpIX effectively when near the wide and strong absorption peak of PpIX, but red light is preferred due to its depth (Ozog, Rkein et al. 2016). The depths for different wavelengths are reported as the depth where 50% of the photons have penetrated, as it is unclear how deep the rest of the photons penetrate (Ozog, Rkein et al. 2016). With narrow band devices like LEDs the relative response to treatment is better when compared to broadband lamps (Morton, Szeimies et al. 2015). With LED light, the photobleaching was more profound through the different layers of the skin when compared to intense pulse light or long-pulsed dye laser (Togsverd-Bo, Idorn et al. 2012).

In the illumination phase of PDT, it is important to consider the fluence ($J/cm^2$) and the irradiance ($mW/cm^2$), which affect the energy of excitation and the achieved photobleaching (Ozog, Rkein et al. 2016). To gain a similar excitation of PpIX, blue light needs a 10 $J/cm^2$ light dose compared to that of red light at 100 J/cm2 (Ozog, Rkein et al. 2016). Irradiance is the rate of the fluence, and it should not be too high as high rates consume tissue oxygen too rapidly and lead to the depletion of oxygen, and lower efficacy (Ozog, Rkein et al. 2016). Irradiance is recommended to be between 150 and 200 $mW/cm^2$, and cumulative doses above 40 $J/cm^2$ consume available oxygen and are thus unnecessary (Ozog, Rkein et al. 2016). The efficacy of PDT in the treatment of sBCC using 5-ALA has been observed to be better when it is delivered with a fractionated protocol, in which there is time for tissue re-oxygenation, compared to continuous illumination. This improved efficacy has not held true when using MAL, or when treating Morbus Bowen (Morton, Szeimies et al. 2015). In a head-to-head trial, Kessler et al. compared conventional MAL-PDT (fluence 37 $J/cm^2$, irradiance 75 $mW/cm^2$) to fractionated 5-ALA-PDT (20+80 $J/cm^2$ with a two-hour dark interval, irradiance 50 mW/cm2), and they achieved a probability for remaining tumour-free at one year of 92.3% for fractionated 5-ALA-PDT, and of 83.4% for conventional MAL-PDT. However, there was no statistical significance in the difference (Kessels, J P H M., Kreukels et al. 2018).

In standard MAL-PDT, the oxygen consumption and photobleaching seem to take place mostly in the first minutes of illumination, and blood perfusion increases towards the end of illumination, which is most likely due to the microvasculature compensating for the used oxygen (Tyrrell, Thorn et al. 2011). Interestingly, in a very recent study by Todd et al., it was shown that by increasing the total dose to 75 J/cm$^2$ in the treatment of BCC or Bowen's disease (carcinoma *in situ*), the efficacy was 90.3% at one year, compared to 67.7% efficacy with the recommended 37 J/cm$^2$ light dose (Todd, Lesar et al. 2019). It seems that at a higher light dose, the PDT reaction happens more efficiently deeper in the tissue, when compared to lower light doses (Todd, Lesar et al. 2019). Thus, photobleaching might not be enough for evaluating the efficacy of the reaction, as the measured fluorescence and photobleaching describe the superficial layers of skin. Furthermore, there could be more available oxygen present deeper in the tissue, even it is depleted in the superficial layers (Todd, Lesar et al. 2019).

5-ALA was used in a dermatological indication for the treatment of BCC for the first time in the 1990's with a 90 % clearance rate (Ozog, Rkein et al. 2016, Kennedy, Pottier et al. 1990). Earlier intravenous photosensitisers were used with photosensitisation lasting for days, but with 5-ALA the effect resolves within 24 to 50 hours, thus making the treatment feasible in clinical practice (Kennedy, Pottier et al. 1990, Ozog, Rkein et al. 2016). Lipophilic esters of 5-ALA can be more powerful than 5-ALA in PDT, as they penetrate the fatty, rate-limiting stratum corneum more efficiently than 5-ALA. However, the vector of choice must be considered in their use, as some aqueous features are also required in order for the photosensitiser to penetrate deeper into the skin. Furthermore, conversion back to 5-ALA is also required for PpIX formation (Lopez, Lange et al. 2004).

There are three currently approved photosensitisers in the European market using red light in their protocols: MAL-containing Metvix (indication for non-hyperkeratotic AKs, Bowen's disease, sBCC and nBCC), 5-ALA-containing patch Alacare (indication for mild AK, without pretreatment), and nanoemulsion of 5-aminolevulinic acid (BF-200 ALA) Ameluz containing 5-ALA in nanoparticles (indication for mild to moderate AK and sBCC) (Morton, Szeimies et al. 2015, Morton, Dominicus et al. 2018). Additionally, in the USA 5-ALA-containing Levulan is approved with a blue light protocol for AKs (Morton, Szeimies et al. 2015, Ozog, Rkein et al. 2016).

MAL is more lipophilic and has a shorter incubation, i.e. occlusion time, compared to 5-ALA (Ozog, Rkein et al. 2016, Morton, Szeimies et al. 2015). Nanoemulsion of BF-200 has a similar incubation time as MAL (Morton, Szeimies

et al. 2015), but a deeper penetration and stronger fluorescence than MAL (Maisch, Santarelli et al. 2010). The nanoparticles improve the stability of 5-ALA (Hurlimann, Hanggi et al. 1998).

Another lipophilic photosensitiser is hexylaminolevulinate (HAL), which is approved for the photodynamic diagnosis of bladder cancers in Europe. HAL was selected for this because of its high fluorescence at low concentrations and satisfactory water solubility compared to 5-ALA, which was previously also used in bladder cancer fluorescence diagnosis (Fotinos, Campo et al. 2006). HAL has been used in the treatment of cervical neoplasia (Hillemanns, Garcia et al. 2015) and bladder cancers (Bader, Stepp et al. 2013).

On nude murine skin, equimolar doses of HAL produce more intense fluorescence and achieve a deeper penetration compared to MAL or 5-ALA (Morrow, McCarron et al. 2010). In the human epidermis and superficial dermis, the fluorescence of 20% HAL is significantly stronger compared to 20% MAL (Togsverd-Bo, Idorn et al. 2012). Additionally, on human skin low concentration HAL and 5-ALA (0.2% and 2%) induced a stronger fluorescence compared to MAL at similar concentrations (Juzeniene, Juzenas et al. 2006). Half of the maximal PpIX fluorescence is reached with 2% 5-ALA, with 1% HAL and with 8% MAL (Juzeniene, Juzenas et al. 2006). Using cream as a vector induces the best fluorescence for HAL and 5-ALA, but the advantage of HAL is its more defined effect on the site of application and less of an effect on surrounding healthy skin compared to 5-ALA (Casas, Perotti et al. 2001).

Different photosensitisers can have a different accumulation of PpIX in the vascular walls during PDT, and thus vascular damage can occur during the treatment (Middelburg, de Vijlder et al. 2014). The effect was stronger for HAL, than for 5-ALA, and for MAL the damage did not differ from normal skin. Thus, the fractioning of illumination might have an effect for HAL and 5-ALA but not for MAL (Middelburg, de Vijlder et al. 2014).

The current protocol with MAL-PDT (curettage + 3 hours occlusion + illumination with Aktilite) seems to allow for a sufficient accumulation and photobleaching of PpIX in all indications (AKs, Morbus Bowen and BCC) regardless of patient age, gender and lesion size (Tyrrell, Campbell et al. 2011).

#### 2.5.4.3 Pretreatment and enhancing of photosensitiser's penetration

For sBCC, it is common practice to remove all scales and crusts as a pretreatment step to allow for the sufficient absorption and penetration of the photosensitiser.

In nBCC, pretreatment with curettage or a scalpel is recommended (Morton, Szeimies et al. 2015). In addition to curettage, there are multiple ways to enhance the penetration by chemical cleansers, tape-stripping, micro-needling and with ablative lasers (Morton, Szeimies et al. 2015, Ozog, Rkein et al. 2016). Regarding pre-handling, curettage is superior and enhances PpIX fluorescence significantly more when compared to a chemical pre-treatment (Nissen, Wiegell et al. 2016). When different pre-treatment modalities are compared, ablative fractional laser enhances PpIX fluorescence the most when compared to other options such as microdermabrasion, micro-needling, and curettage (Bay, Lerche et al. 2017). Bay et al. showed that the fluorescence of PpIX is stronger with more invasive pre-treatment when compared to curettage. It should also be noted that after a certain threshold, the accumulation of PpIX does not improve the efficacy (Nissen, Heerfordt et al. 2017). The use of ablative fractional lasers enhances the accumulation of PpIX and increases the fluorescence and depth penetration (Haak, Christiansen et al. 2016, Haedersdal, Sakamoto et al. 2010). When nBCCs were treated with CO2-laser-assisted MAL-PDT compared to curettage as pre-treatment, a better response rate and fluorescence was achieved in the laser group (Lippert, Smucler et al. 2013).

#### 2.5.4.4 Tolerability

In PDT, post-treatment reactions usually include oedema, erythema, scaling and itching at the site of treatment (Morton, Szeimies et al. 2015, Ozog, Rkein et al. 2016). More unusual, but possible local reactions include pustules, erosions and crusting, especially if treating thicker lesions (Morton, Szeimies et al. 2015). Uncommon reactions include hyperpigmentation, hypopigmentation and scarring, as usually the cosmetic outcome is good in PDT (Morton, Szeimies et al. 2015, Ozog, Rkein et al. 2016). Rare adverse events that are possible to encounter include contact allergy for the photosensitiser, urticaria, post-operative hypertension or localised bullous pemphigoid (Morton, Szeimies et al. 2015). Usually PDT is well tolerated with reasonable post-procedural local reactions. However, the pain during the illumination phase of the treatment can be intense (Morton, Szeimies et al. 2015).

Indeed, the main adverse event for PDT is pain, and a local reaction of some degree is common. Other adverse events are rare (Ibbotson, Wong et al. 2019, Morton, Szeimies et al. 2015, Wang, Shi et al. 2017). The exact mechanism of the pain is still unclear, but it is thought to be caused by the radical oxygen species, i.e.

the same mediators that increase the efficacy (Wang, Shi et al. 2017). It is thought that either radical oxygen species activate nerve endings directly, or they are activated by inflammatory mediators released by the radical oxygen species (Wang, Shi et al. 2017). It has been suggested that nociceptive Aδ nerve fibers could initially deliver the pain in PDT, or that slow-acting C fibers could also play a role (Wang, Shi et al. 2017). GABA has an inhibitive effect on nociceptive neurons, and it seems that radical oxygen species can inhibit GABA-receptors, thus leading to a decrease in GABA activity and an increase in nociceptive signals (Wang, Shi et al. 2017).

The pain is typically unpredictable and individual (Wang, Shi et al. 2017). Typically, pain is more intense on well-innervated sites such as the face and scalp compared to other parts of the body. Pain intensity correlates positively with the size of the treatment area. Furthermore, the lesion type also affects the pain level, as BCC is less painful compared to AKs and Bowen's disease (Wang, Shi et al. 2017, Ang, Riaz et al. 2017). For AKs on the face and scalp the pain scores can be 7.5/10 on the visual analogue scale (VAS) without analgesia, and for nonaggressive BCCs (superficial and thin nodular) the average pain score is 4.5/10 on a numerical scale from one to ten without analgesia (Morton, Szeimies et al. 2015, Morton, Dominicus et al. 2018). In noncancerous indications, the pain is even more severe, as the inflammatory diseases are metabolically active (Wang, Shi et al. 2017). There is no clear evidence that the pain would correlate with gender, age or Fitzpatrick skin type (Wang, Shi et al. 2017).

The above-mentioned factors are not modifiable, but the protocol and treatment-related factors can be customized (Wang, Shi et al. 2017). There is some threshold where a sufficient amount of PpIX is accumulated sufficiently to increase efficacy, as excessive accumulation of PpIX leads to increased pain and erythema (Nissen, Heerfordt et al. 2017). There is no clear evidence that there would be differences in pain between the photosensitisers (Wang, Shi et al. 2017). However, in some studies, 5-ALA has caused more pain than MAL (Wang, Shi et al. 2017). When comparing pain levels in healthy human skin, at low concentrations of 0.2% and 2% HAL caused significantly less pain when compared to BF-200 ALA and MAL, and BF-200 ALA did not significantly differ from MAL (Neittaanmaki-Perttu, Neittaanmaki et al. 2016). In erythema, only 0.2% HAL differed significantly when compared to BF-200 ALA and MAL, but no differences were found between 2% HAL, BF-200 ALA and MAL (Neittaanmaki-Perttu, Neittaanmaki et al. 2016).

For fluence rate and dose, a threshold limit probably exists under which the pain increases with rate and dose, and above the limit a plateau is reached (Wang, Shi et al. 2017). It has been suggested that the limit would be around 60 mW/cm$^2$ for the fluence rate, i.e. irradiance, and around 50 J/cm$^2$ for dose, i.e. fluence (Wang, Shi et al. 2017). Thus, by modifying these parameters some control of pain can be achieved. For example, in daylight PDT the pain levels are clearly lower (Wang, Shi et al. 2017).

Post-procedural pain can also be significant, as pain after PDT on wide areas on the face in the treatment of actinic damage was more severe than after facial surgery, which also included some wide facial operations (Dixon, Anderson et al. 2015).

#### 2.5.4.5 Pain management

Pain management can be divided into interventions on the PDT parameters and to interventions on pain during PDT (Ang, Riaz et al. 2017).

Topically administered local anesthetics like Emla®, lidocaine hydrochlorine 3%, Ampetop® (tetracaine 4%) or morphine gel have not increased the efficacy for pain management during illumination in double-blinded placebo-controlled trials (Wang, Shi et al. 2017).

Nerve blocks using local anesthetics have good results in pain management, but this method is best suited for facial and scalp locations (Wang, Shi et al. 2017). In their study, Paoli et al. introduced nerve blocking in PDT by using trigeminal blocks for extensive facial AKs, and VAS decreased from 7.5/10 to 1.3/10: the change was -6.2 and significant (Paoli, Halldin et al. 2008). In several studies with nerve blocks on facial or scalp sites, the change in pain ranged from -4.2 to -6.3 (Wang, Shi et al. 2017). Nerve blocking is also superior to cold air analgesia or oral analgesia (Wang, Shi et al. 2017). The limitation of the method is its requirement for expertise in the technique and limitation to certain sites (Wang, Shi et al. 2017). However, the most painful sites are covered with this technique.

Nerves can also be blocked by subcutaneous infiltration anesthesia for pain control in PDT (Wang, Shi et al. 2017). The studies on this method are sparse. There is one study which used subcutaneous infusion-tumescent anesthesia, i.e. a continuous infusion during the illumination phase with ropivacaine and prilocaine, where the observed change in VAS was from 8 to 4.5 (Borelli, Herzinger et al. 2007). In a case report, a similar method was used for a child with Gorlin

syndrome. Wide areas of BCC were treated on her back, and good pain management was gained without a loss in efficacy (Debu, Sleth et al. 2012).

#### 2.5.4.6 Efficacy and cosmetic outcome in basal cell carcinoma

In a systematic review and meta-analysis on PDT of low-aggressive BCCs (including superficial and nodular subtypes), the pooled estimate for complete clearance rate was 86.4% (95% CI: 80.0–91.0%) for PDT compared to surgery with 98.2% (95% CI: 95.5-99.3%) complete clearance rate (Wang, Xu et al. 2015). The recurrence rate at one year was 10.3% (95% CI 5.9-17.4%) for PDT and 0.6% (95% CI: 0.1-3.0%) for surgery, with a significant risk ratio of 12.42 (95% CI: 2.34–66.02). However, no significant differences were observed when comparing PDT to cryosurgery with a risk ratio of 1.04 (95% CI: 0.46-2.39) or to pharmacological topical treatment (imiquimod and 5-FU) with a risk ratio of 1.67 (95% CI: 0.97-2.85) (Wang, Xu et al. 2015). At five years, the recurrence rate was higher for PDT with a significant risk ratio of 6.27 (95% CI 2.21-17.75) compared to surgery, but no difference was observed when compared to cryosurgery with a risk ratio of 1.08 (95% CI: 0.62-1.86) (Wang, Xu et al. 2015). In another systematic review on the treatment of sBCC, the pooled complete response rate at twelve weeks was 79% (95% CI 71-87%) for PDT and 86.2% (95% CI 82-90%) for imiquimod (Roozeboom, Arits, A H H M. et al. 2012).

There is only one head-to-head trial in the treatment of superficial BCC which compares different non-invasive options (Jansen, Mosterd et al. 2018). This trial is of good quality, as it is a prospective, controlled, randomised and single-blinded trial with a large sample size. This trial was published after the aforementioned systematic review. In this trial, the efficacy for MAL-PDT was 62.7 (95% CI 55.3-69.2), for 5-FU 70.0 (95% CI 62.9-76.0), and for imiquimod 80.5 (95% CI 74.0-85.6) (Jansen, Mosterd et al. 2018). The hazard ratio for treatment failure was 0.48 (95% CI: 0.32-0.71) when comparing imiquimod to MAL-PDT with a significant difference ($p<0.001$), and 0.74 (95% CI: 0.53-1.05) when comparing 5-FU to MAL-PDT with a non-significant difference ($p=0.09$) (Jansen, Mosterd et al. 2018).

In the systematic review by Wang et al. the probability of a good to excellent cosmetic outcome was significantly higher for PDT, when comparing to surgery with a risk ratio of 1.87 (95% CI 1.54-2.26), or when comparing to cryosurgery with a risk ratio of 1.51 (95% CI 1.30-1.76), but a non-significant difference when comparing to pharmacological topical treatment with a risk ratio of 1.05 (95% CI 0.91-1.21) (Wang, Xu et al. 2015).

In the trial by Jansen et al., pharmacological topical treatments were compared to MAL-PDT. Cosmetic outcome was superior in the MAL-PDT group with 96.3% of patients having a good or excellent outcome as calculated in patients staying recurrence-free at five years, compared to 83.1% in imiquimod and 87% in 5-FU groups. However, it should be noted that the efficacy is lower for MAL-PDT, and 75% of the patients treated with surgery in the second line had a good or excellent cosmetic outcome (Jansen, Koekelkoren et al. 2018).

In any case, the current evidence shows that imiquimod is superior to MAL-PDT and 5-FU, and 5-FU is not inferior when compared to MAL-PDT in efficacy, and furthermore both pharmacological treatments have good cosmetic outcomes (Jansen, Koekelkoren et al. 2018, Jansen, Mosterd et al. 2018). Interestingly, MAL-PDT could be more effective in elderly patients on the lower extremities (Roozeboom, Arits, Aimee H M M. et al. 2016). Thus, there is room for PDT as a non-invasive treatment option.

A recent update on the PDT guideline by the British Association of Dermatologists concluded that PDT should be offered as an option in the treatment of sBCC in the following cases: when the site of the tumour is on a poorly healing site, in cosmetically sensitive areas, or when there are wide or multiple lesions (Wong, Morton et al. 2019). Furthermore, there are multiple parameters in PDT which can be adjusted, and thus it may be that the current protocols are suboptimal. Further research on fractionated PDT, and using higher light doses is required (Todd, Lesar et al. 2019, Collier, Haylett et al. 2018).

#### 2.5.4.7 Photodynamic therapy of lentigo maligna

5-ALA, MAL and BF-200 ALA have been used as off-label indications for the experimental treatment of LM and amelanotic melanoma *in situ* (Chetty, Osborne et al. 2008, Karam, Simon et al. 2013, Rasanen, Neittaanmaki et al. 2019).

Karam et al. retrospectively studied 5-ALA-PDT in the treatment of facial LM with higher light doses (average 60 J/cm2, compared to 37 J/cm2 in non-pigmented lesions) and repeated sessions (from three to nine, compared to the usual two session in non-pigmented lesions). They observed clinical and histological healing in 12/15 lesions at a 10–29 month follow-up, and in 3/15 lesions there was an instant treatment failure (Karam, Simon et al. 2013).

Chetty et al. tried MAL-PDT for amelanotic melanoma *in situ* on the chin with a two-session treatment and a 40 J/cm2 light dose. At one month, the site was clinically showing some fine crusting and possible clearing, but at six months there

was a clinically suspected and histologically proven residual lesion outside of the originally treated area, which was clinically and histologically cleared. At ten months, a recurrence also appeared at the originally treated site (Chetty, Osborne et al. 2008).

Rasanen et al. conducted a prospective, non-sponsored pilot study using ablative fractional laser-assisted PDT with BF-200 ALA in the treatment of facial LM, with three sessions and a 90 J/cm2 light dose. They achieved a histopathologically proven clearance in 7/10 cases. Pain was tolerable, ranging from 2.9 to 3.8 on the VAS, but some severe local adverse events occurred. It was concluded that due to the strong local reactions, PDT of LM should only be used in select, inoperable cases. (Rasanen, Neittaanmaki et al. 2019)

### 2.5.5 Patients' preferences and patient selection in treatment of basal cell carcinoma

BCC is non-lethal but as it is often a chronic condition, it can have an impact on quality of life (Chen, Bertenthal et al. 2007, Chren, Sahay et al. 2007). Thus, patients' preferences and quality of life should also be taken into account when considering treatment options (Essers, Arits et al. 2018, Martin, Schaarschmidt et al. 2016).

In the topical treatment of sBCC, patients valuated different attributes in the following order: efficacy, cosmetic outcome, adverse events and treatment process (Essers, Arits et al. 2018). Interestingly, BCC patients with facial lesions or with multiple lesions were willing to risk the recurrence rate for cosmetic outcome (Martin, Schaarschmidt et al. 2016).

For PDT, there are varying results in the efficacy, and the treatment protocol has many variables which can affect the outcome. The correct lesion and patient selection is essential when considering the outcome of a treatment, but for PDT, there is no clear factor at the individual level which would predict the treatment outcome (Hambly, Mansoor et al. 2017).

# 3 AIMS OF THE STUDY

Skin cancers are a growing problem, and new options and innovations may ease the process and pressure on available resources. This dissertation was designed to test the feasibility of new, non-invasive options in the diagnosis and treatment of skin cancers, thereby contributing to a potentially more smooth and effective treatment process for skin cancer patients in the future.

The specified aims were the following:

1. To test the feasibility of a HIS in separating LM and LMM from each other. Additionally, to test the feasibility of the HIS in localising the invasion site. Separation of these two conditions is crucial for the prognosis, subsequent treatment and follow-up.
2. To test the feasibility of a HIS in the delineation of ill-defined BBCs, which often exist in subclinical extensions, and thus pose a true clinical challenge.
3. To study the efficacy, cosmetic outcome and adverse events of two novel photosensitisers, BF-200 ALA and HAL, compared to the older and widely used MAL in a non-sponsored, prospective, controlled, randomised and double-blinded trial.
4. To test the feasibility of a fluorescence imaging system, which is easy to build up with simple equipment: a digital camera and Woods light, which are usually part of basic dermatological clinic equipment, and a yellow lens.

# 4 MATERIALS AND METHODS

## 4.1 Study design

### 4.1.1 Study I and II: Pilot studies

The two pilot studies were designed to investigate the feasibility of a HIS in the preoperative assessment of skin cancers. In the two non-invasive imaging pilot studies, the lesions were assessed clinically and dermoscopically followed by preoperative hyperspectral imaging. Results were confirmed with histopathology. An experienced dermatopathologist assessed the specimens blinded to the HIS findings.

### 4.1.2 Study III: Clinical trial

The clinical trial was an investigator-initiated, prospective, randomised, double-blinded and controlled trial designed to evaluate the efficacy, adverse events and cosmetic outcome of three different photosensitisers in PDT of non-aggressive BCCs. The patient and observers of outcomes were blinded regarding the photosensitiser that was used.

The primary outcome of study III is the clearance of histologically verified lesions at the three-month follow-up visit. Non-responsive lesions were excised to see if aggressive growth patterns were present. A major secondary outcome included tolerability: pain during illumination with a long-acting local anaesthetic as pain management, and post-treatment reactions. Other secondary outcomes included cosmetic outcome, fluorescence at the beginning of illumination, and photobleaching, i.e. the difference in fluorescence measured in the beginning and end of illumination.

### 4.1.3 Sample size of the studies

For studies I and II, it was not possible to calculate a sample size for the trials as they were pilot studies. We estimated that around 20–30 lesions in each study would be a sufficient sample size to test the feasibility.

For study III, the power of the study was calculated to be 31 lesions per study arm, and this initial set was randomised with a web-based validated program called Research Randomizer (randomizer.org®). To account for error in clinical diagnosis at enrolment and for those patients lost in follow-up, a 25% buffer was added to the sample size. Thus, an additional set of 24 lesions were randomised with closed envelopes, due to problems with the use of Research Randomizer at the time. Thus, we ended up with 117 randomised lesions for the trial: 39 lesions per study arm.

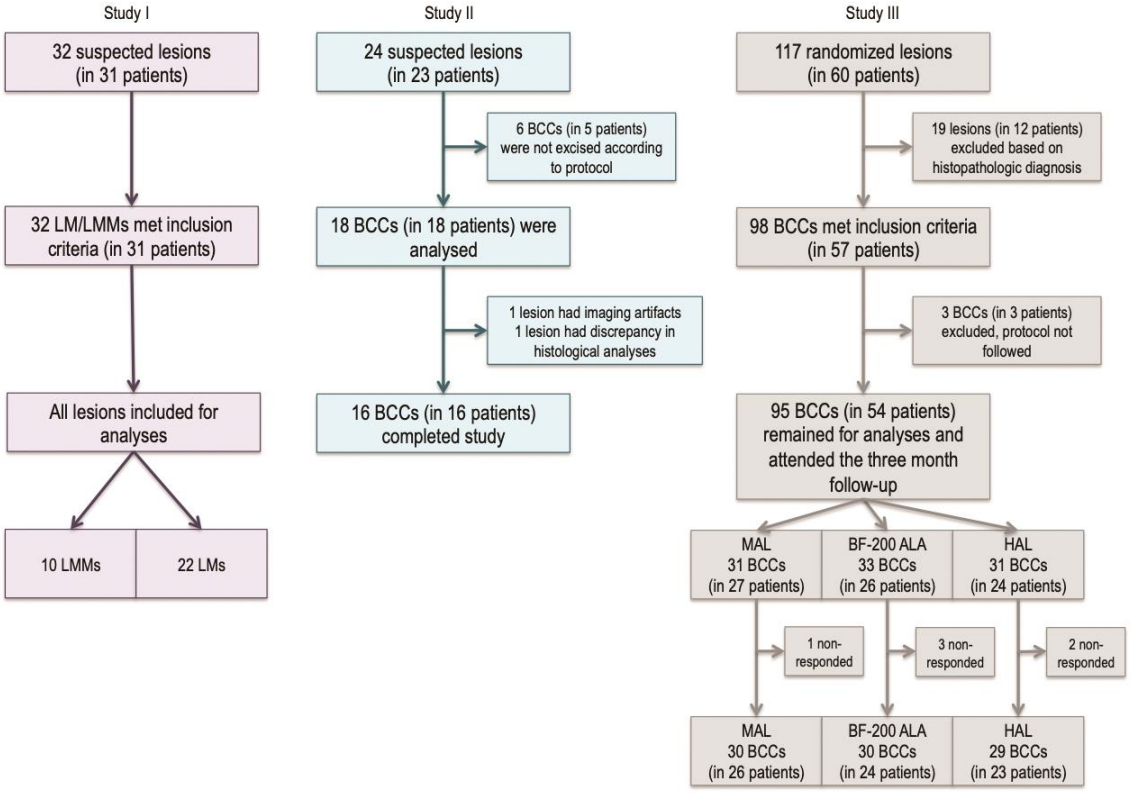


**Figure 7.** Flow-charts of the studies.

### 4.1.4 Ethical aspects and approvals by authorities

In studies I and II on hyperspectral imaging, the Declaration of Helsinki was followed, and protocols were approved by the Ethics committee of Tampere University Hospital and by Valvira (National Supervisory Authority for Welfare and Health). All participants were informed of the study procedures both orally and in writing, and they gave their written consent.

Study III, the clinical trial, was approved by the Ethics committee of Tampere University Hospital and by Fimea (Finnish Medicines Agency), and it abided by the Declaration of Helsinki. All participants were informed orally and in writing, and they provided their written consent.

## 4.2 Patients

All patients were recruited from those referred to the Department of Dermatology and Allergology at the Päijät-Häme Social and Health Care Group in Lahti, Finland. In study I the patients were recruited between January 2012 and January 2015; in study II between March 2014 and March 2017; and in study III between March 2015 and September 2018.

**Table 15.** Patient and lesion characteristics.

| | Study I | Study II | Study III | | |
|---|---|---|---|---|---|
| | | | MAL | BF-200 ALA | HAL |
| **Number of patients** | 31 | 16 | 27 | 26 | 24 |
| with single lesion | 30 | 16 | 14 | 8 | 5 |
| with multiple lesions | 1 | 0 | 13 | 18 | 19 |
| Female | 16 | 7 | 10 | 5 | 12 |
| Male | 15 | 9 | 17 | 21 | 12 |
| Average age in years (range) | 77 (56-97) | 77 (59-91) | 71 (47-91) | 74 (51-91) | 74 (57-91) |
| Skin phototype | | | | | |
| I | 4 | 5 | 6 | 4 | 7 |
| II | 17 | 9 | 10 | 13 | 8 |
| III | 10 | 2 | 11 | 9 | 9 |
| IV | 0 | 0 | 0 | 0 | 0 |
| Immunosuppression, cytostatics or radiotherapy on study area in history | 0 | 1 | 2 | 1 | 2 |
| History of previous skin (pre)malignancies (AK, MB, SCC, BCC, MM) | 15 | 13 | 19 | 20 | 19 |
| | | | | | |
| **Number of lesions** | 32 | 16 | 31 | 33 | 31 |
| Average size in $mm^2$ (range) | - | - | 439 (150-1100) | 377 (130-850) | 376 (160-750) |
| new | 31 | 16 | 30 | 30 | 29 |
| recurrent | 1 | excluded | 1 | 3 | 2 |
| Location on trunk | LMM 1/LM 2 | excluded | 25 | 26 | 25 |
| Location on extremities | LMM 1/LM 0 | excluded | 6 | 7 | 6 |
| Location on head and neck | LMM 8/LM 20 | 16 | excluded | excluded | excluded |

### 4.2.1 Inclusion and exclusion criteria

In study I, patients aged over 18 with clinically and dermoscopically suspected, and histopathologically verified, LM or LMM in any location were included. In study II, patients aged over 18 with clinically and dermoscopically suspected, and histopathologically verified, ill-defined primary BCCs in the head and neck area were included.

In study III, patients aged over 18 with clinically and dermoscopically assessed, mainly superficially growing BCCs on the trunk or extremities were included at enrolment. Multiple lesions on one patient were allowed, but they were required to

be 10 cm apart from each other to avoid mixing up the effect of different photosensitisers. It should also be noted that the lesions were randomised, not the patients. All diagnoses were confirmed with 3-mm punch biopsies. Histopathology excluded lesions other than BCC, i.e. aggressive types of BCC and thick nBCC, in which the bottom of the tumour reaches in to the middle third of the dermis, or deeper. Thus, in histopathology, only superficial and thin nodular BCCs, i.e. the bottom of the tumour reaching into the epidermal junction or into the uppermost third of the dermis, were included and defined as non-aggressive BCCs.

In all studies, special groups such as children and pregnant or breastfeeding women were excluded. Study III also excluded patients with an intolerance or allergy to the used photosensitiser, porphyria or light-sensitivity. Study III required patients to be able to complete VAS pain scores by themselves, thus it was not possible to include patients with a memory illness or with some other diseases affecting their ability to understand instructions on pain scores.

## 4.3 Hyperspectral imaging

For study I and II, a handheld hyperspectral camera prototype with a field of view ranging from 2.5–12 $cm^2$ (VTT FPI VIS-VNIR Spectral Camera) was developed by VTT, the Technical Research Centre of Finland. The camera uses wavelengths from visible light to near infrared light (500-900 nm). The mechanism of the camera is based on a Fabry-Perot interferometer with a tunable air gap between the mirrors inside the interferometer's cavity, allowing the fast capture of 70 different wavelengths. Three wavelength peaks are obtained at one setting of the air gap, and it takes a few milliseconds to change the air gap. Thus the imaging process takes seconds, and the subsequent computational analyses can be completed in 5-10 minutes.

The camera contains objectives, microscope lenses, filters and a beam-splitter which divides the light into visible and near infrared regions. The emitted light (ring light around the lens system, a halogen-based fibre-optic illuminator; Dolan-Jenner Fibre-Lite DC 950) is absorbed and scattered by the imaged tissue, and the remitted light (diffuse reflectance) is recorded with CMOS red-green-blue (RGB) colour sensors (MT009V022) in ENVI standard data format.

A stack of images is created where every pixel has a hyperspectral graph of all imaged wavelengths. Thus, a data cube is created, where the x and y axes are the dimensions of the skin forming a 2D digital image with a resolution of 240x320

pixels, where one pixel is approx. 125 μm in width, and the z-axis is the third, hyperspectral dimension.

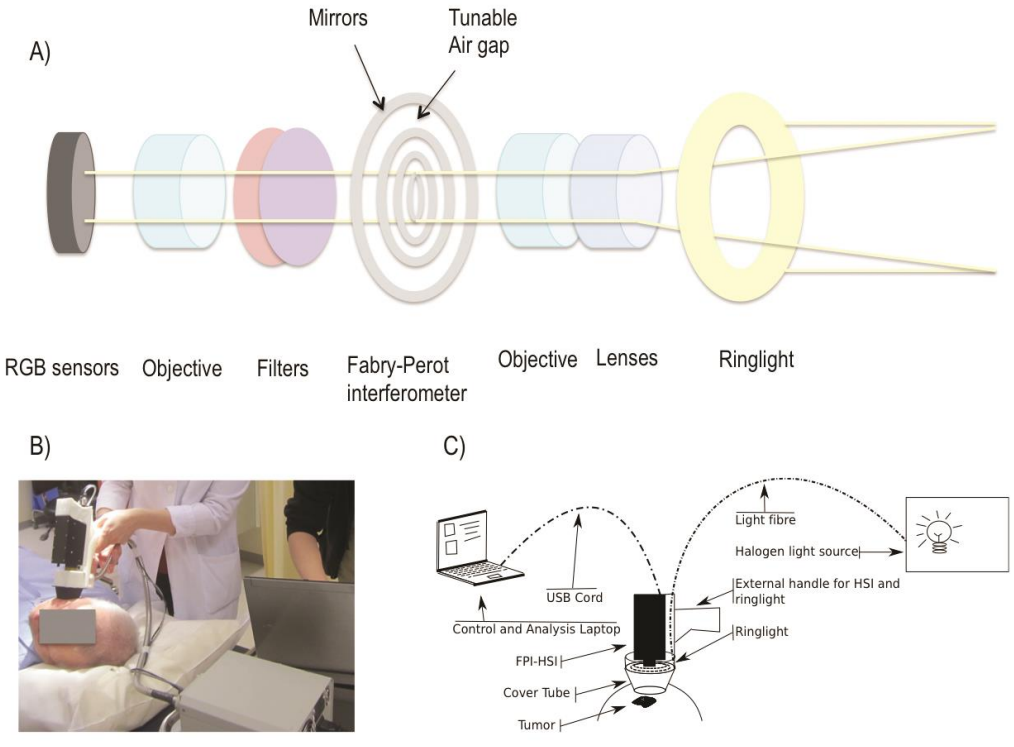


**Figure 8.** A) Structure of the camera B) Clinical imaging C) Function of the camera, courtesy of Ilkka Pölönen.

Visible to near infrared light in hyperspectral imaging is capable of reaching about 2 mm in depth. Short wavelengths penetrate superficially, while longer wavelengths penetrate deeper into the tissue. Thus, it is possible to obtain information beneath the surface of the skin.

Chromophores are biological structures of tissue, which are behind the absorption and scattering of light. In skin, the main chromophores are melanin, hemoglobin and water. The structure of tissue differs between healthy and diseased skin, with the same being true for the number of chromophores. Based on this idea, there could be a unique hyperspectral graph profile for each different tumour or disease.

In the imaging process, the obtained data cube contains a huge amount of spectral information. In order to be able to use this data, it must be processed computationally. The different wavelengths are recorded as different proportions of RGB sensor outputs. This data can be converted into reflectance (in numerical form). Black and white references, which are imaged at the beginning of the imaging process, are used in these calculations.

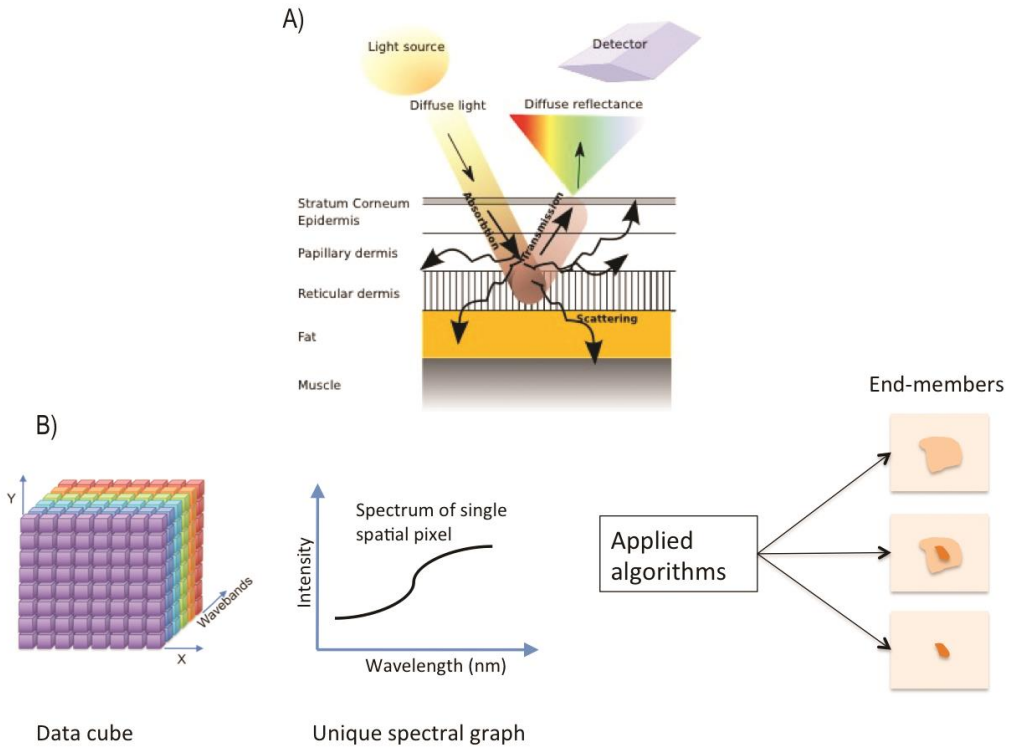


**Figure 9.** A) Recording of diffuse reflectance, courtesy of Ilkka Pölönen B) Data processing, courtesy of Ilkka Pölönen.

There are coefficients for the different chromophores of the skin, and with these coefficients, different algorithms can be applied on the calculated reflectance. Thus, certain chromophores, or a mixture of them, can be extracted from the data as end members, and be presented as an abundance map, i.e. a spectral image of the target, which the clinician can interpret. The used algorithms are mathematical models, and thus assumptions of the reality, but they offer a possibility to visualise the spectral dimension.

### 4.3.1 Mathematical models used and their interpretation

In study I, native imaging of the lesion was performed with an orientation mark, and a mathematical model of linear mixture was used bedside.

In study II, the lesions were natively imaged with HIS using an orientation mark, and again after marking the clinically defined border on the skin with an orientation mark. A linear mixture model was used bedside, and afterwards three other models were developed and applied to the data. Thus, study II utilised a linear mixture, linear mixture with single scattering albedo, chromophore-specific with single-scattering albedo and standard variate model. If three out of four models gave the same borders, those were interpreted as the HIS finding.

### 4.3.2 Linear mixture

A linear mixture model assumes that the recorded reflectance is a linear mixture of limited numbers of characterized spectra of imaged tissue named end members. The model uses vertex component analyses and filter vector analyses to define end members. The recorded reflectance is an equation of mixing matrix and end members. Solved end members are then visually represented as abundance maps.

### 4.3.3 Linear mixture with single scattering albedo

Reflectance spectra of skin are nonlinear. Single-scattering albedo is an estimate calculated based on the scattering and total absorption coefficients of the skin. The non-linear reflectance is converted to be more linear with single-scattering albedo, and then the linear mixture model is applied to solve the end members for abundance maps.

### 4.3.4 Chromophore-specific with single-scattering albedo

Single-scattering albedo is used to describe the recorded reflectance, and the filter vector analysis is used to solve the proportion of chromophores from the recorded reflectance, after which the chromophore coefficient is multiplied by the proportion of the chromophore in question. When this is performed for all chromophores, it is possible to solve chromophore-weighted end members, i.e. the characterized spectra of the chromophore in question, which can be represented as abundance maps of different chromophores.

### 4.3.5 Standard variate

This model has a statistical background, and basically it compares how different spectra differ from the mean spectrum, which is the homogeneous background. Here it is assumed that the lesion is the differing spectrum and the homogeneous background is the healthy skin surrounding the lesion.

## 4.4 Dermoscopy

In all studies, clinical diagnosis was aided by dermoscopy to improve the accuracy of the diagnosis. The dermoscopes used were Dermlite® DL3 or DL3N, 3GenCA, USA, or Heine Delta 20T®.

## 4.5 Photographing and fluorescence imaging

### 4.5.1 Digital photographing

In all studies, the lesions were photographed with a digital camera (Canon Ixus 130, 14.1 megapixel or Canon Ixus 115 HS, 12.1 megapixel). Dermoscopic pictures were obtained with a digital camera through the dermoscope.

### 4.5.2 Fluorescence imaging and Photobleaching

A handheld experimental imaging system including a digital camera (Canon Ixus 130, 14.1 megapixel with set-up: ISO800, FW 2.8, no zoom), Wood's light (Philips Burton®, Somerset, USA, held by hand at about 8 cm distance) and a yellow filter lens (Hoya HMC, yellow-green xo, attached on top of Wood's light) was used to obtain the fluorescence images. Prior to imaging, the photosensitiser cream was wiped off with saline solution. Photobleaching was calculated as the absolute difference of the mean fluorescence before and after illumination.

To quantify the fluorescence, the obtained raw images were processed semi-automatically with an affine transformation and manually selected matching points with Python 3.6, and the intensity was extracted in red-lights channel to get arbitrary units (A.U.) for fluorescence and photobleaching.

## 4.6 Photodynamic therapy and outcome assessments of photodynamic therapy

PDT followed European guidelines except for long-acting local anesthetics which were used prior to curettage (Figure 10). We chose to use local anesthetics as infiltration, which allowed us to retrieve feasible diagnostic punch biopsies during the first PDT session, while simultaneously offering pain management for illumination. The infiltration was repeated during the second session to achieve similar pain management as in the first session.

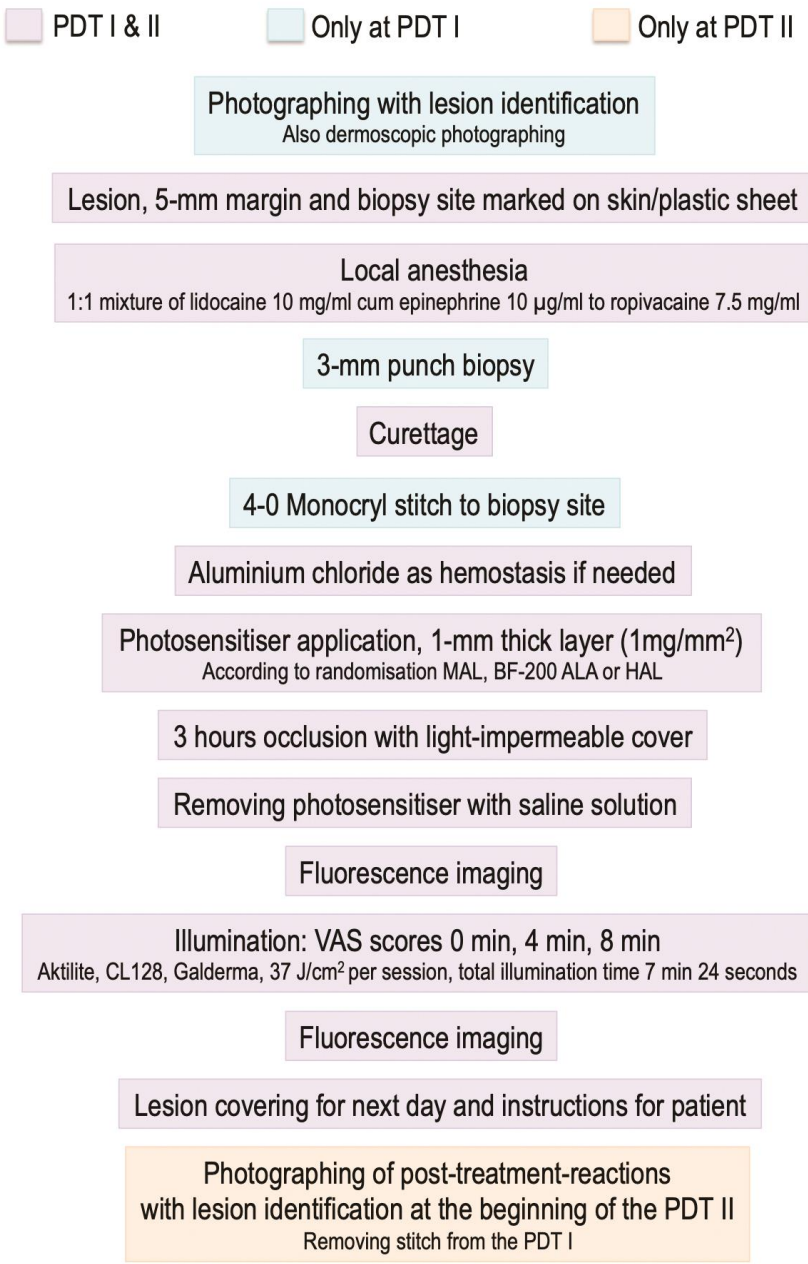


**Figure 10.** Treatment protocol for PDT I and II sessions.

Pain was measured at the beginning, in the middle and at the end of the illumination on a visual analogue scale (VAS). Patients were blinded to the photosensitiser that was used. For patients with multiple lesions, the illumination was performed in the order of randomisation for each lesion at the same session.

Post-treatment reactions were photographed 8–14 days after the first PDT session, prior to the second treatment. Visual evaluation was performed on a five-point-scale (none/minimal/mild/moderate/severe) by an experienced dermatologist blinded to the photosensitiser that was used.

At the three-month follow-up visit, the blinded observer assessed the response to treatment with clinically guided 3-mm punch biopsies. The cosmetic outcome was visually evaluated on a four-point-scale (excellent/good/fair/poor).

## 4.7 Tissue sampling for histopathology

In study I, the first four lesions were excised directly after imaging with a 5-mm margin. In the rest of the LM/LMM, a diagnostic 3-mm punch biopsy was taken from the HIS-suspected site of invasion after imaging and interpretation. Subsequently, LM was excised with a 5-mm margin and LMM with a 10-mm margin. Both biopsies and specimens from the final excision were used in the results to analyse if the HIS-suspected invasion site could be confirmed in histopathology. All specimens were prepared with routine techniques and MART1 staining if needed. All specimens were assessed by an experienced dermatopathologist blinded to the HIS findings.

In study II, post-imaging 3-mm biopsies were taken from HIS-suspected subclinical extension sites, if the patient had an operation scheduled for another day than the imaging day. Finally, all lesions were excised with the same technique, where BCC was excised at the clinically defined tumour border, and the margin was excised as a separate 2-mm circumferential strip. Thus, in analyses we were able to assess if BCC was found in the margin strip specimens, and if a subclinical extension existed. If a margin was reported in the excised tumour piece, this could be interpreted as the actual tumour being smaller than was clinically assessed. If the margin in the tumour piece was reported to be <1 mm, this was interpreted as the tumour being of the same size as was clinically assessed.

All specimens were marked with an orientation for histopathological analyses. Specimens were prepared with routine techniques with tightly sectioned margin strips. If HIS gave grounds for suspecting a subclinical extension, additional slices

were sectioned from the suspected site in the margin strip. HIS findings were compared to histopathology. All specimens were assessed by an experienced dermatopathologist blinded to the HIS findings.

In study III, clinical diagnosis was confirmed with 3-mm punch biopsies. Prior to any procedures, the lesion, 5-mm margin area and the site of the punch biopsy were marked on plastic sheets with scaling (1x1mm squares). These sheets were used as guidance during the follow-up visit to obtain a control 3-mm punch biopsy near the original biopsy site. Additional 3-mm punch biopsies were taken from clinically suspicious sites, if needed. Non-responsive lesions were excised to see if aggressive growth patterns existed. All specimens were assessed by an experienced pathologist blinded to the treatment.

## 4.8 Statistical analyses and calculations on accuracy

In study I and II, the calculations on the performance and accuracy of the imaging system were performed by the authors.

For study III, statistical analyses were performed by a professional statistician, Mika Helminen from Tampere University Hospital, who used SPSS 23.0 (IBM SPSS Statistics for Windows, Version 23.0. Armonk, NY: IBM Corp.), or the mathematician of our study group, Ilkka Pölönen from the University of Jyväskylä, with Python 3.6 using Numpy and Scipy libraries.

To compare the efficacy, cosmetic outcome and post-treatment reactions of the treatment arms, Fisher's exact test was used. In pain results, the comparison between the arms was calculated with the Kruskal-Wallis test, and comparison between the sessions was calculated with the Wilcoxon Signed Rank Test. In fluorescence and photobleaching, the comparison between the arms was calculated with ANOVA, and the Chi Square test was used for studying the correlation between efficacy, fluorescence and photobleaching.

# 5 SUMMARY OF RESULTS

## 5.1 Study I

In histopathology, 10/32 lesions were LMM with a Breslow thickness of 0.4–1.6 mm (mean 0.85mm), and 22/32 were LM. With HIS, 9/10 invasion sites were recognised as LMM (true positives), but in 1/10 of LMM cases the invasion site was not suspected in HIS abundance maps, thus being a false negative.

In 19/22 of LM cases, there was no suspicion of invasion based on HIS abundance maps (true negatives), but in 3/22 LM cases there was a suspected invasion site in HIS abundance maps without histopathological confirmation, thus being false positives.

These results give HIS a positive predictive value of 75%, a negative predictive value of 95%, a sensitivity of 90% and a specificity of 86.3%.

In HIS abundance maps, the LM lesions were seen as white homogeneous areas corresponding to the end member of LM, but in the case of LMM there was a hole (invasion site) inside the homogeneous white area (LM part of LMM). Furthermore, in the case of LMM, an additional end member and thus an additional abundance map was created in HIS analyses from the invasion site. In this map the above-mentioned "hole" was represented as a separate clear white area, representing the end member of LMM. Figure 1 of the original publication I of this dissertation presents an example of a LMM and the abundance maps of the LMM. Thus, the spectra of LMM differed from LM, and furthermore both differed from healthy skin. This can be shown as differing hyperspectral graphs (Figure 11).

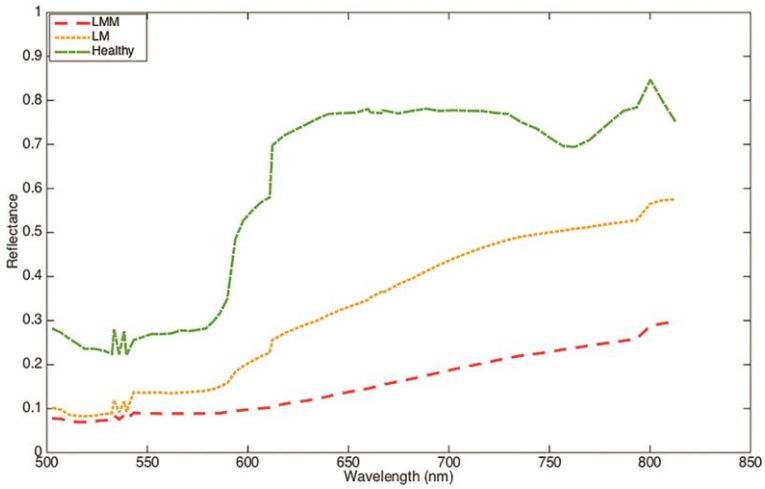


**Figure 11.** Unique hyperspectral graphs of LMM, LM, and healthy skin, Courtesy of Ilkka Pölönen.

## 5.2 Study II

In histopathology, 10/16 BCCs were aggressive subtypes, and 6/16 were nodular, superficial or a mixed type of these two. Clinically, all were ill-defined.

HIS delineated 12/16 BCCs more accurately compared to clinical evaluation. In these, 4/16 were more widely delineated by HIS and confirmed in histopathology. Figure 2 of the original publication II of this dissertation presents an example case of an ill-defined BCC, were HIS delineated the lesion to be wider compared to clinical examination. Furthermore, 8/16 were more narrowly delineated by HIS and confirmed in histopathology. There were 2/16 false positive cases, where HIS delineated the lesion wider without histopathological confirmation, and 2/16 false negative cases, where HIS did not detect the subclinical extension found in histopathology. All four mathematical models gave similar results, but it is still unclear which model works best on BCC, and which has the least artefacts. Based on the results of study II, HIS seems to be a promising clinical aid for a clinician, but the results of the pilot study need to be confirmed in larger trials.

## 5.3 Study III

A total of 54 patients with 95 lesions completed the study. A total of 98 lesions fulfilled all the inclusion criteria, thus the number of 98 lesions is used for the intention-to-treat analyses, even though 117 lesions were randomised. In our protocol of randomised lesions, those which were not BCC were excluded after we received histopathological reports. The protocol was designed in this way due to feasibility and limited resources.

At the three-month follow-up, there were histologically verified, non-responsive lesions in all groups: 1/31 in MAL, 3/33 in BF-200 ALA and 2/31 in HAL group. The efficacies with histological verification with intention-to-treat analyses are 93.8% (95% CI 79.9%-98.3%) for MAL, 90.9% (95% CI 76.4%-96.9%) for BF-200 ALA and 87.9% (95% CI 72.7%-95.2%) for HAL ($p$=0.84).

All secondary outcomes of the trial were analysed as described in the protocol. The cosmetic outcome was good or excellent for 77.4% in MAL group, 75.7% in BF-200 ALA, and 61.3% for HAL with no significant differences between the arms ($p$=0.61).

In tolerability, no differences between the arms were found in post-treatment reaction ($p$=0.49). In pain during illumination, there were no differences between the arms (for 4 min and 8 min timepoints all $p$-values >0.18). In comparison of pain between the sessions, in the HAL group the pain differed between the first and second PDT sessions (4 min $p$=0.006, 8 min $p$=0.005). In other arms, no differences were found in the level of pain between the sessions (MAL 4 min $p$=0.17, 8 min $p$=0.79; BF-200 ALA 4 min $p$=0.45, 8 min $p$=0.43).

Figure 3 of the original publication III of this dissertation presents a visual illustration of the cosmetic outcome, pain and post-treatment reaction results.

There was a loss of images in fluorescence analyses, and thus for the first PDT session 84 lesions in 49 patients were analysed, and for the second PDT session 91 lesions in 51 patients. When the arms were compared, there was lower fluorescence at the beginning of illumination in 2% HAL compared to 16% MAL and 7.8% BF-200 ALA (PDT I $p$=0.043 and PDT II $p$=0.043), but in photobleaching no significant differences were found between the arms (PDT I $p$=0.09 and PDT II $p$=0.42). There was no correlation between the histological clearance and photobleaching (PDT I $p$=0.40, PDT II $p$=0.77) or between the histological clearance and fluorescence (PDT I $p$=0.77, PDT II $p$=0.55) in our material. It should be noted that our fluorescence measurement set-up was experimental and not validated.

# 6 DISCUSSION

This dissertation was the first to report on the feasibility of a HIS in the delineation of ill-defined BCCs, and one of the first ones to report on the preliminary performance of the HIS in separating LMM from LM, and to actually visualise the localisation of the invasion site on a map. In the field of PDT, study III of this dissertation was the first to report on the efficacy of HAL in the treatment of non-aggressive BCCs.

## 6.1 Advantages and disadvantages of the hyperspectral imaging system

When considering the features of a non-invasive imaging system, the following should be discussed: the field of view (FOV), resolution, imaging depth, orientation and form of the provided images, time consumed to obtain the images, and time consumed to acquire the computational analyses. Furthermore, it should be considered whether the system provides a classification or diagnosis for the user, or if the user needs to interpret the images themselves. In the latter situation, the necessary level of expertise is essential when considering the level of healthcare the particular imaging system is practical to use in.

The advantages of HIS in non-invasive optical imaging are the following:

1) An adaptable FOV up to 12 $cm^2$, which is possible to obtain in a few seconds, compared to 1 $mm^2$ in conventional RCM, where it is possible to obtain 14 $mm^2$ per minute with mosaicking (Kose, Cordova et al. 2014), or compared to conventional OCT, where 25 $mm^2$ is obtained in 40 seconds (Cheng, Guitera 2015).

2) The adaptable filter is capable of reaching otherwise impracticable areas such as around the eyes and ears.

3) An imaging depth of approximately 2 mm. The depth of HIS is similar to that achieved with conventional OCT, compared to 250–300 µm in RCM. However, in OCT the superior resolution achieved with newer devices is compromised with a

loss in imaging depth (Cheng, Guitera 2015, Kang, Bahadoran et al. 2010, Reddy, Nguyen 2019).

4) Computational analyses are quick, taking about 5–10 minutes to provide the HIS images, i.e. abundance maps. As computational analyses are part of the imaging system, in the future it will be easy to add artificial intelligence to the analyses.

5) The interpretation of the abundance maps is easy to learn.

The disadvantages of the HIS are the following:

1) Lateral resolution of approximately 125 μm, compared to 1 μm in RCM (Que 2016), or to 10–15 μm in conventional OCT (with 2 mm depth), or 1–3 μm in high-definition OCT (with 570–750 μm depth), or 7.5 μm in frequency/Fourier-domain OCT (with 1.2–1.8 mm depth) (Reddy, Nguyen 2019).

2) Artefacts of the imaging, which can reduce the quality of abundance maps. Artefacts that we have noticed are very light skin type, which can cause excessive reflectance, and rounded or sharp surfaces, which can also create artefacts in the imaging.

3) Exact depth measurements are not provided. At the moment, HIS does not provide vertical sections or 3D images. With the current system it is possible to obtain 2D images, although in these 2D abundance maps the information is obtained from the hyperspectral graph, which contains information from the whole imaging depth.

4) Mathematical modelling and computational analyses only provide assumptions of the reality, but if the assumptions can be proved to be correct in a clinical trial, then the system is useful.

5) At the moment, we do not have any knowledge concerning how the system works on dark skin types.

Considering the current features of our HIS, i.e. easy, fast, and adaptable, the possible users could be specialists from different fields who treat large numbers of lesions, like dermatologists, ear-nose-throat specialists and plastic surgeons. HIS could be a useful tool in preoperative margin assessment and a useful tool for clinicians to obtain biopsies from an optimal site to achieve a correct histopathological diagnosis.

At the moment, HIS is not a diagnostic tool that could provide the diagnosis in equivocal lesions akin to RCM, but HIS can provide additional information when the diagnosis is based on some other method. The right place for RCM could be highly specialized skin cancer centers, as RCM demands a high level of expertise, and extensive training to learn how to interpret the images on the cellular level.

HIS is a more straightforward system compared to RCM when considering the interpretation. Thus, HIS could also be useful in places with less expertise, but HIS could also be useful in high expertise centers, as another option in the toolbox.

HIS is currently an add-on tool, which provides subclinical information not possible to obtain by visual inspection or by a dermoscope.

## 6.2 Separating *in situ* melanoma versus invasive melanoma, and localising the site of invasion

Our results from study I showed that the hyperspectral graph is unique to LM and LMM, and thus these two lesions differ from each other in diffuse reflectance. Thus, it is possible to distinguish the two from each other based on the hyperspectral data. Nagaoka et al. have shown that the hyperspectral graphs of melanocytic nevi and LMM also differ from each other (Nagaoka, Kiyohara et al. 2015). Nagaoka et al. created a discrimination index from a hyperspectral data cube, which is capable of distinguishing melanoma from other pigmented skin lesions with good accuracy (Nagaoka, Kiyohara et al. 2015). We chose to create abundance maps, which also appeared capable of separating LM and LMM from each other with good accuracy. Furthermore, our abundance maps had the particular advantage of being able to localise and visualise the exact invasion site.

RCM performs well in the diagnosis of LM from other flat facial lesions with a LM score developed by Guitera et al., and interestingly in separating amelanotic lesions only, the sensitivity and specificity are higher for the LM score (Guitera, Pellacani et al. 2010). Pellacani et al. have introduced a RCM score for separating melanoma from equivocal melanocytic lesions with good accuracy (Pellacani, Guitera et al. 2007). However, if the goal is to separate LM from LMM, RCM is not the most suitable modality. This is due to its limited penetration depth: RCM reaches the epidermis and superficial papillary dermis (Que 2016), and the invasion is below these structures.

Mataca et al. showed that RCM is as just as useful as dermoscopy in guiding the clinician to obtain a representative biopsy (Mataca, Migaldi et al. 2018). When considering which method is capable of achieving the most robust histopathological criteria for diagnosis of LM/LMM, RCM is more accurate than dermoscopy and the naked eye, and dermoscopy is more accurate than the naked eye in guiding the biopsy site selection (Mataca, Migaldi et al. 2018). When these

two methods are compared to HIS, the advantage of HIS is its ability to visualise the exact invasion site *in vivo*.

In separating LM and LMM, measuring the depth of the lesion could be one option. Scanning the lesion with an imaging system that provides vertical sections also enables the localisation and measurement of the invasion site. OCT or high-frequency ultrasound (HFUS) are capable of measuring tumour depth. When comparing spectral-domain OCT (axial resolution 5.5 μm) to HFUS (axial resolution 16 μm) in the measurement of melanocytic lesions, Varkentin et al. reported that OCT is more precise than HFUS in measuring the depth, but both methods underestimated the depth when the thickness of the lesion increased. Thus, both perform best in lesions less than 1 mm in thickness (Varkentin, Mazurenka et al. 2017). Another study by Hinz et al. compared conventional OCT to HFUS in measuring the depth of melanocytic lesions, with the result of OCT having better correlation with histopathology. However, both technologies overestimated the depth (Hinz, Ehler et al. 2011). Conventional OCT with vertical sections seems to be capable of distinguishing melanoma *in situ*, invasive melanoma, junctional nevus, and compound nevus from each other (Moraes Pinto Blumetti, Tatiana Cristina, Cohen et al. 2015).

Dynamic OCT provides horizontal sections while speckle-variance OCT provides horizontal and vertical sections of the tumour microvasculature. De Carvalho et al. demonstrated that the microvascular pattern of melanoma correlates with the Breslow thickness (De Carvalho, Welzel et al. 2018). In a case report, De Carvalho et al. demonstrated that by imaging the microvasculature, the transformation of a junctional nevus to melanoma *in situ* could be visualised and localised with speckle-variance OCT (De Carvalho, Ciardo et al. 2016). Thus, both dynamic and speckle-variance OCT, and HIS seem to be promising options in preoperatively localising the site of invasion *in vivo*.

Furthermore, in LM/LMM the value of non-invasive imaging lies especially in its ability to guide the pathologist in obtaining the sections from the right place, as with wide lesions there exists a risk for error when using the traditional bread loafing technique. Thus, with correct diagnosis, the treatment and follow-up can be planned appropriately. HIS is an interesting option for this, as we demonstrated in our pilot study.

## 6.3 Detecting subclinical extensions in ill-defined basal cell carcinomas and recognising the true borders of the lesion

This study is the first to report results on non-invasive imaging of BCCs with a HIS. Our study showed that the HIS delineated the margins more accurately in 75% of the clinically ill-defined lesions and revealed a subclinical extension in 25% of the lesions, compared to clinical evaluation with a dermoscope.

Even though dermoscopy is an excellent aid for diagnosing BCC, it has not proved to be capable of revealing subclinical extensions in ill-defined BCC. For example, dermoscopic margin assessment has not reduced the stages in MMS compared to visual inspection alone (Jayasekera, Dodd et al. 2018). The same is true for high-frequency ultrasound, which also did not reduce the stages in MMS compared to visual inspection (Marmur, Berkowitz et al. 2010).

Similarly to what we showed, Venturini et al. demonstrated that with RCM, in 30 % of cases a subclinical extension in ill-defined BCC was revealed (Venturini, Gualdi et al. 2016). Aggressive BCCs are often ill-defined, and subclinical extensions can lie deeper than the maximum penetration depth of RCM. Thus, the HIS makes it possible to obtain more subclinical information.

With Fourier-domain OCT, the subclinical extension was revealed to be present in 21 % of the BCCs treated with MMS, with no false positive or false negative cases (Wang, Meekings et al. 2013). Interestingly, Fourier-domain combined with dynamic OCT is capable of visualising BCCs in 3D form, which is an exciting step toward detecting the true dimensions of BCC *in vivo*.

Non-invasive imaging could have an impact on treatment capacity as the number of re-excisions could be reduced, and resources of MMS could be directed to the most high-risk cases where it is truly needed. It could be speculated that non-invasive imaging could reduce the number of high-risk BCCs by preventing several recurrent lesions. A recurrence in high-risk location is always a high-risk BCC, and aggressive subtypes often have subclinical extensions. Thus, if subclinical extensions are revealed, perhaps recurrences could be avoided.

The performance of the HIS should be confirmed in larger trials than this pilot study, but based on our results, HIS seems to be an interesting option for preoperative lateral margin assessment in ill-defined BCC.

## 6.4 Advantages and disadvantages of non-invasive treatments of non-aggressive basal cell carcinoma

Efficacy and recurrence rate are not the only parameters affecting a clinician's treatment decision for BCC. If the lesion is solitary and operable, the decision is easy, as surgery is the most effective treatment with few recurrences.

Sometimes, BCC can be a chronic condition with multiple primaries and multiple recurrences. When the treatment needs to be repeated multiple times, surgery is not always the best option. The patient's preferences and demographics can also affect the choice of treatment. Examples of these are cosmetic outcome, age of the patient, or the logistics involved in patients coming to the treatment. In the case of aggressive BCCs, the choice is easy: surgery is the most effective and recommended option. However, in the case of non-aggressive and low risk tumours, there is room for non-invasive options. When there are multiple options for non-invasive treatment, the decision on the choice of treatment should be made in cooperation with the patient by explaining the adverse events and treatment protocols.

The following can be regarded as advantages of non-invasive treatment:

1) Cost-effectiveness
2) Cosmetic outcome
3) Possibility to treat multiple lesions at once
4) Possibility to easily treat wide areas
5) Possibility for application at home (easy for patient, if arriving to treatment or time spent in treatment are an issue, minimization of consumed resources)

The following can be regarded as disadvantages:

6) Loss of control in histological clearance
7) Lower efficacy compared to surgery
8) Higher risk for recurrence compared to surgery
9) Possibility for application at home (demands good patient selection and compliance, as there is a loss of control for treatment delivery)

As the number of BCCs is constantly rising, the number of non-invasive treatments is also likely to increase in the future. In non-invasive treatment, the control of treatment outcome and follow-up are essential when considering the risk

for recurrence. At the moment, the clinical practice is to evaluate the treatment outcome visually with a dermoscope, and by obtaining punch biopsies, if needed. Non-invasive imaging could offer a more accurate surveillance of the treatment in the future, and thus decrease the risk for error in the assessment of treatment outcome.

## 6.5 Possible advantages of hexylaminolevulinate

In our results, we showed that with 2% HAL, a similar lesion clearance can be achieved as with 7.8% BF-200 ALA or 16% MAL in PDT of non-aggressive BCCs, with no differences in adverse events.

Preclinical studies present some evidence that HAL could be more effective in equimolar doses compared to MAL and 5-ALA (Morrow, McCarron et al. 2010). Preclinical evidence also shows that due to its lipophilic nature, HAL could be used in PDT at lower concentrations, as HAL induces stronger fluorescence, i.e. PpIX accumulation, when compared to the more hydrophilic MAL or 5-ALA (Kiesslich, Helander et al. 2014, Togsverd-Bo, Lerche et al. 2012, Togsverd-Bo, Idorn et al. 2012). Our results support these findings from preclinical studies.

In a safety study, Neittaanmäki-Perttu et al. reported that 0.2% and 2% HAL are significantly less painful on healthy human skin compared to 7.8% BF-200 ALA and 16% MAL, when illuminated with red light (Neittaanmaki-Perttu, Neittaanmaki et al. 2016). Thus, it seems that with a low concentration, pain could be reduced. In our results, there were no differences between the three photosensitisers in the level of pain when treating BCC with red light. One reason behind this could be that the accumulation of an exogenous photosensitiser is tumour tissue-selective (Kennedy, Pottier et al. 1990), and that metabolically active and proliferating tumour cells accumulate more PpIX (Wang, Shi et al. 2017). We did not find differences in the level of pain for sBCC. Perhaps the pain sensation threshold is exceeded anyhow in tumour cells, and when using low concentrations on healthy human skin, this threshold is not exceeded, but higher concentrations on healthy human skin exceed the threshold.

With regard to the efficacy of HAL, the 2% concentration might be suboptimal for the treatment of sBCC. The same may also be true for the three-hour incubation time. Thus, a dose-determining study with different concentrations and incubation times should be performed with HAL in the future. By optimizing the protocol, the efficacy of low concentration HAL-PDT could potentially be

increased. Interestingly, when an ultralow concentration of 0.2% HAL was used for daylight-PDT of thin actinic keratosis, Neittaanmäki et al. achieved a similar lesion clearance as with 16% MAL at the one-year time point (Neittaanmaki-Perttu, Karppinen et al. 2017). So, for different types of lesions the optimal concentration could vary.

With regard to the cost-effectiveness, some savings could be made in manufacturing a low-concentration HAL cream, as a good outcome is achieved already at low concentrations. Furthermore, new and effective options in photosensitisers provide competition to the market, as there are currently few photosensitiser options in dermatological PDT. Thus, HAL is an interesting option for dermatological PDT, as there could be some advantages in the use of low concentrations without compromising the response rate, as we showed in our trial.

## 6.6 Usefulness of local infiltration anesthesia

The exact mechanism of pain during PDT is unclear, but the pain sensation probably arises from apoptosis and necrosis caused by radical oxygen species created during the PDT reaction, or due to the direct effect of radical oxygen species on neurons (Wang, Shi et al. 2017). Regardless of the exact mechanism, nociceptive neurons are stimulated and thus a sensation of pain is created. In the head and neck area, nerve blocking is a good pain management method (Wang, Shi et al. 2017, Paoli, Halldin et al. 2008), but for solitary lesions local anesthetics are more practical.

The studies on local infiltration anesthesia are few. Borelli et al. used subcutaneous infiltration anesthesia during illumination as a continuous infusion of Ringer solution with ropivacaine, prilocaine and epinephrine in a split-half-face-trial, in the treatment of treated extensive facial actinic keratosis with 5-ALA-PDT (Borelli, Herzinger et al. 2007). There was a significant difference in pain, as subcutaneous infiltration anesthesia was a more effective pain management method when compared to oral analgesia with an air-cooling device (Borelli, Herzinger et al. 2007). Debu et al. have a case report on a paediatric patient with Gorlin syndrome, where a similar continuous infusion was used subcutaneously with good success in the treatment of multiple BCCs on the patient's back (Debu, Sleth et al. 2012).

In our results, the mean and median pain score was 2.3 on the VAS scale for the treatment of sBCC with a local, long-acting infiltration anesthetic which was

injected three hours prior to illumination. In the PDT study on non-aggressive BCCs by Morton et al., the mean pain score on a numerical scale (1-10) was 4.5 without analgesia (Morton, Dominicus et al. 2018). Our study had similar inclusion criteria for tumour subtype and similar incubation time in PDT as Morton et al. Interestingly, Morton et al. used RhodoLED as a light source, which has a gradual increase in light dose, but a similar total dose of 37 J/cm$^2$ as Aktilite, which was used in our study. Zaar et al. have shown that RhodoLED causes significantly less pain compared to Aktilite (Zaar, Sjoholm Hylen et al. 2018). Yet, our pain scores were lower with our pain management method compared to Morton et al., even though we had the more painful light source.

Solid conclusions cannot be made when two different studies are compared. However, if our mean pain score of 2.3 is compared to the mean pain score of 4.5 in Morton et al.'s study, it seems that with our method some pain management is achieved, and thus further studies are warranted.

## 6.7 Strengths and limitations of the study

The strengths of the hyperspectral imaging studies were histopathological controls for the camera findings, the comparison of different mathematical models, and our operation technique in the ill-defined BCC study. MMS was not available to us, but with our operation technique the clinically assessed border was clearly marked, and comparisons to the findings of the hyperspectral camera were straightforward to do. An additional strength was that if there was a subclinical extension suspected by HIS in a specific site, additional sections were made for the histopathology of this site.

The limitations in the hyperspectral imaging studies include the rather small number of imaged lesions, the lack of in-depth visualisation, and the possible sources of artefacts in the imaging. Due to study I and II being pilot studies, it was not possible to calculate sample sizes.

In our clinical trial, strengths included the non-sponsored, randomised, controlled, prospective and double-blinded design, the histopathological confirmation of diagnosis and treatment outcome, as well as the excision of non-responsive lesions, as this allowed to evaluate if there were aggressive underlying subtypes of BCC.

The limitations of our PDT trial were its small sample size, and optimistic assumptions in the power calculations, including multiple lesions (possible

confounding factors for results), and taking biopsies during the first PDT session (healing due to inflammation induced by the biopsy can be a confounding factor). In pain analyses, the lack of a control group was a limitation. In fluorescence analyses, the lack of a validated fluorescence imaging system was a major limitation. It should also be noted that it was optimistic to assume that a low concentration HAL could be more effective than a high concentration MAL. Evaluating retrospectively, perhaps equal or non-inferior efficacies would have been more accurate assumptions.

## 6.8 Clinical implications

Our results showed the capability of the HIS to localise the invasion site in LMM and to detect the borders of ill-defined BCCs more accurately than by clinical assessment. Additionally, Neittaanmäki-Perttu et al. have shown that the same HIS is useful in the preoperative *in viv*o margin delineation of LM/LMM by revealing subclinical extensions (Neittaanmaki-Perttu, Gronroos et al. 2015). Thus, with HIS, the accuracy of diagnostic biopsies could be increased, the subclinical extensions could be revealed, and the number of re-excisions could be reduced by avoiding repeated visits and operations. In the future, the results of the pilot studies need to be confirmed. The HIS could be a useful aid for clinicians and should be further developed.

In PDT, our results support the findings of previous studies for the use of BF-ALA for PDT of sBCC. BF-200 ALA is a commercial product of Ameluz, and thus easily available for clinicians. Our results also provide a new HAL option, but as it is currently more for research use, it is not yet easily accessible. HAL is available as a powder used for the photodynamic diagnosis of bladder cancer, but should be commercialised as a cream before wider use in dermatological PDT. As photosensitisers are expensive raw materials, a low concentration cream could provide cost benefits in manufacturing. Although we did not find the novel photosensitisers to be superior, our results support the similarity of them, and thus offer more options for clinicians in PDT. Usually, multiple options are beneficial in the treatment of patients.

## 6.9 Future prospects

In the future, it would be interesting to explore whether the HIS is capable of converting the information into a 3D map of the tumour, or at least capable of obtaining vertical sections, which combined with current horizontal images would provide additional information for the clinician. The 3D information could potentially be acquired by combining hyperspectral imaging with OCT.

In the case of aggressive BCCs, it would be interesting to repeat the design of study II, but compare the results to MMS where 100% of the margins are assessed. In this way, it is likely that more precise information on the performance of HIS would be gained. This design could also possibly allow for the evaluation of whether hyperspectral imaging could reduce the stages of MMS. Furthermore, in the case of aggressive BCC, it would be interesting to investigate if the HIS could recognise a perineural invasion, as in LMM we showed that the invasion site could be localised. Perhaps the hyperspectral signature of perineural invasion is also unique.

Far in the future, if hyperspectral imaging proves to be an advantageous method in skin imaging, a library of skin lesions could be collected, and artificial intelligence could be combined to data processing. Thus, the HIS could also be used as a diagnostic method.

Furthermore, it would be interesting to study if the use of photosensitisers could improve the results of the HIS in tumour delineation. It would also be worthwhile to explore the performance of HIS in non-invasive treatment monitoring.

In PDT for HAL, a dose-finding study is warranted in the future. It would also be intriguing to study which incubation and illumination time (i.e. total light dose) are optimal in the treatment of non-aggressive BCCs. Additionally, it would be interesting to study if the efficacy of fractionated illumination increases with low-concentration HAL. Studies using HAL-PDT on carcinomas *in situ* and thick actinic keratosis are warranted and interesting to perform. Pain would be valuable to study with our pain management method in a controlled and randomised fashion in non-aggressive BCC and in carcinoma *in situ*, and it would also be interesting to include some pain measurement for a few post-procedural days.

# 7 CONCLUSIONS

The results of this dissertation introduce the potential of hyperspectral imaging in the treatment of BCC and LMM. Furthermore, this dissertation presents a first-time report on the efficacy of HAL in the treatment of non-aggressive BCCs.

The following conclusions can be drawn from the results of this dissertation:

1) The HIS is an interesting option in optical, non-invasive skin imaging in preoperative tumour assessment due to its demonstrated potential in visualising and localising subclinical findings.
2) Hyperspectral imaging could be a useful clinical tool as the system provides a large imaging field, good penetration depth, and fast reception and processing of subclinical visual data, which can be interpreted bedside.
3) Novel photosensitisers, BF-200 ALA and HAL, are not superior in efficacy, but have similar adverse event profiles as the widely used MAL in PDT of non-aggressive BCCs. HAL in particular is a new, interesting option for dermatological PDT, because it achieves a good efficacy already at low concentrations.
4) Infiltration of long-acting local anesthetics seems to reduce pain in non-aggressive BCCs during illumination.
5) A validated imaging system should be used to obtain reliable fluorescence images.

Thus, new options for skin cancer diagnosis and treatment are presented, although these results need to be confirmed in larger trials. This dissertation also provides plenty of ideas for further research.

# REFERENCES


AHLGRIMM-SIESS, V., HORN, M., KOLLER, S., LUDWIG, R., GERGER, A. and HOFMANN-WELLENHOF, R., 2009. Monitoring efficacy of cryotherapy for superficial basal cell carcinomas with in vivo reflectance confocal microscopy: a preliminary study. *Journal of Dermatological Science,* **53**(1), pp. 60-64.

AHNLIDE, I. and BJELLERUP, M., 2013. Accuracy of clinical skin tumour diagnosis in a dermatological setting. *Acta Dermato-Venereologica,* **93**(3), pp. 305-308.

ALARCON, I., CARRERA, C., ALOS, L., PALOU, J., MALVEHY, J. and PUIG, S., 2014. In vivo reflectance confocal microscopy to monitor the response of lentigo maligna to imiquimod. *Journal of the American Academy of Dermatology,* **71**(1), pp. 49-55.

ANG, J.M., RIAZ, I.B., KAMAL, M.U., PARAGH, G. and ZEITOUNI, N.C., 2017. Photodynamic therapy and pain: A systematic review. *Photodiagnosis & Photodynamic Therapy,* **19**, pp. 308-344.

AOUDE, L.G., WADT, K.A.W., PRITCHARD, A.L. and HAYWARD, N.K., 2015. Genetics of familial melanoma: 20 years after CDKN2A. *Pigment Cell & Melanoma Research,* **28**(2), pp. 148-160.

APALLA, Z., LALLAS, A., SOTIRIOU, E., LAZARIDOU, E., VAKIRLIS, E., TRAKATELLI, M., KYRGIDIS, A. and IOANNIDES, D., 2016. Farmers develop more aggressive histologic subtypes of basal cell carcinoma. Experience from a Tertiary Hospital in Northern Greece. *Journal of the European Academy of Dermatology & Venereology,* **30**(Suppl 3), pp. 17-20.

APALLA, Z., LALLAS, A., TZELLOS, T., SIDIROPOULOS, T., LEFAKI, I., TRAKATELLI, M., SOTIRIOU, E., LAZARIDOU, E., EVANGELOU, G., PATSATSI, A., KYRGIDIS, A., STRATIGOS, A., ZALAUDEK, I., ARGENZIANO, G. and IOANNIDES, D., 2014. Applicability of dermoscopy for evaluation of patients' response to nonablative therapies for the treatment of superficial basal cell carcinoma. *British Journal of Dermatology,* **170**(4), pp. 809-815.

ARITS, A H M M., SCHLANGEN, M.H.J., NELEMANS, P.J. and KELLENERS-SMEETS, N.W.J., 2011. Trends in the incidence of basal cell carcinoma by histopathological subtype. *Journal of the European Academy of Dermatology & Venereology,* **25**(5), pp. 565-569.

ARITS, AIMEE H M M, MOSTERD, K., ESSERS, B.A., SPOORENBERG, E., SOMMER, A., DE ROOIJ, MICHETTE J M, VAN PELT, HAN P A, QUAEDVLIEG, P.J.F., KREKELS, G.A.M., VAN NEER, PIERRE A F A, RIJZEWIJK, J.J., VAN GEEST, A.J., STEIJLEN, P.M., NELEMANS, P.J. and KELLENERS-SMEETS, N.W.J., 2013. Photodynamic therapy versus topical imiquimod versus topical fluorouracil for treatment of superficial basal-cell carcinoma: a single blind, non-inferiority, randomised controlled trial. *Lancet Oncology,* **14**(7), pp. 647-654.

ARMSTRONG, B.K. and KRICKER, A., 2001. The epidemiology of UV induced skin cancer. *Journal of Photochemistry & Photobiology.B - Biology,* **63**(1-3), pp. 8-18.

ARMSTRONG, B.K. and CUST, A.E., 2017. Sun exposure and skin cancer, and the puzzle of cutaneous melanoma: A perspective on Fears et al. Mathematical models of age and ultraviolet effects on the incidence of skin cancer among whites in the United States. American Journal of Epidemiology 1977; 105: 420-427. *Cancer Epidemiology,* **48**, pp. 147-156.

AXELROD, M.L., JOHNSON, D.B. and BALKO, J.M., 2018. Emerging biomarkers for cancer immunotherapy in melanoma. *Seminars in Cancer Biology,* **52**(Pt 2), pp. 207-215.

BADER, M.J., STEPP, H., BEYER, W., PONGRATZ, T., SROKA, R., KRIEGMAIR, M., ZAAK, D., WELSCHOF, M., TILKI, D., STIEF, C.G. and WAIDELICH, R., 2013. Photodynamic therapy of bladder cancer - a phase I study using hexaminolevulinate (HAL). *Urologic Oncology,* **31**(7), pp. 1178-1183.

BARTON, D.T., ZENS, M.S., NELSON, H.H., CHRISTENSEN, B.C., STORM, C.A., PERRY, A.E. and KARAGAS, M.R., 2016. Distinct Histologic Subtypes and Risk Factors for Early Onset Basal Cell Carcinoma: A Population-Based Case Control Study from New Hampshire. *Journal of Investigative Dermatology,* **136**(2), pp. 533-535.

BARTON, V., ARMESON, K., HAMPRAS, S., FERRIS, L.K., VISVANATHAN, K., ROLLISON, D. and ALBERG, A.J., 2017. Nonmelanoma skin cancer and risk of all-cause and cancer-related mortality: a systematic review. *Archives of Dermatological Research,* **309**(4), pp. 243-251.

BATH-HEXTALL, F., LEONARDI-BEE, J., SOMCHAND, N., WEBSTER, A., DELITT, J. and PERKINS, W., 2007. Interventions for preventing non-melanoma skin cancers in high-risk groups. *Cochrane Database of Systematic Reviews,* (4), pp. CD005414.

BAY, C., LERCHE, C.M., FERRICK, B., PHILIPSEN, P.A., TOGSVERD-BO, K. and HAEDERSDAL, M., 2017. Comparison of Physical Pretreatment Regimens to Enhance Protoporphyrin IX Uptake in Photodynamic Therapy: A Randomized Clinical Trial. *JAMA Dermatology,* **153**(4), pp. 270-278.

BENTZEN, J., KJELLBERG, J., THORGAARD, C., ENGHOLM, G., PHILLIP, A. and STORM, H.H., 2013. Costs of illness for melanoma and nonmelanoma skin cancer in Denmark. *European Journal of Cancer Prevention,* **22**(6), pp. 569-576.

BERLIN, N.L., FERRUCCI, L.M., CARTMEL, B., WANG, S., LEFFELL, D.J., MCNIFF, J.M. and MAYNE, S.T., 2015. Subsequent skin cancer in patients with early-onset basal cell carcinoma. *Australasian Journal of Dermatology,* **56**(3), pp. 236-237.

BETTI, R., RADAELLI, G., BOMBONATO, C., CROSTI, C., CERRI, A. and MENNI, S., 2010. Anatomic location of Basal cell carcinomas may favor certain histologic subtypes. *Journal of Cutaneous Medicine & Surgery,* **14**(6), pp. 298-302.

BOEHRINGER, A., ADAM, P., SCHNABL, S., HAFNER, H. and BREUNINGER, H., 2015. Analysis of incomplete excisions of basal-cell carcinomas after breadloaf microscopy compared with 3D-microscopy: a prospective randomized and blinded study. *Journal of Cutaneous Pathology,* **42**(8), pp. 542-553.

BORELLI, C., HERZINGER, T., MERK, K., BERKING, C., KUNTE, C., PLEWIG, G. and DEGITZ, K., 2007. Effect of subcutaneous infiltration anesthesia on pain in photodynamic therapy: a controlled open pilot trial. *Dermatologic Surgery,* **33**(3), pp. 314-318.

BORSARI, S., PAMPENA, R., LALLAS, A., KYRGIDIS, A., MOSCARELLA, E., BENATI, E., RAUCCI, M., PELLACANI, G., ZALAUDEK, I., ARGENZIANO, G. and LONGO, C., 2016. Clinical Indications for Use of Reflectance Confocal Microscopy for Skin Cancer Diagnosis. *JAMA Dermatology,* **152**(10), pp. 1093-1098.

BRUNSSEN, A., WALDMANN, A., EISEMANN, N. and KATALINIC, A., 2017. Impact of skin cancer screening and secondary prevention campaigns on skin cancer incidence and mortality: A systematic review. *Journal of the American Academy of Dermatology,* **76**(1), pp. 129-139.e10.

BURDON-JONES, D. and THOMAS, P.W., 2006. One-fifth of basal cell carcinomas have a morphoeic or partly morphoeic histology: implications for treatment. *Australasian Journal of Dermatology,* **47**(2), pp. 102-105.

CAKIR, B.O., ADAMSON, P. and CINGI, C., 2012. Epidemiology and economic burden of nonmelanoma skin cancer. *Facial Plastic Surgery Clinics of North America,* **20**(4), pp. 419-422.

CAMPBELL, C.L., BROWN, C.T.A., WOOD, K., SALVIO, A.G., INADA, N.M., BAGNATO, V.S. and MOSELEY, H., 2017. A quantitative study of in vivo protoporphyrin IX fluorescence build up during occlusive treatment phases. *Photodiagnosis & Photodynamic Therapy,* **18**, pp. 204-207.

CANCER GENOME ATLAS NETWORK, 2015. Genomic Classification of Cutaneous Melanoma. *Cell,* **161**(7), pp. 1681-1696.

CASAS, A., PEROTTI, C., FUKUDA, H., ROGERS, L., BUTLER, A.R. and BATLLE, A., 2001. ALA and ALA hexyl ester-induced porphyrin synthesis in chemically induced skin tumours: the role of different vehicles on improving photosensitization. *British Journal of Cancer,* **85**(11), pp. 1794-1800.

CHEN, A.C., MARTIN, A.J., CHOY, B., FERNANDEZ-PENAS, P., DALZIELL, R.A., MCKENZIE, C.A., SCOLYER, R.A., DHILLON, H.M., VARDY, J.L., KRICKER, A., ST GEORGE, G., CHINNIAH, N., HALLIDAY, G.M. and DAMIAN, D.L., 2015. A Phase 3 Randomized Trial of Nicotinamide for Skin-Cancer Chemoprevention. *New England Journal of Medicine,* **373**(17), pp. 1618-1626.

CHEN, T., BERTENTHAL, D., SAHAY, A., SEN, S. and CHREN, M., 2007. Predictors of skin-related quality of life after treatment of cutaneous basal cell carcinoma and squamous cell carcinoma. *Archives of Dermatology,* **143**(11), pp. 1386-1392.

CHENG, H.M. and GUITERA, P., 2015. Systematic review of optical coherence tomography usage in the diagnosis and management of basal cell carcinoma. *British Journal of Dermatology,* **173**(6), pp. 1371-1380.

CHETTY, N.C., OSBORNE, V. and HARLAND, C., 2008. Amelanotic melanoma in situ: lack of sustained response to photodynamic therapy. *Clinical & Experimental Dermatology,* **33**(2), pp. 204-206.

CHREN, M., SAHAY, A.P., BERTENTHAL, D.S., SEN, S. and LANDEFELD, C.S., 2007. Quality-of-life outcomes of treatments for cutaneous basal cell carcinoma and squamous cell carcinoma. *Journal of Investigative Dermatology,* **127**(6), pp. 1351-1357.

CINOTTI, E., LABEILLE, B., DEBARBIEUX, S., CARRERA, C., LACARRUBBA, F., WITKOWSKI, A.M., MOSCARELLA, E., ARZBERGER, E., KITTLER, H., BAHADORAN, P., GONZALEZ, S., GUITERA, P., AGOZZINO, M., FARNETANI, F., HOFMANN-WELLENHOF, R., ARDIGO, M., RUBEGNI, P., TOGNETTI, L., LUDZIK, J., ZALAUDEK, I., ARGENZIANO, G., LONGO, C., RIBERO, S., MALVEHY, J., PELLACANI, G., CAMBAZARD, F. and PERROT, J.L., 2018. Dermoscopy vs. reflectance confocal microscopy for the diagnosis of lentigo maligna. *Journal of the European Academy of Dermatology & Venereology,* **32**(8), pp. 1284-1291.

COLLIER, N.J., HAYLETT, A.K., WONG, T.H., MORTON, C.A., IBBOTSON, S.H., MCKENNA, K.E., MALLIPEDDI, R., MOSELEY, H., SEUKERAN, D., WARD, K.A., MOHD MUSTAPA, M.F., EXTON, L.S., GREEN, A.C. and RHODES, L.E., 2018. Conventional and combination topical photodynamic therapy for basal cell carcinoma: systematic review and meta-analysis. *British Journal of Dermatology,* **179**(6), pp. 1277-1296.

COORY, M., BAADE, P., AITKEN, J., SMITHERS, M., MCLEOD, G.R.C. and RING, I., 2006. Trends for in situ and invasive melanoma in Queensland, Australia, 1982-2002. *Cancer Causes & Control,* **17**(1), pp. 21-27.

COUZAN, C., CINOTTI, E., LABEILLE, B., VERCHERIN, P., RUBEGNI, P., CAMBAZARD, F. and PERROT, J.L., 2018. Reflectance confocal microscopy identification of subclinical basal cell carcinomas during and after vismodegib treatment. *Journal of the European Academy of Dermatology & Venereology,* **32**(5), pp. 763-767.

COX, N.H., AITCHISON, T.C. and MACKIE, R.M., 1998. Extrafacial lentigo maligna melanoma: analysis of 71 cases and comparison with lentigo maligna melanoma of the head and neck. *British Journal of Dermatology,* **139**(3), pp. 439-443.

COX, N.H., AITCHISON, T.C., SIREL, J.M. and MACKIE, R.M., 1996. Comparison between lentigo maligna melanoma and other histogenetic types of malignant melanoma of the head and neck. Scottish Melanoma Group. *British Journal of Cancer,* **73**(7), pp. 940-944.

CROWSON, A.N., 2006. Basal cell carcinoma: biology, morphology and clinical implications. *Modern Pathology,* **19**(Suppl 2), pp. 127.

CUST, A.E., MISHRA, K. and BERWICK, M., 2018. Melanoma - role of the environment and genetics. *Photochemical & Photobiological Sciences,* **17**(12), pp. 1853-1860.

DE CARVALHO, N., CIARDO, S., CESINARO, A.M., JEMEC, G., ULRICH, M., WELZEL, J., HOLMES, J. and PELLACANI, G., 2016. In vivo micro-angiography by means of speckle-variance optical coherence tomography (SV-OCT) is able to detect microscopic vascular changes in naevus to melanoma transition. *Journal of the European Academy of Dermatology & Venereology,* **30**(10), pp. e67-e68.

DE CARVALHO, N., WELZEL, J., SCHUH, S., THEMSTRUP, L., ULRICH, M., JEMEC, G.B.E., HOLMES, J., KALECI, S., CHESTER, J., BIGI, L., CIARDO, S. and PELLACANI, G., 2018. The vascular morphology of melanoma is related to Breslow index: An in vivo study with dynamic optical coherence tomography. *Experimental dermatology,* **27**(11), pp. 1280-1286.

DE VRIES, E., MICALLEF, R., BREWSTER, D.H., GIBBS, J.H., FLOHIL, S.C., SAKSELA, O., SANKILA, R., FORREST, A.D., TRAKATELLI, M., COEBERGH, J.W.W., PROBY, C.M. and EPIDERM GROUP, 2012. Population-based estimates of the occurrence of multiple vs first primary basal cell carcinomas in 4 European regions. *Archives of Dermatology,* **148**(3), pp. 347-354.

DEADY, S., SHARP, L. and COMBER, H., 2014. Increasing skin cancer incidence in young, affluent, urban populations: a challenge for prevention. *British Journal of Dermatology,* **171**(2), pp. 324-331.

DEBU, A., SLETH, J., GIRARD, C., BESSIS, D., GUILLOT, B. and BLATIERE, V., 2012. The use of subcutaneous infusion tumescent anesthesia in photodynamic therapy pain control. *Paediatric Anaesthesia,* **22**(6), pp. 600-601.

DESSINIOTI, C., ANTONIOU, C., KATSAMBAS, A. and STRATIGOS, A.J., 2010. Basal cell carcinoma: what's new under the sun. *Photochemistry & Photobiology,* **86**(3), pp. 481-491.

DEWANE, M.E., KELSEY, A., OLIVIERO, M., RABINOVITZ, H. and GRANT-KELS, J.M., 2019. Melanoma on chronically sun-damaged skin: Lentigo maligna and desmoplastic melanoma. *Journal of the American Academy of Dermatology,* **81**(3), pp. 823-833.

DICKER, D.T., LERNER, J., VAN BELLE, P., BARTH, S.F., GUERRY D 4TH, HERLYN, M., ELDER, D.E. and EL-DEIRY, W.S., 2006. Differentiation of normal skin and melanoma using high resolution hyperspectral imaging. *Cancer Biology & Therapy,* **5**(8), pp. 1033-1038.

DICKER, D.T., KAHN, N., FLAHERTY, K.T., LERNER, J. and EL-DEIRY, W.S., 2011. Hyperspectral imaging: a non-invasive method of imaging melanoma lesions in a patient with stage IV melanoma, being treated with a RAF inhibitor. *Cancer Biology & Therapy,* **12**(4), pp. 326-334.

DINNES, J., DEEKS, J.J., CHUCHU, N., FERRANTE DI RUFFANO, L., MATIN, R.N., THOMSON, D.R., WONG, K.Y., ALDRIDGE, R.B., ABBOTT, R., FAWZY, M., BAYLISS, S.E., GRAINGE, M.J., TAKWOINGI, Y., DAVENPORT, C., GODFREY, K., WALTER, F.M., WILLIAMS, H.C. and COCHRANE SKIN CANCER DIAGNOSTIC TEST ACCURACY GROUP, 2018a. Dermoscopy, with and without visual inspection, for diagnosing melanoma in adults. *Cochrane Database of Systematic Reviews,* **12**, pp. 011902.

DINNES, J., DEEKS, J.J., CHUCHU, N., SALEH, D., BAYLISS, S.E., TAKWOINGI, Y., DAVENPORT, C., PATEL, L., MATIN, R.N., O'SULLIVAN, C., PATALAY, R., WILLIAMS, H.C. and COCHRANE SKIN CANCER DIAGNOSTIC TEST ACCURACY GROUP, 2018b. Reflectance confocal microscopy for diagnosing keratinocyte skin cancers in adults. *Cochrane Database of Systematic Reviews,* **12**, pp. 013191.

DINNES, J., DEEKS, J.J., SALEH, D., CHUCHU, N., BAYLISS, S.E., PATEL, L., DAVENPORT, C., TAKWOINGI, Y., GODFREY, K., MATIN, R.N., PATALAY, R., WILLIAMS, H.C. and COCHRANE SKIN CANCER DIAGNOSTIC TEST ACCURACY GROUP, 2018c. Reflectance confocal microscopy for diagnosing cutaneous melanoma in adults. *Cochrane Database of Systematic Reviews,* **12**, pp. 013190.

DIXON, A.J., ANDERSON, S.J., DIXON, M.P. and DIXON, J.B., 2015. Post procedural pain with photodynamic therapy is more severe than skin surgery. *Journal of Plastic, Reconstructive & Aesthetic Surgery,* **68**(2), pp. 28.

EDWARDS, S.J., OSEI-ASSIBEY, G., PATALAY, R., WAKEFIELD, V. and KARNER, C., 2017. Diagnostic accuracy of reflectance confocal microscopy using VivaScope for detecting and monitoring skin lesions: a systematic review. *Clinical & Experimental Dermatology,* **42**(3), pp. 266-275.

EISEMANN, N., WALDMANN, A., GELLER, A.C., WEINSTOCK, M.A., VOLKMER, B., GREINERT, R., BREITBART, E.W. and KATALINIC, A., 2014. Non-melanoma skin cancer incidence and impact of skin cancer screening on incidence. *Journal of Investigative Dermatology,* **134**(1), pp. 43-50.

ERICSON, M.B., GRAPENGIESSER, S., GUDMUNDSON, F., WENNBERG, A., LARKO, O., MOAN, J. and ROSEN, A., 2003. A spectroscopic study of the photobleaching of protoporphyrin IX in solution. *Lasers in Medical Science,* **18**(1), pp. 56-62.

ESSERS, B.A.B., ARITS, A.H., HENDRIKS, M.R., MOSTERD, K. and KELLENERS-SMEETS, N.W., 2018. Patient preferences for the attributes of a noninvasive treatment for superficial basal cell carcinoma: a discrete choice experiment. *British Journal of Dermatology,* **178**(1), pp. e26-e27.

FANTINI, F., GRECO, A., CESINARO, A.M., SURRENTI, T., PERIS, K., VASCHIERI, C., MARCONI, A., GIANNETTI, A. and PINCELLI, C., 2008. Pathologic changes after photodynamic therapy for Basal cell carcinoma and Bowen disease: a histologic and immunohistochemical investigation. *Archives of Dermatology,* **144**(2), pp. 186-194.

FARNETANI, F., MANFREDINI, M., CHESTER, J., CIARDO, S., GONZALEZ, S. and PELLACANI, G., 2019. Reflectance confocal microscopy in the diagnosis of pigmented macules of the face: differential diagnosis and margin definition. *Photochemical & Photobiological Sciences,* **18**(5), pp. 963-969.

FERRANTE DI RUFFANO, L., DINNES, J., DEEKS, J.J., CHUCHU, N., BAYLISS, S.E., DAVENPORT, C., TAKWOINGI, Y., GODFREY, K., O'SULLIVAN, C., MATIN, R.N., TEHRANI, H., WILLIAMS, H.C. and COCHRANE SKIN CANCER DIAGNOSTIC TEST ACCURACY GROUP, 2018. Optical coherence tomography for diagnosing skin cancer in adults. *Cochrane Database of Systematic Reviews,* **12**, pp. 013189.

FINK, C. and HAENSSLE, H.A., 2017. Non-invasive tools for the diagnosis of cutaneous melanoma. *Skin Research & Technology,* **23**(3), pp. 261-271.

FINNISH CANCER REGISTRY, Cancer 2017, a yearly report on the cancer statistics in Finland. Accessed [February 20th, 2020], *available online at https://syoparekisteri.fi/tilastot/syopa-2017-raportti/*

FLOHIL, S.C., PROBY, C.M., FORREST, A.D., VAN TIEL, S., SAKSELA, O., PITKANEN, S., AHTI, T., MICALLEF, R., DE VRIES, E. and EPIDERM GROUP, 2012. Basal cell carcinomas without histological confirmation and their treatment: an audit in four European regions. *British Journal of Dermatology,* **167**(Suppl 2), pp. 22-28.

FLOHIL, S.C., VAN DER LEEST, ROBERT J T, ARENDS, L.R., DE VRIES, E. and NIJSTEN, T., 2013. Risk of subsequent cutaneous malignancy in patients with prior keratinocyte carcinoma: a systematic review and meta-analysis. *European Journal of Cancer,* **49**(10), pp. 2365-2375.

FOTINOS, N., CAMPO, M.A., POPOWYCZ, F., GURNY, R. and LANGE, N., 2006. 5-Aminolevulinic acid derivatives in photomedicine: Characteristics, application and perspectives. *Photochemistry & Photobiology,* **82**(4), pp. 994-1015.

FRIEDMAN, R.J., GUTKOWICZ-KRUSIN, D., FARBER, M.J., WARYCHA, M., SCHNEIDER-KELS, L., PAPASTATHIS, N., MIHM MC JR, GOOGE, P., KING, R., PRIETO, V.G., KOPF, A.W., POLSKY, D., RABINOVITZ, H., OLIVIERO, M., COGNETTA, A., RIGEL, D.S., MARGHOOB, A., RIVERS, J., JOHR, R., GRANT-KELS, J.M. and TSAO, H., 2008. The diagnostic performance of expert dermoscopists vs a computer-vision system on small-diameter melanomas. *Archives of Dermatology,* **144**(4), pp. 476-482.

GAMBICHLER, T., SCHMID-WENDTNER, M.H., PLURA, I., KAMPILAFKOS, P., STUCKER, M., BERKING, C. and MAIER, T., 2015. A multicentre pilot study investigating high-definition optical coherence tomography in the differentiation of cutaneous melanoma and melanocytic naevi. *Journal of the European Academy of Dermatology & Venereology,* **29**(3), pp. 537-541.

GAMO-VILLEGAS, R., PAMPIN-FRANCO, A., FLORISTAN-MURUZABAL, U., GARCIA-ZAMORA, E., PINEDO-MORALEDA, F. and LOPEZ-ESTEBARANZ, J.L., 2019. Key dermoscopic signs in the diagnosis and progression of extrafacial lentigo maligna: Evaluation of a series of 41 cases. *Australasian Journal of Dermatology,* **60**(4), pp. 288-293.

GARBE, C., PERIS, K., HAUSCHILD, A., SAIAG, P., MIDDLETON, M., BASTHOLT, L., GROB, J., MALVEHY, J., NEWTON-BISHOP, J., STRATIGOS, A.J., PEHAMBERGER, H., EGGERMONT, A.M., EUROPEAN DERMATOLOGY FORUM, (., EUROPEAN ASSOCIATION OF DERMATO-ONCOLOGY, (EADO) and EUROPEAN ORGANISATION FOR RESEARCH AND TREATMENT OF CANCER, (EORTC), 2016. Diagnosis and treatment of melanoma: European consensus-based interdisciplinary guideline - Update 2016. *European Journal of Cancer,* 63, pp. 201-217.

GAUDI, S., MEYER, R., RANKA, J., GRANAHAN, J.C., ISRAEL, S.A., YACHIK, T.R. and JUKIC, D.M., 2014. Hyperspectral imaging of melanocytic lesions. *American Journal of Dermatopathology,* **36**(2), pp. 131-136.

GAUDY-MARQUESTE, C., MADJLESSI, N., GUILLOT, B., AVRIL, M. and GROB, J., 2009. Risk factors in elderly people for lentigo maligna compared with other melanomas: a double case-control study. *Archives of Dermatology,* **145**(4), pp. 418-423.

GAULIN, C., SEBARATNAM, D.F. and FERNANDEZ-PENAS, P., 2015. Quality of life in non-melanoma skin cancer. *Australasian Journal of Dermatology,* **56**(1), pp. 70-76.

GERSHENWALD, J.E. and SCOLYER, R.A., 2018. Melanoma Staging: American Joint Committee on Cancer (AJCC) 8th Edition and Beyond. *Annals of Surgical Oncology,* **25**(8), pp. 2105-2110.

GERSHENWALD, J.E., SCOLYER, R.A., HESS, K.R., SONDAK, V.K., LONG, G.V., ROSS, M.I., LAZAR, A.J., FARIES, M.B., KIRKWOOD, J.M., MCARTHUR, G.A., HAYDU, L.E., EGGERMONT, A.M.M., FLAHERTY, K.T., BALCH, C.M., THOMPSON, J.F. and FOR MEMBERS OF THE AMERICAN JOINT COMMITTEE ON CANCER MELANOMA EXPERT PANEL AND THE INTERNATIONAL MELANOMA DATABASE AND DISCOVERY PLATFORM, 2017. Melanoma staging: Evidence-based changes in the American Joint Committee on Cancer eighth edition cancer staging manual. *CA: a Cancer Journal for Clinicians,* **67**(6), pp. 472-492.

GLOSTER, H.M.J. and NEAL, K., 2006. Skin cancer in skin of color. *Journal of the American Academy of Dermatology,* **55**(5), pp. 741-760.

GLUD, M., GNIADECKI, R. and DRZEWIECKI, K.T., 2009. Spectrophotometric intracutaneous analysis versus dermoscopy for the diagnosis of pigmented skin lesions: prospective, double-blind study in a secondary reference centre. *Melanoma Research,* **19**(3), pp. 176-179.

GOLDENBERG, G., KARAGIANNIS, T., PALMER, J.B., LOTYA, J., O'NEILL, C., KISA, R., HERRERA, V. and SIEGEL, D.M., 2016. Incidence and prevalence of basal cell carcinoma (BCC) and locally advanced BCC (LABCC) in a large commercially insured population in the United States: A retrospective cohort study. *Journal of the American Academy of Dermatology,* **75**(5), pp. 957-966.e2.

GREVELING, K., WAKKEE, M., NIJSTEN, T., VAN DEN BOS, RENATE R. and HOLLESTEIN, L.M., 2016. Epidemiology of Lentigo Maligna and Lentigo Maligna Melanoma in the Netherlands, 1989-2013. *Journal of Investigative Dermatology,* **136**(10), pp. 1955-1960.

GUITERA, P., PELLACANI, G., CROTTY, K.A., SCOLYER, R.A., LI, L.X., BASSOLI, S., VINCETI, M., RABINOVITZ, H., LONGO, C. and MENZIES, S.W., 2010. The impact of in vivo reflectance confocal microscopy on the diagnostic accuracy of lentigo maligna and equivocal pigmented and nonpigmented macules of the face. *Journal of Investigative Dermatology,* **130**(8), pp. 2080-2091.

GULLETH, Y., GOLDBERG, N., SILVERMAN, R.P. and GASTMAN, B.R., 2010. What is the best surgical margin for a Basal cell carcinoma: a meta-analysis of the literature. *Plastic & Reconstructive Surgery,* **126**(4), pp. 1222-1231.

HAAK, C.S., CHRISTIANSEN, K., ERLENDSSON, A.M., TAUDORF, E.H., THAYSEN-PETERSEN, D., WULF, H.C. and HAEDERSDAL, M., 2016. Ablative fractional laser enhances MAL-induced PpIX accumulation: Impact of laser channel density, incubation time and drug concentration. *Journal of Photochemistry & Photobiology.B - Biology,* **159**, pp. 42-48.

HAEDERSDAL, M., SAKAMOTO, F.H., FARINELLI, W.A., DOUKAS, A.G., TAM, J. and ANDERSON, R.R., 2010. Fractional CO(2) laser-assisted drug delivery. *Lasers in Surgery & Medicine,* **42**(2), pp. 113-122.

HAMBLY, R., MANSOOR, N., QUINLAN, C., SHAH, Z., LENANE, P., RALPH, N. and MOLONEY, F.J., 2017. Topical photodynamic therapy for primary Bowen disease and basal cell carcinoma: optimizing patient selection. *British Journal of Dermatology,* **177**(3), pp. e55-e57.

HARTMANN, D., KRAMMER, S., RUINI, C., RUZICKA, T. and VON BRAUNMUHL, T., 2016. Correlation of histological and ex-vivo confocal tumor thickness in malignant melanoma. *Lasers in Medical Science,* **31**(5), pp. 921-927.

HAUSCHILD, A., CHEN, S.C., WEICHENTHAL, M., BLUM, A., KING, H.C., GOLDSMITH, J., SCHARFSTEIN, D. and GUTKOWICZ-KRUSIN, D., 2014. To excise or not: impact of MelaFind on German dermatologists' decisions to biopsy atypical lesions. *Journal der Deutschen Dermatologischen Gesellschaft,* **12**(7), pp. 606-614.

HELVIND, N.M., HOLMICH, L.R., SMITH, S., GLUD, M., ANDERSEN, K.K., DALTON, S.O. and DRZEWIECKI, K.T., 2015. Incidence of In Situ and Invasive Melanoma in Denmark From 1985 Through 2012: A National Database Study of 24,059 Melanoma Cases. *JAMA Dermatology,* **151**(10), pp. 1087-1095.

HIGGINS, H.W.2., LEE, K.C., GALAN, A. and LEFFELL, D.J., 2015. Melanoma in situ: Part I. Epidemiology, screening, and clinical features. *Journal of the American Academy of Dermatology,* **73**(2), pp. 181-190.

HILLEMANNS, P., GARCIA, F., PETRY, K.U., DVORAK, V., SADOVSKY, O., IVERSEN, O. and EINSTEIN, M.H., 2015. A randomized study of hexaminolevulinate photodynamic therapy in patients with cervical intraepithelial neoplasia 1/2. *American Journal of Obstetrics & Gynecology,* **212**(4), pp. 465.e1-465.e7.

HINZ, T., EHLER, L.K., VOTH, H., FORTMEIER, I., HOELLER, T., HORNUNG, T. and SCHMID-WENDTNER, M.H., 2011. Assessment of tumor thickness in melanocytic skin lesions: comparison of optical coherence tomography, 20-MHz ultrasound and histopathology. *Dermatology,* **223**(2), pp. 161-168.

HOLM, A., NISSEN, C.V. and WULF, H.C., 2016. Basal Cell Carcinoma is as Common as the Sum of all Other Cancers: Implications for Treatment Capacity. *Acta Dermato-Venereologica,* **96**(4), pp. 505-509.

HOLMES, J., VON BRAUNMUHL, T., BERKING, C., SATTLER, E., ULRICH, M., REINHOLD, U., KURZEN, H., DIRSCHKA, T., KELLNER, C., SCHUH, S. and WELZEL, J., 2018. Optical coherence tomography of basal cell carcinoma: influence of location, subtype, observer variability and image quality on diagnostic performance. *British Journal of Dermatology,* **178**(5), pp. 1102-1110.

HURLIMANN, A.F., HANGGI, G. and PANIZZON, R.G., 1998. Photodynamic therapy of superficial basal cell carcinomas using topical 5-aminolevulinic acid in a nanocolloid lotion. *Dermatology,* **197**(3), pp. 248-254.

IBBOTSON, S.H., WONG, T.H., MORTON, C.A., COLLIER, N.J., HAYLETT, A., MCKENNA, K.E., MALLIPEDDI, R., MOSELEY, H., RHODES, L.E., SEUKERAN, D.C., WARD, K.A., MOHD MUSTAPA, M.F. and EXTON, L.S., 2019. Adverse effects of topical photodynamic therapy: a consensus review and approach to management. *British Journal of Dermatology,* **180**(4), pp. 715-729.

INSKIP, M. and ROSENDAHL, C., 2016. Extrafacial lentigo maligna melanoma is reported often in Australia, more so at lower latitudes. *Australasian Journal of Dermatology,* **57**(1), pp. 70-71.

JACQUES, S.L., 2013. Optical properties of biological tissues: a review. *Physics in Medicine & Biology,* **58**(11), pp. 37.

JAIMES, N. and MARGHOOB, A.A., 2013. The morphologic universe of melanoma. *Dermatologic Clinics,* **31**(4), pp. 599-613.

JANSEN, M.H.E., KOEKELKOREN, F.H.J., NELEMANS, P.J., ARITS, AIMEE H M M., ROOZEBOOM, M.H., KELLENERS-SMEETS, N.W.J. and MOSTERD, K., 2018. Comparison of long-term cosmetic outcomes for different treatments of superficial basal cell carcinoma. *Journal of the American Academy of Dermatology,* **79**(5), pp. 961-964.

JANSEN, M.H.E., MOSTERD, K., ARITS, AIMEE H M M, ROOZEBOOM, M.H., SOMMER, A., ESSERS, B.A.B., VAN PELT, HAN P A, QUAEDVLIEG, P.J.F., STEIJLEN, P.M., NELEMANS, P.J. and KELLENERS-SMEETS, N.W.J., 2018. Five-Year Results of a Randomized Controlled Trial Comparing Effectiveness of Photodynamic Therapy, Topical Imiquimod, and Topical 5-Fluorouracil in Patients with Superficial Basal Cell Carcinoma. *Journal of Investigative Dermatology,* **138**(3), pp. 527-533.

JAYASEKERA, P.S.A., DODD, J., OLIPHANT, T., LANGTRY, J.A.A. and LAWRENCE, C.M., 2018. Dermoscopy prior to Mohs micrographic surgery does not improve tumour margin assessment and leads to fewer Mohs stages. *British Journal of Dermatology,* **178**(2), pp. 565-566.

JENSEN, A.O., BAUTZ, A., OLESEN, A.B., KARAGAS, M.R., SORENSEN, H.T. and FRIIS, S., 2008. Mortality in Danish patients with nonmelanoma skin cancer, 1978-2001. *British Journal of Dermatology,* **159**(2), pp. 419-425.

JERJES, W., HAMDOON, Z., AL RAWI, N. and HOPPER, C., 2019. OCT in the diagnosis of head and neck pre-cancerous and cancerous cutaneous lesions: An immediate ex vivo study. *Photodiagnosis & Photodynamic Therapy,* **27**, pp. 481-486.

JUZENIENE, A., JUZENAS, P., MA, L., IANI, V. and MOAN, J., 2006. Topical application of 5-aminolaevulinic acid, methyl 5-aminolaevulinate and hexyl 5-aminolaevulinate on normal human skin. *British Journal of Dermatology,* **155**(4), pp. 791-799.

KADOUCH, D.J., LEEFLANG, M.M., ELSHOT, Y.S., LONGO, C., ULRICH, M., VAN DER WAL, A C., WOLKERSTORFER, A., BEKKENK, M.W. and DE RIE, M.A., 2017. Diagnostic accuracy of confocal microscopy imaging vs. punch biopsy for diagnosing and subtyping basal cell carcinoma. *Journal of the European Academy of Dermatology & Venereology,* **31**(10), pp. 1641-1648.

KANG, H.Y., BAHADORAN, P. and ORTONNE, J.P., 2010. Reflectance confocal microscopy for pigmentary disorders. *Experimental Dermatology,* **19**(3), pp. 233-239.

KARAM, A., SIMON, M., LEMASSON, G. and MISERY, L., 2013. The use of photodynamic therapy in the treatment of lentigo maligna. *Pigment Cell & Melanoma Research,* **26**(2), pp. 275-277.

KENNEDY, J.C., POTTIER, R.H. and PROSS, D.C., 1990. Photodynamic therapy with endogenous protoporphyrin IX: basic principles and present clinical experience. *Journal of Photochemistry & Photobiology.B - Biology,* **6**(1-2), pp. 143-148.

KESSELS, J P H M., KREUKELS, H., NELEMANS, P.J., ROOZEBOOM, M.H., VAN PELT, H., MOSTERD, K., DE HAAS, E R M. and KELLENERS-SMEETS, N.W.J., 2018. Treatment of superficial basal cell carcinoma by topical photodynamic therapy with fractionated 5-aminolaevulinic acid 20% vs. two-stage topical methyl aminolaevulinate: results of a randomized controlled trial. *British Journal of Dermatology,* **178**(5), pp. 1056-1063.

KIESSLICH, T., HELANDER, L., ILLIG, R., OBERDANNER, C., WAGNER, A., LETTNER, H., JAKAB, M. and PLAETZER, K., 2014. Real-time analysis of endogenous protoporphyrin IX fluorescence from delta-aminolevulinic acid and its derivatives reveals distinct time- and dose-dependent characteristics in vitro. *Journal of Biomedical Optics,* **19**(8), pp. 085007.

KIMYAI-ASADI, A., KATZ, T., GOLDBERG, L.H., AYALA, G.B., WANG, S.Q., VUJEVICH, J.J. and JIH, M.H., 2007. Margin involvement after the excision of melanoma in situ: the need for complete en face examination of the surgical margins. *Dermatologic Surgery,* **33**(12), pp. 1434-1439.

KOH, D., WANG, H., LEE, J., CHIA, K.S., LEE, H.P. and GOH, C.L., 2003. Basal cell carcinoma, squamous cell carcinoma and melanoma of the skin: analysis of the Singapore Cancer Registry data 1968-97. *British Journal of Dermatology,* **148**(6), pp. 1161-1166.

KOSE, K., CORDOVA, M., DUFFY, M., FLORES, E.S., BROOKS, D.H. and RAJADHYAKSHA, M., 2014. Video-mosaicing of reflectance confocal images for examination of extended areas of skin in vivo. *British Journal of Dermatology,* **171**(5), pp. 1239-1241.

KRAFT, S. and GRANTER, S.R., 2014. Molecular pathology of skin neoplasms of the head and neck. *Archives of Pathology & Laboratory Medicine,* **138**(6), pp. 759-787.

KUO, K.Y., BATRA, P., CHO, H.G., LI, S., CHAHAL, H.S., RIEGER, K.E., TANG, J.Y. and SARIN, K.Y., 2017. Correlates of multiple basal cell carcinoma in a retrospective cohort study: Sex, histologic subtypes, and anatomic distribution. *Journal of the American Academy of Dermatology,* **77**(2), pp. 233-234.e2.

KVASKOFF, M., SISKIND, V. and GREEN, A.C., 2012. Risk factors for lentigo maligna melanoma compared with superficial spreading melanoma: a case-control study in Australia. *Archives of Dermatology,* **148**(2), pp. 164-170.

LAI, V., CRANWELL, W. and SINCLAIR, R., 2018. Epidemiology of skin cancer in the mature patient. *Clinics in Dermatology,* **36**(2), pp. 167-176.

LALLAS, A., APALLA, Z., ARGENZIANO, G., LONGO, C., MOSCARELLA, E., SPECCHIO, F., RAUCCI, M. and ZALAUDEK, I., 2014. The dermatoscopic universe of basal cell carcinoma. *Dermatology Practical & Conceptual,* **4**(3), pp. 11-24.

LALLAS, A., ARGENZIANO, G., MOSCARELLA, E., LONGO, C., SIMONETTI, V. and ZALAUDEK, I., 2014. Diagnosis and management of facial pigmented macules. *Clinics in Dermatology,* **32**(1), pp. 94-100.

LALLAS, A., TZELLOS, T., KYRGIDIS, A., APALLA, Z., ZALAUDEK, I., KARATOLIAS, A., FERRARA, G., PIANA, S., LONGO, C., MOSCARELLA, E., STRATIGOS, A. and ARGENZIANO, G., 2014. Accuracy of dermoscopic criteria for discriminating superficial from other subtypes of basal cell carcinoma. *Journal of the American Academy of Dermatology,* **70**(2), pp. 303-311.

LANGLEY, R.G., WALSH, N., SUTHERLAND, A.E., PROPPEROVA, I., DELANEY, L., MORRIS, S.F. and GALLANT, C., 2007. The diagnostic accuracy of in vivo confocal scanning laser microscopy compared to dermoscopy of benign and malignant melanocytic lesions: a prospective study. *Dermatology,* **215**(4), pp. 365-372.

LASITHIOTAKIS, K.G., PETRAKIS, I.E. and GARBE, C., 2010. Cutaneous melanoma in the elderly: epidemiology, prognosis and treatment. *Melanoma research,* **20**(3), pp. 163-170.

LINDELOF, B., LAPINS, J. and DAL, H., 2017. Shift in Occupational Risk for Basal Cell Carcinoma from Outdoor to Indoor Workers: A Large Population-based Case-control Register Study from Sweden. *Acta Dermato-Venereologica,* **97**(7), pp. 830-833.

LINOS, E., LI, W.Q., HAN, J., LI, T., CHO, E. and QURESHI, A.A., 2017. Lifetime ultraviolet radiation exposure and lentigo maligna melanoma. *British Journal of Dermatology,* **176**(6), pp. 1666-1668.

LIPPERT, J., SMUCLER, R. and VLK, M., 2013. Fractional carbon dioxide laser improves nodular basal cell carcinoma treatment with photodynamic therapy with methyl 5-aminolevulinate. *Dermatologic Surgery,* **39**(8), pp. 1202-1208.

LIU, V. and MIHM, M.C., 2003. Pathology of malignant melanoma. *Surgical Clinics of North America,* **83**(1), pp. 31-60.

LOMAS, A., LEONARDI-BEE, J. and BATH-HEXTALL, F., 2012. A systematic review of worldwide incidence of nonmelanoma skin cancer. *British Journal of Dermatology,* **166**(5), pp. 1069-1080.

LOPEZ, R.F.V., LANGE, N., GUY, R. and BENTLEY, MARIA VITORIA LOPES BADRA, 2004. Photodynamic therapy of skin cancer: controlled drug delivery of 5-ALA and its esters. *Advanced Drug Delivery Reviews,* **56**(1), pp. 77-94.

LOWENSTEIN, S.E., GARRETT, G., TOLAND, A.E., JAMBUSARIA-PAHLAJANI, A., ASGARI, M.M., GREEN, A., ENGELS, E.A., ARRON, S.T. and NATIONAL CANCER INSTITUTE KERATINOCYTE CARCINOMA CONSORTIUM, 2017. Risk prediction tools for keratinocyte carcinoma after solid organ transplantation: a review of the literature. *British Journal of Dermatology,* **177**(5), pp. 1202-1207.

LU, G., and FEI, B., 2014. Medical hyperspectral imaging: a review. *Journal Biomedical optics,* 19(1):10901, 2014 Jan.

LUBEEK, S.F.K., VAN VUGT, L.J., ABEN, K.K.H., VAN DE KERKHOF, PETER C M. and GERRITSEN, M.P., 2017. The Epidemiology and Clinicopathological Features of Basal Cell Carcinoma in Patients 80 Years and Older: A Systematic Review. *JAMA Dermatology,* **153**(1), pp. 71-78.

LUI, H., ZHAO, J., MCLEAN, D. and ZENG, H., 2012. Real-time Raman spectroscopy for in vivo skin cancer diagnosis. *Cancer Research,* **72**(10), pp. 2491-2500.

MAHER, N.G., BLUMETTI, T.P., GOMES, E.E., CHENG, H.M., SATGUNASEELAN, L., LO, S., REZZE, G.G., SCOLYER, R.A. and GUITERA, P., 2017. Melanoma diagnosis may be a pitfall for optical coherence tomography assessment of equivocal amelanotic or hypomelanotic skin lesions. *British Journal of Dermatology,* **177**(2), pp. 574-577.

MAHER, N.G., SOLINAS, A., SCOLYER, R.A., PUIG, S., PELLACANI, G. and GUITERA, P., 2017. Detection of desmoplastic melanoma with dermoscopy and reflectance confocal microscopy. *Journal of the European Academy of Dermatology & Venereology,* **31**(12), pp. 2016-2024.

MAISCH, T., SANTARELLI, F., SCHREML, S., BABILAS, P. and SZEIMIES, R., 2010. Fluorescence induction of protoporphyrin IX by a new 5-aminolevulinic acid nanoemulsion used for photodynamic therapy in a full-thickness ex vivo skin model. *Experimental Dermatology,* **19**(8), pp. 302.

MALLIDI, S., ANBIL, S., LEE, S., MANSTEIN, D., ELRINGTON, S., KOSITRATNA, G., SCHOENFELD, D., POGUE, B., DAVIS, S.J. and HASAN, T., 2014. Photosensitizer fluorescence and singlet oxygen luminescence as dosimetric predictors of topical 5-aminolevulinic acid photodynamic therapy induced clinical erythema. *Journal of Biomedical Optics,* **19**(2), pp. 028001.

MANESTAR-BLAZIC, T., BATINAC, T., HADZISEJDIC, I. and BRAJAC, I., 2007. Apoptosis and immune response are responsible for the site-specific incidence of non-melanoma skin cancer. *Medical Hypotheses,* **68**(4), pp. 853-855.

MARMUR, E.S., BERKOWITZ, E.Z., FUCHS, B.S., SINGER, G.K. and YOO, J.Y., 2010. Use of high-frequency, high-resolution ultrasound before Mohs surgery. *Dermatologic Surgery,* **36**(6), pp. 841-847.

MARRA, K., LAROCHELLE, E.P., CHAPMAN, M.S., HOOPES, P.J., LUKOVITS, K., MAYTIN, E.V., HASAN, T. and POGUE, B.W., 2018. Comparison of Blue and White Lamp Light with Sunlight for Daylight-Mediated, 5-ALA Photodynamic Therapy, in vivo. *Photochemistry & Photobiology,* **94**(5), pp. 1049-1057.

MARTIN, I., SCHAARSCHMIDT, M., GLOCKER, A., HERR, R., SCHMIEDER, A., GOERDT, S. and PEITSCH, W.K., 2016. Patient Preferences for Treatment of Basal Cell Carcinoma: Importance of Cure and Cosmetic Outcome. *Acta Dermato-Venereologica,* **96**(3), pp. 355-360.

MATACA, E., MIGALDI, M. and CESINARO, A.M., 2018. Impact of Dermoscopy and Reflectance Confocal Microscopy on the Histopathologic Diagnosis of Lentigo Maligna/Lentigo Maligna Melanoma. *American Journal of Dermatopathology,* **40**(12), pp. 884-889.

MAZURENKA, M., BEHRENDT, L., MEINHARDT-WOLLWEBER, M., MORGNER, U. and ROTH, B., 2017. Development of a combined OCT-Raman probe for the prospective in vivo clinical melanoma skin cancer screening. *Review of Scientific Instruments,* **88**(10), pp. 105103.

MIDDELBURG, T.A., DE VIJLDER, H.C., DE BRUIJN, H.S., VAN DER PLOEG-VAN DEN HEUVEL, ANGELIQUE, NEUMANN, H.A.M., DE HAAS, ELLEN R M. and ROBINSON, D.J., 2014. Topical photodynamic therapy using different porphyrin precursors leads to differences in vascular photosensitization and vascular damage in normal mouse skin. *Photochemistry & Photobiology,* **90**(4), pp. 896-902.

MIRZOYEV, S.A., KNUDSON, R.M., REED, K.B., HOU, J.L., LOHSE, C.M., FROHM, M.L., BREWER, J.D., OTLEY, C.C. and ROENIGK, R.K., 2014. Incidence of lentigo maligna in Olmsted County, Minnesota, 1970 to 2007. *Journal of the American Academy of Dermatology,* **70**(3), pp. 443-448.

MOAN, J., BERG, K., GADMAR, O.B., IANI, V., MA, L. and JUZENAS, P., 1999. The temperature dependence of protoporphyrin IX production in cells and tissues. *Photochemistry & Photobiology,* **70**(4), pp. 669-673.

MOHAN, S.V. and CHANG, A.L.S., 2014. Advanced Basal Cell Carcinoma: Epidemiology and Therapeutic Innovations. *Current Dermatology Reports,* **3**, pp. 40-45.

MOHR, P., BIRGERSSON, U., BERKING, C., HENDERSON, C., TREFZER, U., KEMENY, L., SUNDERKOTTER, C., DIRSCHKA, T., MOTLEY, R., FROHM-NILSSON, M., REINHOLD, U., LOQUAI, C., BRAUN, R., NYBERG, F. and PAOLI, J., 2013. Electrical impedance spectroscopy as a potential adjunct diagnostic tool for cutaneous melanoma. *Skin Research & Technology,* **19**(2), pp. 75-83.

MONCRIEFF, M., COTTON, S., CLARIDGE, E. and HALL, P., 2002. Spectrophotometric intracutaneous analysis: a new technique for imaging pigmented skin lesions. *British Journal of Dermatology,* **146**(3), pp. 448-457.

MONHEIT, G., COGNETTA, A.B., FERRIS, L., RABINOVITZ, H., GROSS, K., MARTINI, M., GRICHNIK, J.M., MIHM, M., PRIETO, V.G., GOOGE, P., KING, R., TOLEDANO, A., KABELEV, N., WOJTON, M. and GUTKOWICZ-KRUSIN, D., 2011. The performance of MelaFind: a prospective multicenter study. *Archives of Dermatology,* **147**(2), pp. 188-194.

MORAES PINTO BLUMETTI, TATIANA CRISTINA, COHEN, M.P., GOMES, E.E., PETACCIA DE MACEDO, M., FERREIRA DE SOUZA BEGNAMI, MARIA DIRLEI, TAVARES GUERREIRO FREGNANI, JOSE HUMBERTO, DUPRAT, J.P., PELLACANI, G. and REZZE, G.G., 2015. Optical coherence tomography (OCT) features of nevi and melanomas and their association with intraepidermal or dermal involvement: A pilot study. *Journal of the American Academy of Dermatology,* **73**(2), pp. 315-317.

MORROW, D.I.J., MCCARRON, P.A., WOOLFSON, A.D., JUZENAS, P., JUZENIENE, A., IANI, V., MOAN, J. and DONNELLY, R.F., 2010. Hexyl aminolaevulinate is a more effective topical photosensitiser precursor than methyl aminolaevulinate and 5-aminolaevulinic acids when applied in equimolar doses. *Journal of Pharmaceutical Sciences,* **99**(8), pp. 3486-3498.

MORTON, C.A., DOMINICUS, R., RADNY, P., DIRSCHKA, T., HAUSCHILD, A., REINHOLD, U., ASCHOFF, R., ULRICH, M., KEOHANE, S., EKANAYAKE-BOHLIG, S., IBBOTSON, S., OSTENDORF, R., BERKING, C., GRONE, D., SCHULZE, H.J., OCKENFELS, H.M., JASNOCH, V., KURZEN, H., SEBASTIAN, M., STEGE, H., STAUBACH, P., GUPTA, G., HUBINGER, F., ZIABREVA, I., SCHMITZ, B., GERTZMANN, A., LUBBERT, H. and SZEIMIES, R., 2018. A randomized, multinational, noninferiority, phase III trial to evaluate the safety and efficacy of BF-200 aminolaevulinic acid gel vs. methyl aminolaevulinate cream in the treatment of nonaggressive basal cell carcinoma with photodynamic therapy. *British Journal of Dermatology,* **179**(2), pp. 309-319.

MORTON, C., SZEIMIES, R., SIDOROFF, A., WENNBERG, A., BASSET-SEGUIN, N., CALZAVARA-PINTON, P., GILABERTE, Y., HOFBAUER, G., HUNGER, R., KARRER, S., LEHMANN, P., PIASERICO, S., ULRICH, C., BRAATHEN, L. and EUROPEAN DERMATOLOGY FORUM, 2015. European Dermatology Forum Guidelines on topical photodynamic therapy. *European Journal of Dermatology,* **25**(4), pp. 296-311.

MOSTERD, K., KREKELS, G.A.M., NIEMAN, F.H., OSTERTAG, J.U., ESSERS, B.A.B., DIRKSEN, C.D., STEIJLEN, P.M., VERMEULEN, A., NEUMANN, H. and KELLENERS-SMEETS, N.W.J., 2008. Surgical excision versus Mohs' micrographic surgery for primary and recurrent basal-cell carcinoma of the face: a prospective randomised controlled trial with 5-years' follow-up. *Lancet Oncology,* **9**(12), pp. 1149-1156.

MURRAY, C., SIVAJOHANATHAN, D., HANNA, T.P., BRADSHAW, S., SOLISH, N., MORAN, B., HEKKENBERG, R., WEI, A.C. and PETRELLA, T., 2019a. Patient indications for Mohs micrographic surgery: a clinical practice guideline. *Current Oncology,* **26**(1), pp. e94-e99.

MURRAY, C., SIVAJOHANATHAN, D., HANNA, T.P., BRADSHAW, S., SOLISH, N., MORAN, B., HEKKENBERG, R., WEI, A.C. and PETRELLA, T., 2019b. Patient Indications for Mohs Micrographic Surgery: A Systematic Review. *Journal of Cutaneous Medicine & Surgery,* **23**(1), pp. 75-90.

NAGAOKA, T., KIYOHARA, Y., KOGA, H., NAKAMURA, A., SAIDA, T. and SOTA, T., 2015. Modification of a melanoma discrimination index derived from hyperspectral data: a clinical trial conducted in 2 centers between March 2011 and December 2013. *Skin Research & Technology,* **21**(3), pp. 278-283.

NAGAOKA, T., NAKAMURA, A., OKUTANI, H., KIYOHARA, Y., KOGA, H., SAIDA, T. and SOTA, T., 2013. Hyperspectroscopic screening of melanoma on acral volar skin. *Skin Research & Technology,* **19**(1), pp. 290.

NAGAOKA, T., NAKAMURA, A., OKUTANI, H., KIYOHARA, Y. and SOTA, T., 2012. A possible melanoma discrimination index based on hyperspectral data: a pilot study. *Skin Research & Technology,* **18**(3), pp. 301-310.

NASSIRI-KASHANI, M., SADR, B., FANIAN, F., KAMYAB, K., NOORMOHAMMADPOUR, P., SHAHSHAHANI, M.M., ZARTAB, H., NAGHIZADEH, M., SARRAF-YAZDY, M. and FIROOZ, A., 2013. Pre-operative assessment of basal cell carcinoma dimensions using high frequency ultrasonography and its correlation with histopathology. *Skin Research & Technology,* **19**(1), pp. 132.

NCCN Clinical Practice Guidelines In Oncology, NCCN Guidelines®: Referenced with permission from the **NCCN Guidelines® for Basal Cell Skin Cancer V.1.2020** © National Comprehensive Cancer Network, Inc. 2019. All rights reserved. Accessed [February 20th, 2020]. *Available online at www.NCCN.org*. NCCN makes no warranties of any kind whatsoever regarding their content, use or application and disclaims any responsibility for their application or use in any way.

NEITTAANMAKI-PERTTU, N., GRONROOS, M., JESKANEN, L., POLONEN, I., RANKI, A., SAKSELA, O. and SNELLMAN, E., 2015. Delineating margins of lentigo maligna using a hyperspectral imaging system. *Acta Dermato-Venereologica,* **95**(5), pp. 549-552.

NEITTAANMAKI-PERTTU, N., KARPPINEN, T.T., TANI, T., SNELLMAN, E. and GRONROOS, M., 2017. Long-term Outcome of Low-concentration Hexyl-5-aminolaevulinate Daylight Photodynamic Therapy for Treatment of Actinic Keratoses. *Acta Dermato-Venereologica,* **97**(1), pp. 120-121.

NEITTAANMAKI-PERTTU, N., NEITTAANMAKI, E., POLONEN, I., SNELLMAN, E. and GRONROOS, M., 2016. Safety of Novel Amino-5-laevulinate Photosensitizer Precursors in Photodynamic Therapy for Healthy Human Skin. *Acta Dermato-Venereologica,* **96**(1), pp. 108-110.

NGUYEN-NIELSEN, M., WANG, L., PEDERSEN, L., OLESEN, A.B., HOU, J., MACKEY, H., MCCUSKER, M., BASSET-SEGUIN, N., FRYZEK, J. and VYBERG, M., 2015. The incidence of metastatic basal cell carcinoma (mBCC) in Denmark, 1997-2010. *European Journal of Dermatology,* **25**(5), pp. 463-468.

NIKOLAOU, V. and STRATIGOS, A.J., 2014. Emerging trends in the epidemiology of melanoma. *British Journal of Dermatology,* **170**(1), pp. 11-19.

NISSEN, C.V., HEERFORDT, I.M., WIEGELL, S.R., MIKKELSEN, C.S. and WULF, H.C., 2017. Increased protoporphyrin IX accumulation does not improve the effect of photodynamic therapy for actinic keratosis: a randomized controlled trial. *British Journal of Dermatology,* **176**(5), pp. 1241-1246.

NISSEN, C.V., PHILIPSEN, P.A. and WULF, H.C., 2015. Protoporphyrin IX formation after topical application of methyl aminolaevulinate and BF-200 aminolaevulinic acid declines with age. *British Journal of Dermatology,* **173**(3), pp. 760-766.

NISSEN, C.V., WIEGELL, S.R., PHILIPSEN, P.A. and WULF, H.C., 2016. Short-term chemical pretreatment cannot replace curettage in photodynamic therapy. *Photodermatology, Photoimmunology & Photomedicine,* **32**(3), pp. 146-152.

OLSEN, C.M., CARROLL, H.J. and WHITEMAN, D.C., 2010. Familial melanoma: a meta-analysis and estimates of attributable fraction. *Cancer Epidemiology, Biomarkers & Prevention,* **19**(1), pp. 65-73.

OZOG, D.M., RKEIN, A.M., FABI, S.G., GOLD, M.H., GOLDMAN, M.P., LOWE, N.J., MARTIN, G.M. and MUNAVALLI, G.S., 2016. Photodynamic Therapy: A Clinical Consensus Guide. *Dermatologic Surgery,* **42**(7), pp. 804-827.

PAMPENA, R., KYRGIDIS, A., LALLAS, A., MOSCARELLA, E., ARGENZIANO, G. and LONGO, C., 2017. A meta-analysis of nevus-associated melanoma: Prevalence and practical implications. *Journal of the American Academy of Dermatology,* **77**(5), pp. 938-945.e4.

PAOLI, J., HALLDIN, C., ERICSON, M.B. and WENNBERG, A., 2008. Nerve blocks provide effective pain relief during topical photodynamic therapy for extensive facial actinic keratoses. *Clinical & Experimental Dermatology,* **33**(5), pp. 559-564.

PAOLI, J., DARYONI, S., WENNBERG, A., MOLNE, L., GILLSTEDT, M., MIOCIC, M. and STENQUIST, B., 2011. 5-year recurrence rates of Mohs micrographic surgery for aggressive and recurrent facial basal cell carcinoma. *Acta Dermato-Venereologica,* **91**(6), pp. 689-693.

PELLACANI, G., GUITERA, P., LONGO, C., AVRAMIDIS, M., SEIDENARI, S. and MENZIES, S., 2007. The impact of in vivo reflectance confocal microscopy for the diagnostic accuracy of melanoma and equivocal melanocytic lesions. *Journal of Investigative Dermatology,* **127**(12), pp. 2759-2765.

PELUCCHI, C., DI LANDRO, A., NALDI, L., LA VECCHIA, C. and ONCOLOGY STUDY GROUP OF THE ITALIAN GROUP FOR EPIDEMIOLOGIC RESEARCH IN DERMATOLOGY, (GISED), 2007. Risk factors for histological types and anatomic sites of cutaneous basal-cell carcinoma: an italian case-control study. *Journal of Investigative Dermatology,* **127**(4), pp. 935-944.

PERNICIARO, C., 1997. Dermatopathologic variants of malignant melanoma. *Mayo Clinic proceedings,* **72**(3), pp. 273-279.

PIACENTINI, R.D., DELLA CECA, L.S. and IPINA, A., 2018. Climate change and its relationship with non-melanoma skin cancers. *Photochemical & Photobiological Sciences,* **17**(12), pp. 1913-1917.

PONKA, D. and BADDAR, F., 2012. Wood lamp examination. *Canadian Family Physician,* **58**(9), pp. 976

PUIG, S. and BERROCAL, A., 2015. Management of high-risk and advanced basal cell carcinoma. *Clinical & Translational Oncology: Official Publication of the Federation of Spanish Oncology Societes & of the National Cancer Institute of Mexico,* **17**(7), pp. 497-503.

PYNE, J.H., MYINT, E., BARR, E.M., CLARK, S.P., DAVID, M., NA, R. and HOU, R., 2017. Superficial basal cell carcinoma: A comparison of superficial only subtype with superficial combined with other subtypes by age, sex and anatomic site in 3150 cases. *Journal of Cutaneous Pathology,* **44**(8), pp. 677-683.

QUE, S.K.T., 2016. Research Techniques Made Simple: Noninvasive Imaging Technologies for the Delineation of Basal Cell Carcinomas. *Journal of Investigative Dermatology,* **136**(4), pp. 33.

RAASCH, B.A., BUETTNER, P.G. and GARBE, C., 2006. Basal cell carcinoma: histological classification and body-site distribution. *British Journal of Dermatology,* **155**(2), pp. 401-407.

RASANEN, J.E., NEITTAANMAKI, N., JESKANEN, L., POLONEN, I., SNELLMAN, E. and GRONROOS, M., 2019. Ablative fractional laser-assisted photodynamic therapy for lentigo maligna: a prospective pilot study. *Journal of the European Academy of Dermatology & Venereology,* ahead of print, DOI: 10.1111/jdv.15925.

RASHED, D., SHAH, D., FREEMAN, A., COOK, R.J., HOPPER, C. and PERRETT, C.M., 2017. Rapid ex vivo examination of Mohs specimens using optical coherence tomography. *Photodiagnosis & Photodynamic Therapy,* **19**, pp. 243-248.

REDDY, N. and NGUYEN, B.T., 2019. The utility of optical coherence tomography for diagnosis of basal cell carcinoma: a quantitative review. *British Journal of Dermatology,* **180**(3), pp. 475-483.

REITER, O., MIMOUNI, I., GDALEVICH, M., MARGHOOB, A.A., LEVI, A., HODAK, E. and LESHEM, Y.A., 2019. The diagnostic accuracy of dermoscopy for basal cell carcinoma: A systematic review and meta-analysis. *Journal of the American Academy of Dermatology,* **80**(5), pp. 1380-1388.

RICHMOND-SINCLAIR, N.M., PANDEYA, N., WARE, R.S., NEALE, R.E., WILLIAMS, G.M., VAN DER POLS, JOLIEKE C and GREEN, A.C., 2009. Incidence of basal cell carcinoma multiplicity and detailed anatomic distribution: longitudinal study of an Australian population. *Journal of Investigative Dermatology,* **129**(2), pp. 323-328.

ROBINSON, J.K., 2004. Use of Digital Epiluminescence Microscopy to Help Define the Edge of Lentigo Maligna. *Archives of Dermatology.* **140**(9), pp. 1095-100

ROMANO, E., SCHWARTZ, G.K., CHAPMAN, P.B., WOLCHOCK, J.D. and CARVAJAL, R.D., 2011. Treatment implications of the emerging molecular classification system for melanoma. *Lancet Oncology,* **12**(9), pp. 913-922.

ROOZEBOOM, M.H., ARITS, A H H M., NELEMANS, P.J. and KELLENERS-SMEETS, N.W.J., 2012. Overall treatment success after treatment of primary superficial basal cell carcinoma: a systematic review and meta-analysis of randomized and nonrandomized trials. *British Journal of Dermatology,* **167**(4), pp. 733-756.

ROOZEBOOM, M.H., ARITS, AIMEE H M M., MOSTERD, K., SOMMER, A., ESSERS, B.A.B., DE ROOIJ, MICHETTE J M., QUAEDVLIEG, P.J.F., STEIJLEN, P.M., NELEMANS, P.J. and KELLENERS-SMEETS, N.W.J., 2016. Three-Year Follow-Up Results of Photodynamic Therapy vs. Imiquimod vs. Fluorouracil for Treatment of Superficial Basal Cell Carcinoma: A Single-Blind, Noninferiority, Randomized Controlled Trial. *Journal of Investigative Dermatology,* **136**(8), pp. 1568-1574.

SAHU, A., YELAMOS, O., IFTIMIA, N., CORDOVA, M., ALESSI-FOX, C., GILL, M., MAGULURI, G., DUSZA, S.W., NAVARRETE-DECHENT, C., GONZALEZ, S., ROSSI, A.M., MARGHOOB, A.A., RAJADHYAKSHA, M. and CHEN, C.J., 2018. Evaluation of a Combined Reflectance Confocal Microscopy-Optical Coherence Tomography Device for Detection and Depth Assessment of Basal Cell Carcinoma. *JAMA Dermatology,* **154**(10), pp. 1175-1183.

SANCHEZ, G., NOVA, J., RODRIGUEZ-HERNANDEZ, A.E., MEDINA, R.D., SOLORZANO-RESTREPO, C., GONZALEZ, J., OLMOS, M., GODFREY, K. and AREVALO-RODRIGUEZ, I., 2016. Sun protection for preventing basal cell and squamous cell skin cancers. *Cochrane Database of Systematic Reviews,* **7**, pp. 011161.

SCRIVENER, Y., GROSSHANS, E. and CRIBIER, B., 2002. Variations of basal cell carcinomas according to gender, age, location and histopathological subtype. *British Journal of Dermatology,* **147**(1), pp. 41-47.

SGOUROS, D., LALLAS, A., JULIAN, Y., RIGOPOULOS, D., ZALAUDEK, I., LONGO, C., MOSCARELLA, E., SIMONETTI, V. and ARGENZIANO, G., 2014. Assessment of SIAscopy in the triage of suspicious skin tumours. *Skin Research & Technology,* **20**(4), pp. 440-444.

SILVA, E.S.D., TAVARES, R., PAULITSCH, F.D.S. and ZHANG, L., 2018. Use of sunscreen and risk of melanoma and non-melanoma skin cancer: a systematic review and meta-analysis. *European Journal of Dermatology,* **28**(2), pp. 186-201.

SONG, E., GRANT-KELS, J.M., SWEDE, H., D'ANTONIO, J.L., LACHANCE, A., DADRAS, S.S., KRISTJANSSON, A.K., FERENCZI, K., MAKKAR, H.S. and ROTHE, M.J., 2016. Paired comparison of the sensitivity and specificity of multispectral digital skin lesion analysis and reflectance confocal microscopy in the detection of melanoma in vivo: A cross-sectional study. *Journal of the American Academy of Dermatology,* **75**(6), pp. 1187-1192.e2.

SU, W.P., 1997. Malignant melanoma: basic approach to clinicopathologic correlation. *Mayo Clinic Proceedings,* **72**(3), pp. 267-272.

SWETTER, S.M., BOLDRICK, J.C., JUNG, S.Y., EGBERT, B.M. and HARVELL, J.D., 2005. Increasing incidence of lentigo maligna melanoma subtypes: northern California and national trends 1990-2000. *Journal of Investigative Dermatology,* **125**(4), pp. 685-691.

SWETTER, S.M., TSAO, H., BICHAKJIAN, C.K., CURIEL-LEWANDROWSKI, C., ELDER, D.E., GERSHENWALD, J.E., GUILD, V., GRANT-KELS, J.M., HALPERN, A.C., JOHNSON, T.M., SOBER, A.J., THOMPSON, J.A., WISCO, O.J., WYATT, S., HU, S. and LAMINA, T., 2019. Guidelines of care for the management of primary cutaneous melanoma. *Journal of the American Academy of Dermatology,* **80**(1), pp. 208-250.

SZEWCZYK, M., PAZDROWSKI, J., GOLUSINSKI, P., DANCZAK-PAZDROWSKA, A., LUCZEWSKI, L., MARSZALEK, S., MAJCHRZAK, E. and GOLUSINSKI, W., 2016. Basal cell carcinoma in farmers: an occupation group at high risk. *International Archives of Occupational & Environmental Health,* **89**(3), pp. 497-501.

TANKAM, P., SOH, J., CANAVESI, C., LANIS, M., HAYES, A., COGLIATI, A., ROLLAND, J.P. and IBRAHIM, S.F., 2019. Gabor-domain optical coherence tomography to aid in Mohs resection of basal cell carcinoma. *Journal of the American Academy of Dermatology,* **80**(6), pp. 1766-1769.

TCHANQUE-FOSSUO, C.N. and EISEN, D.B., 2018. A systematic review on the use of cryotherapy versus other treatments for basal cell carcinoma. *Dermatology Online Journal,* **24**(11):3, DOI: 10.1111/jdv.15925.

THEMSTRUP, L., BANZHAF, C.A., MOGENSEN, M. and JEMEC, G.B.E., 2014. Optical coherence tomography imaging of non-melanoma skin cancer undergoing photodynamic therapy reveals subclinical residual lesions. *Photodiagnosis & Photodynamic Therapy,* **11**(1), pp. 7-12.

THEMSTRUP, L., DE CARVALHO, N., NIELSEN, S.M., OLSEN, J., CIARDO, S., SCHUH, S., NORNBERG, B.M., WELZEL, J., ULRICH, M., PELLACANI, G. and JEMEC, G.B.E., 2018. In vivo differentiation of common basal cell carcinoma subtypes by microvascular and structural imaging using dynamic optical coherence tomography. *Experimental Dermatology,* **27**(2), pp. 156-165.

TIODOROVIC-ZIVKOVIC, D., ARGENZIANO, G., LALLAS, A., THOMAS, L., IGNJATOVIC, A., RABINOVITZ, H., MOSCARELLA, E., LONGO, C., HOFMANN-WELLENHOF, R. and ZALAUDEK, I., 2015. Age, gender, and topography influence the clinical and dermoscopic appearance of lentigo maligna. *Journal of the American Academy of Dermatology,* **72**(5), pp. 801-808.

TKACZYK, E., 2017. Innovations and Developments in Dermatologic Non-invasive Optical Imaging and Potential Clinical Applications. *Acta Dermato-Venereologica,* (Suppl 218), pp. 5-13.

TODD, B.K., LESAR, A., O'MAHONEY, P., EADIE, E. and IBBOTSON, S.H., 2019. Is there an optimal irradiation dose for PDT: 37 $Jcm^{-2}$ or 75 $Jcm^{-2}$ ?. *British Journal of Dermatology,* ahead of print, DOI: 10.1111/bjd.18644.

TOENDER, A., KJAER, S.K. and JENSEN, A., 2014. Increased incidence of melanoma in situ in Denmark from 1997 to 2011: results from a nationwide population-based study. *Melanoma Research,* **24**(5), pp. 488-495.

TOGSVERD-BO, K., IDORN, L.W., PHILIPSEN, P.A., WULF, H.C. and HAEDERSDAL, M., 2012. Protoporphyrin IX formation and photobleaching in different layers of normal human skin: methyl- and hexylaminolevulinate and different light sources. *Experimental Dermatology,* **21**(10), pp. 745-750.

TOGSVERD-BO, K., LERCHE, C.M., PHILIPSEN, P.A., POULSEN, T., WULF, H.C. and HAEDERSDAL, M., 2012. Porphyrin biodistribution in UV-exposed murine skin after methyl- and hexyl-aminolevulinate incubation. *Experimental Dermatology,* **21**(4), pp. 260-264.

TOLKACHJOV, S.N., BRODLAND, D.G., COLDIRON, B.M., FAZIO, M.J., HRUZA, G.J., ROENIGK, R.K., ROGERS, H.W., ZITELLI, J.A., WINCHESTER, D.S. and HARMON, C.B., 2017. Understanding Mohs Micrographic Surgery: A Review and Practical Guide for the Nondermatologist. *Mayo Clinic Proceedings,* **92**(8), pp. 1261-1271.

TRAKATELLI, M., MORTON, C., NAGORE, E., ULRICH, C., DEL MARMOL, V., PERIS, K., BASSET-SEGUIN, N. and BCC SUBCOMMITTEE OF THE GUIDELINES COMMITTEE OF THE EUROPEAN DERMATOLOGY FORUM, 2014. Update of the European guidelines for basal cell carcinoma management. *European Journal of Dermatology,* **24**(3), pp. 312-329.

TSCHANDL, P., ROSENDAHL, C. and KITTLER, H., 2015. Dermatoscopy of flat pigmented facial lesions. *Journal of European Academy of Dermatology and Venereology,* **29**(1), pp.120-127.

TYRRELL, J.S., MORTON, C., CAMPBELL, S.M. and CURNOW, A., 2011. Comparison of protoporphyrin IX accumulation and destruction during methylaminolevulinate photodynamic therapy of skin tumours located at acral and nonacral sites. *British Journal of Dermatology,* **164**(6), pp. 1362-1368.

TYRRELL, J., THORN, C., SHORE, A., CAMPBELL, S. and CURNOW, A., 2011. Oxygen saturation and perfusion changes during dermatological methylaminolaevulinate photodynamic therapy. *British Journal of Dermatology,* **165**(6), pp. 1323-1331.

TYRRELL, J.S., CAMPBELL, S.M. and CURNOW, A., 2010a. The relationship between protoporphyrin IX photobleaching during real-time dermatological methyl-aminolevulinate photodynamic therapy (MAL-PDT) and subsequent clinical outcome. *Lasers in Surgery & Medicine,* **42**(7), pp. 613-619.

TYRRELL, J., CAMPBELL, S.M. and CURNOW, A., 2011. Monitoring the accumulation and dissipation of the photosensitizer protoporphyrin IX during standard dermatological methyl-aminolevulinate photodynamic therapy utilizing non-invasive fluorescence imaging and quantification. *Photodiagnosis & Photodynamic Therapy,* **8**(1), pp. 30-38.

TYRRELL, J., CAMPBELL, S. and CURNOW, A., 2010b. Validation of a non-invasive fluorescence imaging system to monitor dermatological PDT. *Photodiagnosis & Photodynamic Therapy,* **7**(2), pp. 86-97.

TYRRELL, J., PATERSON, C. and CURNOW, A., 2019. Regression Analysis of Protoporphyrin IX Measurements Obtained During Dermatological Photodynamic Therapy. *Cancers,* **11**(1),.

VAN DEN AKKER, J T., IANI, V., STAR, W.M., STERENBORG, H.J. and MOAN, J., 2000. Topical application of 5-aminolevulinic acid hexyl ester and 5-aminolevulinic acid to normal nude mouse skin: differences in protoporphyrin IX fluorescence kinetics and the role of the stratum corneum. *Photochemistry & Photobiology,* **72**(5), pp. 681-689.

VAN DER LEUN, JAN C., PIACENTINI, R.D. and DE GRUIJL, F.R., 2008. Climate change and human skin cancer. *Photochemical & Photobiological Sciences,* **7**(6), pp. 730-733.

VAN LOO, E., MOSTERD, K., KREKELS, G.A., ROOZEBOOM, M.H., OSTERTAG, J.U., DIRKSEN, C.D., STEIJLEN, P.M., NEUMANN, H.A., NELEMANS, P.J. and KELLENERS-SMEETS, N.W., 2014. Surgical excision versus Mohs' micrographic surgery for basal cell carcinoma of the face: A randomised clinical trial with 10 year follow-up. *European Journal of Cancer,* **50**(17), pp. 3011-3020.

VARKENTIN, A., MAZURENKA, M., BLUMENROTHER, E., BEHRENDT, L., EMMERT, S., MORGNER, U., MEINHARDT-WOLLWEBER, M., RAHLVES, M. and ROTH, B., 2018. Trimodal system for in vivo skin cancer screening with combined optical coherence tomography-Raman and colocalized optoacoustic measurements. *Journal of Biophotonics,* **11**(6), pp. e201700288.

VARKENTIN, A., MAZURENKA, M., BLUMENROTHER, E., MEINHARDT-WOLLWEBER, M., RAHLVES, M., BROEKAERT, S.M.C., SCHAD-TRCKA, S., EMMERTINST, S., MORGNER, U. and ROTH, B., 2017. Comparative study of presurgical skin infiltration depth measurements of melanocytic lesions with OCT and high frequency ultrasound. *Journal of Biophotonics,* **10**(6-7), pp. 854-861.

VENTURINI, M., SALA, R., GONZALEZ, S. and CALZAVARA-PINTON, P.G., 2013. Reflectance confocal microscopy allows in vivo real-time noninvasive assessment of the outcome of methyl aminolaevulinate photodynamic therapy of basal cell carcinoma. *British Journal of Dermatology,* **168**(1), pp. 99-105.

VENTURINI, M., GUALDI, G., ZANCA, A., LORENZI, L., PELLACANI, G. and CALZAVARA-PINTON, P.G., 2016. A new approach for presurgical margin assessment by reflectance confocal microscopy of basal cell carcinoma. *British Journal of Dermatology,* **174**(2), pp. 380-385.

VERKOUTEREN, J.A.C., RAMDAS, K.H.R., WAKKEE, M. and NIJSTEN, T., 2017. Epidemiology of basal cell carcinoma: scholarly review. *British Journal of Dermatology,* **177**(2), pp. 359-372.

VERKOUTEREN, J.A.C., SMEDINGA, H., STEYERBERG, E.W., HOFMAN, A. and NIJSTEN, T., 2015. Predicting the Risk of a Second Basal Cell Carcinoma. *Journal of Investigative Dermatology,* **135**(11), pp. 2649-2656.

VERNE, S.H., MAGNO, R.J., EBER, A.E., CERVANTES, J., PERPER, M. and NOURI, K., 2018. Optical coherence tomography image processing for in vivo 3-dimensional visualization of basal cell carcinoma. *Skin Research & Technology,* **24**(3), pp. 509-511.

VILLARREAL-MARTINEZ, A., BENNASSAR, A., GONZALEZ, S., MALVEHY, J. and PUIG, S., 2018. Application of in vivo reflectance confocal microscopy and ex vivo fluorescence confocal microscopy in the most common subtypes of basal cell carcinoma and correlation with histopathology. *British Journal of Dermatology,* **178**(5), pp. 1215-1217.

VON BRAUNMUHL, T., HARTMANN, D., TIETZE, J.K., CEKOVIC, D., KUNTE, C., RUZICKA, T., BERKING, C. and SATTLER, E.C., 2016. Morphologic features of basal cell carcinoma using the en-face mode in frequency domain optical coherence tomography. *Journal of the European Academy of Dermatology & Venereology,* **30**(11), pp. 1919-1925.

WALDMAN, R.A. and GRANT-KELS, J.M., 2019. The role of sunscreen in the prevention of cutaneous melanoma and nonmelanoma skin cancer. *Journal of the American Academy of Dermatology,* **80**(2), pp. 574-576.e1.

WANG, B., SHI, L., ZHANG, Y.F., ZHOU, Q., ZHENG, J., SZEIMIES, R.M. and WANG, X.L., 2017. Gain with no pain? Pain management in dermatological photodynamic therapy. *British Journal of Dermatology,* **177**(3), pp. 656-665.

WANG, G.Y., WANG, J., MANCIANTI, M. and EPSTEIN, E.H.J., 2011. Basal cell carcinomas arise from hair follicle stem cells in Ptch1(+/-) mice. *Cancer Cell,* **19**(1), pp. 114-124.

WANG, H., XU, Y., SHI, J., GAO, X. and GENG, L., 2015. Photodynamic therapy in the treatment of basal cell carcinoma: a systematic review and meta-analysis. *Photodermatology, Photoimmunology & Photomedicine,* **31**(1), pp. 44-53.

WANG, K.X., MEEKINGS, A., FLUHR, J.W., MCKENZIE, G., LEE, D.A., FISHER, J., MARKOWITZ, O. and SIEGEL, D.M., 2013. Optical coherence tomography-based optimization of mohs micrographic surgery of Basal cell carcinoma: a pilot study. *Dermatologic Surgery,* **39**(4), pp. 627-633.

WEISS, S.A., HANNIFORD, D., HERNANDO, E. and OSMAN, I., 2015. Revisiting determinants of prognosis in cutaneous melanoma. *Cancer,* **121**(23), pp. 4108-4123.

WELLS, R., GUTKOWICZ-KRUSIN, D., VELEDAR, E., TOLEDANO, A. and CHEN, S.C., 2012. Comparison of diagnostic and management sensitivity to melanoma between dermatologists and MelaFind: a pilot study. *Archives of Dermatology,* **148**(9), pp. 1083-1084.

WHITEMAN, D.C., BRAY, C.A., SISKIND, V., GREEN, A.C., HOLE, D.J. and MACKIE, R.M., 2008. Changes in the incidence of cutaneous melanoma in the west of Scotland and Queensland, Australia: hope for health promotion?. *European Journal of Cancer Prevention,* **17**(3), pp. 243-250.

WHITEMAN, D.C., PAVAN, W.J. and BASTIAN, B.C., 2011. The melanomas: a synthesis of epidemiological, clinical, histopathological, genetic, and biological aspects, supporting distinct subtypes, causal pathways, and cells of origin. *Pigment Cell & Melanoma Research,* **24**(5), pp. 879-897.

WHITEMAN, D.C., THOMPSON, B.S., THRIFT, A.P., HUGHES, M., MURANUSHI, C., NEALE, R.E., GREEN, A.C., OLSEN, C.M. and QSKIN STUDY, 2016. A Model to Predict the Risk of Keratinocyte Carcinomas. *Journal of Investigative Dermatology,* **136**(6), pp. 1247-1254.

WIEGELL, S.R., SKODT, V. and WULF, H.C., 2014. Daylight-mediated photodynamic therapy of basal cell carcinomas - an explorative study. *Journal of the European Academy of Dermatology & Venereology,* **28**(2), pp. 169-175.

WONG, T.H., MORTON, C.A., COLLIER, N., HAYLETT, A., IBBOTSON, S., MCKENNA, K.E., MALLIPEDDI, R., MOSELEY, H., SEUKERAN, D.C., RHODES, L.E., WARD, K.A., MOHD MUSTAPA, M.F. and EXTON, L.S., 2019. British Association of Dermatologists and British Photodermatology Group guidelines for topical photodynamic therapy 2018. *British Journal of Dermatology,* **180**(4), pp. 730-739.

WORK GROUP, INVITED REVIEWERS, KIM, J.Y.S., KOZLOW, J.H., MITTAL, B., MOYER, J., OLENCKI, T. and RODGERS, P., 2018. Guidelines of care for the management of basal cell carcinoma. *Journal of the American Academy of Dermatology,* **78**(3), pp. 540-559.

WORLD HEALTH ORGANIZATION, 2008. *The global burden of disease : 2004 update.* Geneva: World Health Organization||World Health Organization.

WORLD HEALTH ORGANIZATION and LUCAS, R., MCMICHAEL, T., SMITH, W., ARMSTRONG, B., PRÜSS-ÜSTÜN, A., 2006. *Solar Ultraviolet Radiation: global burden of disease from solar ultraviolet radiation.* Geneva: World Health Organization||World Health Organization.

WRIGHT, F.C., SOUTER, L.H., KELLETT, S., EASSON, A., MURRAY, C., TOYE, J., MCCREADY, D., NESSIM, C., GHAZARIAN, D., HONG, N.J.L., JOHNSON, S., GOLDSTEIN, D.P., PETRELLA, T. and MELANOMA DISEASE SITE GROUP, 2019. Primary excision margins, sentinel lymph node biopsy, and completion lymph node dissection in cutaneous melanoma: a clinical practice guideline. *Current Oncology,* **26**(4), pp. e541-e550.

XIANG, F., LUCAS, R., HALES, S. and NEALE, R., 2014. Incidence of nonmelanoma skin cancer in relation to ambient UV radiation in white populations, 1978-2012: empirical relationships. *JAMA Dermatology,* **150**(10), pp. 1063-1071.

YELAMOS, O., BRAUN, R.P., LIOPYRIS, K., WOLNER, Z.J., KERL, K., GERAMI, P. and MARGHOOB, A.A., 2019. Usefulness of dermoscopy to improve the clinical and histopathologic diagnosis of skin cancers. *Journal of the American Academy of Dermatology,* **80**(2), pp. 365-377.

YOULDEN, D.R., YOUL, P.H., SOYER, H.P., AITKEN, J.F. and BAADE, P.D., 2014. Distribution of subsequent primary invasive melanomas following a first primary invasive or in situ melanoma Queensland, Australia, 1982-2010. *JAMA Dermatology,* **150**(5), pp. 526-534.

ZAAR, O., SJOHOLM HYLEN, A., GILLSTEDT, M. and PAOLI, J., 2018. A prospective, randomized, within-subject study of ALA-PDT for actinic keratoses using different irradiation regimes. *Photodermatology, Photoimmunology & Photomedicine,* **34**(5), pp. 338-342.

ZHOU, W., CHEN, Z., YANG, S. and XING, D., 2017. Optical biopsy approach to basal cell carcinoma and melanoma based on all-optically integrated photoacoustic and optical coherence tomography. *Optics Letters,* **42**(11), pp. 2145-2148.

# PUBLICATIONS

# PUBLICATION I

**Hyperspectral imaging in detecting dermal invasion in lentigo maligna melanoma**

Neittaanmäki N, Salmivuori M, Pölönen I, Jeskanen L, Ranki A, Saksela O, Snellman E, Grönroos M

Br J Dermatol. 177(6):1742-1744, 2017 Dec.

KMA 8 June 2017
Research letter 16/924R2

**Hyperspectral imaging in detecting dermal invasion in lentigo maligna melanoma**

Dear Editor, Invasive lentigo maligna melanoma (LMM) and its *in situ* precursor lentigo maligna (LM) are the most common melanoma types on sun-damaged skin.[1] Clinically unsuspected invasion is revealed histologically in 5–52% of LMs.[2] Correct early diagnoses are crucial for determining accurate resection margins and discussion of sentinel lymph node examination.[3]

Hyperspectral imaging is based on the detection of spectral differences reflecting a tissue's biological properties.[4,5] We determined how accurately a hyperspectral imaging system (HIS) detected LMM invasion. A total of 31 patients, with 32 lesions, with histologically confirmed LM or LMM, participated in the study. Of the 32 LM/LMM lesions, 10 were histologically defined as LMMs (eight on the face or scalp, two on the trunk) with Breslow thicknesses between 0.4 and 1.6 mm (mean 0.85 mm). The remaining 22 lesions were histologically LMs (20 on the face or scalp, two on the trunk).

All lesions were evaluated with dermatoscopy (DermLite®, 3Gen Inc., San Juan Capistrano, CA, U.S.A.) and photographed (Canon Ixus 115 HS, 12.1 megapixel, Canon Inc., Tokyo, Japan). Hyperspectral images were taken *in vivo* using a HIS camera prototype (VTT FPI VIS-VNIR Spectral Camera, VTT Technical Research Centre of Finland, Espoo, Finland), based on a Fabry-Perot interferometer. Within seconds HIS captures the diffuse reflectance of visible and near-infrared light (500–900 nm), with a 12 $cm^2$ field of view (spatial resolution 6400 pixels $cm^{-2}$, pixel = 125 μm) and imaging depth of approximately 2 mm. In acquired hyperspectral images every pixel represents a diffuse reflectance spectrum, formed from mixing of spectra from the image's different materials. With mathematical modelling this spectrum can be separated into 'pure' or 'endmember' spectra. Endmembers can further be used to create abundance images showing localization of these spectra in the imaged area. A detailed description of the technique has been reported elsewhere.[4,5]

For the first four patients, the lesions were excised with 5-mm margins after imaging. In the subsequent cases, punch biopsies were taken from the suspected invasion sites, and thereafter excised completely, using a 5-mm margin for LM and a 10-mm margin for LMM. Specimens were processed routinely and stained with haematoxylin and eosin.

In abundance images, *in situ* LMs were seen as homogeneous white areas. In LMMs, abundance maps showed a dark hole on the invasion site, while the rest of lesion was seen as a homogeneous white area, as in LM. These areas, which represented the LMM invasion, were seen as clear white areas in separate abundance maps (Fig. 1). This finding was seen in nine of 10 LMMs (true positives). HIS did not detect the invasion in one of the 10 LMMs, where the Breslow thickness was 0.5 mm (false negative). In 19 of 22 LMs HIS did not indicate any sites of invasion (true negatives), but in three of 22 cases did suggest invasion where it was not detected histologically (false positives). Thus, HIS achieved a positive predictive value of 75%, a negative predictive value of 95%, sensitivity of 90% and specificity of 86.3%.

Diffuse reflectance records both light absorption and scattering, and thus provides information on skin morphology and chromophore content. In this study the abundance images showed clear differences between LM and LMM. Most likely, absorption of the skin chromophores (like melanin) at different skin levels explains most of the differences between spectra.

Many techniques have been developed for melanoma diagnostics. Of these, dermatoscopy and reflectance confocal microscopy (RCM) are widely used.[6] Both techniques are imprecise in determining melanoma thickness and early invasion. Multispectral imaging devices use four to 15 noncontinuous bands of wavelengths resulting in discrete spectral images, while HIS uses continuous narrow wavebands delivered from a tuneable filter. The HIS method used in this study showed potential in guiding practitioners to obtain more targeted diagnostic biopsies of LMM, improving early staging of LMM. HIS could also be developed further to measure the thickness of LMM noninvasively prior to surgery.

A limitation in our study was its small sample size. Although the analysis method is objective, clinicians still need to interpret the HIS images, albeit this needs less expertise than the interpretation of near-histological RCM images. The quality of the HIS images may be affected by imaging artefacts. A future goal is to image a large set

of various skin tumours for the development of a classification algorithm for noninvasive tumour diagnostics based on spectral data.

In conclusion, HIS is a promising tool to detect basal membrane invasion in LMM, and thus to separate in situ and invasive LMs for more accurate presurgical diagnostics.

## Acknowledgments

This study was funded by the Novo Nordisk Foundation's Novo PreSeed Grant and by the Instrumentarium Foundation and by the Finnish Cancer foundation.

N. Neittaanmäki[1]

M. Salmivuori[2]

I. Pölönen[3]

L. Jeskanen[4]

A. Ranki[4]

O. Saksela[4]

E. Snellman[5]

M. Grönroos[2]

[1]Department of Clinical Pathology, Sahlgrenska University Hospital, Institute of Biomedicine at the Sahlgrenska Academy, University of Gothenburg, Gothenburg, Sweden

[2]Department of Dermatology and Allergology, Päijät-Häme Social and Health Care Group, Lahti, Finland

[3]Department of Mathematical Information Technology, University of Jyväskylä, Jyväskylä, Finland

[4]Departments of Dermatology and Allergology, University of Helsinki and Helsinki University Hospital, Helsinki, Finland

[5]Department of Dermatology, University of Tampere and Tampere University Hospital, Tampere, Finland

E-mail: noora.neittaanmaki@fimnet.fi

## References

1 Bosbous MW, Dzwierzynski WW, Neuburg M. Lentigo maligna: diagnosis and treatment. *Clin Plast Surg* 2010; **37**:35–46.

2 McGuire LK, Disa JJ, Lee EH *et al*. Melanoma of the lentigo maligna subtype: diagnostic challenges and current treatment paradigms. *Plast Reconstr Surg* 2012; **129**:288e–99e.

3 Hieken TJ, Hernández-Irizarry R, Boll JM, Jones Coleman JE. Accuracy of diagnostic biopsy for cutaneous melanoma: implications for surgical oncologists. *Int J Surg Oncol* 2013; **2013**:196493.

4 Neittaanmaki-Perttu N, Grönroos M, Tani T *et al*. Detecting field cancerization using a hyperspectral imaging system. *Lasers Surg Med* 2013; **45**:410–17.

5 Neittaanmaki-Perttu N, Gronroos M, Jeskanen L *et al*. Delineating margins of lentigo maligna using a hyperspectral imaging system. *Acta Derm Venereol* 2015; **95**:549–52.

6 Smith L, Macneil S. State of the art in non-invasive imaging of cutaneous melanoma. *Skin Res Technol* 2011; **17**:257–69.

7 Glud M, Gniadecki R, Drzewiecki KT. Spectrophotometric intracutaneous analysis versus dermoscopy for the diagnosis of pigmented skin lesions: prospective, double-blind study in a secondary reference centre. *Melanoma Res* 2009; **19**:176–9.

Funding sources**:** this study was funded by the Novo Nordisk Foundation's Novo PreSeed Grant, by the Instrumentarium Foundation and by the Finnish Cancer foundation.

Conflicts of interest: none declared.

**Figure legend**

**Fig 1.** Clinical images, histological images and hyperspectral abundance images representing lentigo maligna melanoma (LMM) (true positive). (a) Photograph of LMM. (b) Dermatoscopic image of LMM. (c) Hyperspectral abundance map representing the healthy skin around the lesion (white). (d) Hyperspectral abundance map representing the noninvasive part of the LMM lesion (white). (e) Hyperspectral abundance map representing the dermal invasion in LMM seen in a separate

abundance map; the red arrow points to the invasion area. (f) Haematoxylin and eosin staining of LMM (Breslow thickness 1.6 mm). (g) Immunohistochemistry for MART1 in LMM (Breslow thickness 1.6 mm).

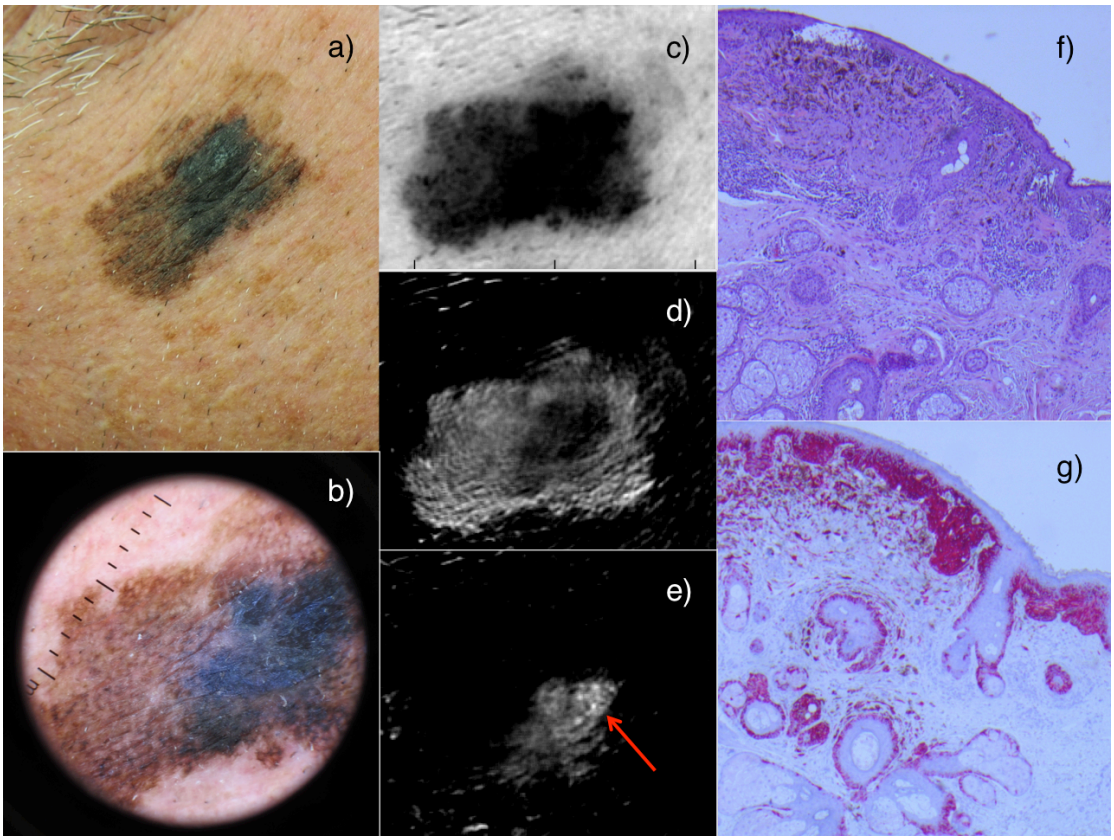

# PUBLICATION
# II

**Hyperspectral Imaging System in the Delineation of Ill-defined Basal Cell Carcinomas: a pilot study**

Salmivuori M, Neittaanmäki N, Pölönen I, Jeskanen L, Snellman E, Grönroos M.

J Eur Acad Dermatol Venereol. 33(1):71-78, 2019 Jan.

DR. MARI SALMIVUORI (Orcid ID : 0000-0003-0193-0552)

Article type : Original Article

# Hyperspectral Imaging System in the Delineation of Ill-defined Basal Cell Carcinomas: A Pilot Study

M. Salmivuori MD[1,5]; N. Neittaanmäki MD, PhD[2]; I. Pölönen PhD[3]; L. Jeskanen MD[4]; E. Snellman MD, PhD[1,5]; M. Grönroos MD, PhD[1]

1) Department of Dermatology and Allergology, Päijät-Häme Social and Health Care Group, Lahti, Finland

2) Departments of Pathology and Dermatology, Institutes of Biomedicine and Clinical Sciences, Sahlgrenska Academy, University of Gothenburg, Gothenburg, Sweden

3) Faculty of Mathematical Information Technology, University of Jyväskylä, Finland

4) Department of Dermatology and Allergology, Helsinki University Central Hospital, Finland

5) Department of Dermatology, Tampere University and Tampere University Hospital, Finland

This article has been accepted for publication and undergone full peer review but has not been through the copyediting, typesetting, pagination and proofreading process, which may lead to differences between this version and the Version of Record. Please cite this article as doi: 10.1111/jdv.15102

**Corresponding author:** Mari Salmivuori, Ihotautien poliklinikka, Keskussairaalankatu 7, 15830 Lahti, Finland

Mobile: +358505355616, E-mail: salmivuori.mari.k@student.uta.fi

**Funding:** This study was funded by research grants from the SILY, Finnish Dermatological Society, the Cancer Foundation Finland, the Foundation for Clinical Chemistry Research, and the Instrumentarium Science Foundation.

**Conflict of interest:** The authors declare no conflicts of interest.

## ABSTRACT

**Background** Basal cell carcinoma (BCC) is the most common skin cancer in the Caucasian population. Eighty percent of BCCs are located on the head and neck area. Clinically ill-defined BCCs often represent histologically aggressive subtypes, and they can have subtle subclinical extensions leading to recurrence and the need for re-excisions.

**Objectives** The aim of this pilot study was to test the feasibility of a hyperspectral imaging system (HIS) *in vivo* in delineating the preoperatively lateral margins of ill-defined BCCs on the head and neck area.

**Methods** Ill-defined BCCs were assessed clinically with a dermatoscope, photographed, and imaged with HIS. This was followed by surgical procedures where the BCCs were excised at the clinical border and the marginal strip separately. HIS, with a 12 $cm^2$ field of view and fast data processing, records a hyperspectral graph for every pixel in the imaged area, thus creating a data cube. With automated computational modelling, the spectral data is converted into localisation maps showing the tumour borders. Interpretation of these maps was compared to the histologically verified tumour borders.

**Results** Sixteen BCCs were included. Of these cases, 10/16 were the aggressive subtype of BCC and 6/16 were nodular, superficial, or a mixed type. HIS delineated the lesions more accurately in 12/16 of the BCCs compared to the clinical evaluation (4/16 wider and 8/16 smaller by HIS). In 2/16 cases, the HIS-delineated lesion was wider without histopathological confirmation. In 2/16 cases, HIS did not detect the histopathologically confirmed subclinical extension.

**Conclusions** HIS has the potential to be an easy and fast aid in the preoperative delineation of ill-defined BCCs, but further adjustment and larger studies are warranted for an optimal outcome.

## INTRODUCTION

Basal cell carcinoma (BCC) is a locally destructive and rarely metastasising non-melanoma skin cancer (NMSC), which comprises 40% of all cancers worldwide[1].

Eighty percent of NMSCs are BCCs[2]. The incidence of BCC is as high as the incidence of all other cancers combined, and its incidence continues to increase, also affecting ever-younger populations[3-5]. BCC is causing a remarkable burden via healthcare costs, treatment capacity, and the morbidity of affected individuals[1,2,4].

Histologically, BCCs can be classified by their morphological growth pattern into indolent (nodular and superficial) or aggressive (micronodular, morpheaform, infiltrative, and metatypical – i.e. basosquamous) types[6]. In 27–43% of cases, a combination of different patterns – i.e. a mixed histology – exists[6-8]. The histological subtype affects the clinical choice of treatment and the prognosis[6]. A high risk of recurrence is associated most importantly with aggressive growth patterns along with location in high-risk anatomic areas (nose, ears, eyes, and periocular areas), clinically unclear visualisation of the border, immunosuppression, recurrence, and perineural involvement[9]. Clinically, BCCs are classified by visual assessment as either indolent (nodular, superficial) or ill-defined (aggressive subtypes)[9]. Roughly one out of five BCCs is the histologically verified aggressive subtype[6,10]. However, the proportion might be even higher. The accuracy of a punch biopsy in the interpretation of a mixed histology is 37%[11]. Moreover, in 39.1% of aggressive BBCs, the punch biopsy fails to identify the subtype correctly compared to the following excision, and 11–14.1% of any type of BCC shows an unsuspected aggressive component in the excision compared to the preceding punch biopsy[8,11].

The incidence of BCC is highest in the most sun-exposed anatomic locations[12]. Thus 80% of BCCs – and most of the aggressive types – are located on the head and neck area[2,13], where preserving the anatomy and function plays a major role. Surgery and, if

available, Mohs micrographic surgery (MMS) with a 100% margin control is the treatment of choice for high-risk BCCs[9].

Hyperspectral imaging is based on tissue chromophores (like melanin if present, haemoglobin, proteins, and water) affecting the absorption and scattering of emitted light, thus causing, together with autofluorescence, a unique spectral graph for different biological tissues[14]. A hyperspectral imaging system (HIS) has shown potential in the preoperative delineation of lentigo maligna[15] and the detection of field-cancerised skin[16]. In this pilot study, the aim was to test the feasibility of HIS in the preoperative delineation of the lateral margins of ill-defined BCCs on the head and neck area.

## MATERIALS AND METHODS

We followed the Declaration of Helsinki, and the Ethics Committee of the Tampere University Hospital District, Finland, approved our study protocol. All the recruited volunteering patients were informed orally and in writing, and they provided their written consent.

### *Patients*

Twenty-three patients with 24 lesions were recruited prospectively between March 2014 and March 2017 at the Department of Dermatology and Allergology at the Päijät-Häme Social and Health Care Group, Lahti, Finland. The inclusion criterion was a clinically assessed primary BCC with a visually ill-defined margin on the head and neck area, and which was later histologically confirmed to be a BCC. Eight BCCs

from seven patients were excluded: six because these were not treated according to the study protocol (3 represented only the superficial subtype and were treated with cryosurgery, and 3 were operated on without a separate circumferential marginal strip). Furthermore, one patient was excluded due to the imaging artefacts and one due to discrepancy in the histopathological statement (subclinical extension shown only in the preoperative biopsies and not in the separate margin strip).

Thus, 16 patients (7 female and 9 male) with 16 lesions completed the study. The mean age of the patients was 77 years (range 59–91 years). Five patients displayed anamnestic skin phototype I, nine patients displayed skin phototype II, and two patients displayed skin phototype III. Thirteen patients had a previous history of skin malignancy or its precursor, and seven of them had multiple conditions (basal cell carcinoma n=12, actinic keratosis n=8, and melanoma n=2). None of the patients had received cytostatics or radiotherapy in the study areas or received phototherapy for any skin condition. One patient had received immunosuppressive treatments.

*Imaging processes*

All the lesions were initially evaluated clinically and with a dermatoscope (Dermlite® 3GenCA, USA). They were photographed native with a digital camera (Canon Ixus 115 HS, 12.1 megapixel or Canon Ixus 130, 14.1 megapixel) and with the dermatoscope linked to the digital camera. The hyperspectral imaging process was performed initially without drawing the clinically assessed tumour border, and then after marking the clinical borders on the skin. The prototype of HIS is described more detailed elsewhere [15]. (In short, the VTT FPI VIS-VNIR Spectral Camera uses visible-to-near infrared light – i.e. wavelengths 500–900 nm based on a Fabry-Perot

interferometer – which enables the use of tuneable waveband selection. It has a large, 12 $cm^2$ field of view (FOV) with a spatial resolution of 6,400 pixels/$cm^2$, where one pixel is approx. 125 µm, and an imaging depth of approx. 2 mm.) [15] The hyperspectral imaging took only seconds to capture the hyperspectral data cube, which thereafter was analysed computationally in 5–10 minutes.

*Data analysis*

The hyperspectral data cube is a three-dimensional data cube, where the x-axis and y-axis are the dimensions on the skin surface, and the z-axis is the 70 layered hyperspectral images, where every layer is imaged on a narrow waveband. Every pixel on the skin's surface has a unique hyperspectral graph – i.e. an end-member – from which the abundance maps are calculated based on mathematical modelling (see *Fig.1*).

In this pilot study, we used mathematical modelling of linear mixture, as used in our previous studies[15,16]. These abundance maps were interpreted on site by the test-readers (M.S., M.G., I.P. and N.N.). Additionally, we developed three diverse enhanced mathematical models to create more sensitive ways to characterise the visually ill-defined margins of BCCs. Finally, the mathematical models used for the results were 1) an inversion of linear mixture model using iterative Vertex Component Analysis – i.e. the linear mixture (the one used on site), 2) an inversion of linear mixture model from the estimated single scattering albedo (SSA) using iterative Vertex Component Analysis – i.e. the linear mixture with SSA, 3) a closed form chromophore-specific approximation for the estimated SSA – i.e. chromophore specific with SSA, and 4) a modified standard normal variate correction algorithm – i.e. a standard variate. All abundance maps from these four models were interpreted

by the same test-readers. A summarised technical and mathematical presentation of the imaging system used, the algorithms, and simulated results are presented in the supplementary material, *S1*.

Each of the mathematical models used has advantages and disadvantages. The standard variate model is quite sensitive to all changes in spectra that differ from the mean spectra of the imaged area. When there is either a lot of normal skin or an ill-defined BCC, the standard variate model will distinguish the areas well. The linear mixture and linear mixture with SSA both capture changes in the concentration of skin chromophores. The chromophore specific with SSA is sensitive to skin scattering and absorption. The results from calculations with the linear mixture, the linear mixture with SSA, and the chromophore specific with SSA models can be used to simulate an imaged spectral cube. The simulated cube is a characterisation of the originally acquired image presented in the form of an abundance map for interpretation.

*Surgical procedures and the histopathological sampling*

After the imaging and analysis processes, and if the patient did not have an appointment for an operation on the same day, we took biopsies from the lesions and the areas where the HIS imaging indicated the BCC may be spreading. For all cases, we used a special operation technique to verify whether a subclinical extension was detected by HIS (see *Fig.1*). This included an initial excision of the tumour from the clinically and dermatoscopically detected border followed by a separately operated 2 mm circumferential marginal strip, both with orientation marks. The circumferential strip allowed us to evaluate whether there was a subclinical extension in the marginal

area. If a free margin was found in the separately excised tumour specimen, this allowed us to evaluate if the BCC was smaller than the clinical evaluation with dermatoscopy. All the samples were orientated, fixed in 10% formalin, embedded in paraffin, and cut into 3 µm thick slices, which were stained with haematoxylin and eosin and, if necessary, with CK-PAN staining for the evaluation of perineural involvement. The tumour specimens were sectioned using the normal "bread-loaf" technique. The circumferential strips were sectioned closely in vertical slices. The histopathological samples were analysed by an experienced dermatopathologist blinded to the HIS outcome. If the circumferential marginal strip was BCC-positive, a re-excision was performed.

**RESULTS**

The histopathological subtypes of the 16 included BCCs are shown in Table 1. 10/16 BCCs represented the aggressive subtype (infiltrative, infiltrative with perineural invasion, morpheaform, or micronodular features) in the final excision. In 6/16 BCCs the subtype was nodular, superficial, or a mixed histology of these two in the final excision, even though clinically all the included lesions were ill defined.

In 12/16 cases, HIS was capable of delineating the BCCs more accurately than the conventional clinical evaluation by the naked eye and with a dermatoscope. HIS-delineated lesions were wider in 4/16 of the BCCs (see *Fig.2*), and in 8/16 BCCs the lesions were delineated to be smaller than the clinical evaluation. In 2/16 cases, the HIS-delineated lesion was wider but could not be confirmed histopathologically (false positives). In 2/16 cases, HIS did not detect the histopathologically confirmed BCC in the circumferential strip (false negatives).

The results were quite similar in the four different mathematical models. If three out of four models showed similar tumour borders, those were regarded as the HIS-defined borders (see *Table 1*). However, it is still unclear which model is best for the imaging of BCC.

## DISCUSSION

This study shows that HIS is feasible in detecting the borders of ill-defined BCCs, but further development work is needed to determine the optimal model for data processing.

To our knowledge, there are no earlier studies on delineating BCC margins using hyperspectral imaging technology.

Other non-invasive imaging techniques for delineating the lateral margins of BCCs include dermatoscopy, reflectance confocal microscopy (RCM), and optical coherence tomography (OCT)/high-definition optical coherence tomography (HD-OCT). In clinical practice, dermatoscopy is the most widely used for the detection of lateral margins, although its use preoperatively has not reduced the excision stages in MMS, and thus evidence of its accuracy is lacking[17]. It has been previously shown that preoperative *in vivo* use of RCM and OCT can reduce the number of excision stages in the MMS of BCCs[17].

The advantages of HIS compared to the previously studied imaging techniques in the preoperative assessment of the lateral surgical margin are the following: i) adjustable FOV up to a maximum of 12 $m^2$ in HIS captured and processed in 5–10 min compared to 1 $cm^2$ (with mosaicking) in RCM captured and processed in 2 min[18], and

6x6 mm (0.36 $cm^2$) in OCT, where 5x5 mm is captured and processed in 40 s[19]; ii) imaging depth of approx. 2 mm for HIS compared to 200 µm for RCM[17] and 0.2–2.5 mm for OCT, though one should note that the higher resolution is compromised by the penetration depth[19]; and iii) interpretation of HIS images is quick, easy to learn with a little experience, and does not require histological knowledge, unlike HD-OCT and RCM[17,19]. It seems that the interpretation of HIS images can be straightforward, but currently in some cases more combined information is needed from different models to conclude the interpretation, and thus further development of HIS is warranted.

Our result for 4/16 BCCs revealed that subclinical extension by HIS is quite similar to RCM in the preoperative *in vivo* assessment of the margins, as in Venturini et al.'s study, RCM found subclinical extension in 3/10 cases compared to the dermatoscopically assessed margins prior to excision[20]. OCT found the subclinical extension of BCC in 11/52 cases compared to clinical evaluation by a Mohs surgeon[21]. Wang et al. [21] had a 100% evaluation of the margins in MMS excision compared to our design with vertical sections, which is clearly a limitation in our study. Furthermore, OCT delineated the lateral margins to be smaller by 1.4 +/-1.3 mm than the clinical evaluation[21]. HIS delineated the lesion as being smaller in 8/16 cases.

In addition, high frequency ultrasound (HFUS) and fluorescence diagnosis have earlier been studied for the *in vivo* preoperative delineation of BCC. In lateral margin delineation, ultrasound has a low correlation compared to histopathology[22]. The subclinical extensions of the infiltrative and micronodular subtypes of BCC in particular are less likely to be detected by HFUS[23]. In deep margin assessment, the correlation using HFUS is intermediate[22], and in facial BCCs, there is even a good

correlation for the deep margin with histopathology[24]. HFUS has the advantage of showing underlying structures like cartilage and bone[24]. In the fluorescence diagnosis of facial BCCs, the exogenic fluorescence diagnosis has no benefit in margin assessment compared to clinical evaluation in high risk areas (though most of the BCCs were nodular in this study) [25], but in aggressive types bispectral fluorescence imaging (using autogenic and exogenic fluorescence) had some potential in delineating the margins of BCC, with a 42% agreement in lateral margin assessment compared to the histopathology of MMS[26].

A limitation of HIS is its poorer resolution compared to OCT and RCM. In this study, HIS was not used to evaluate the deep margin, which in the future might be possible with further developments given the approx. 2 mm penetration depth of HIS. However, the assessment of deep margins is also limited with RCM and HD-OCT[17]. Artefacts in HIS abundance maps can be caused by an uneven imaging surface – i.e. round and sharp forms in the imaging area, and thus one case locating on nose was excluded with low quality in the abundance maps for interpretation. With further developments of HIS, it might be possible to handle these artefacts better. Additional pathological findings (i.e. actinic keratoses, etc.) in the imaging area might also be confounding factors in the interpretation of the HIS abundance maps, and thus further development work with HIS is needed. The limitations in our pilot study design were the small number of the cases, and thus these results are preliminary. This study was not performed to distinguish BCCs from other lesions on sun-damaged skin, but rather to visualise the borders of the lesions. Thus, larger studies are warranted in the future.

Subclinical extension in aggressive BCCs can consist of cords with a thickness of a few cells[6]. Thus, in the future it would be interesting to repeat this study design by

assessing 100% of the margin and comparing the results to MMS. At the clinic where patients were recruited, MMS is not available, and thus we used the presented operation technique. Compared to MMS, in our method the separate circumferential strip was not assessed with a 100% margin control. In one true positive case, we were able to confirm subclinical extension of the marginal strip after additional histological sectioning based on the suspected subclinical extension in the HIS abundance maps. However, additional sectioning failed to reveal the subclinical extension in the two other false positive cases. It can be speculated that MMS with a 100% margin control would have revealed the histological extension in these false positive cases.

It would be interesting to investigate if HIS could be useful in MMS by reducing the number of stages by defining the margins preoperatively more accurately than the clinical evaluation, and by being faster than RCM. HIS might be also useful in reducing the number of re-excisions by more accurate preoperative assessment in intermediate- or low-risk anatomic locations, and also in high-risk areas if MMS is not available. After MMS, primary BCCs have a 4.4% recurrence and recurrent BCCs have a 3.9% recurrence in the 10-year follow-up; after traditional excision, the corresponding rates are 12.2% and 13.5%[27]. In traditional excision, the recurrence rates varies according to the width of the surgical margin, where a 2, 3, 4 or 5 mm announced negative margin has a recurrence rate of 3.96, 2.56, 1.62 and 0.39% respectively; if a positive margin is announced, the overall recurrence is 27%[28]. In the future with HIS, it might be possible to save tissues in cosmetically sensitive areas.

With the increasing incidence of BCCs, there is a need for new technologies to make the treatment of BCC less time-consuming and more cost-effective. With preliminary results of 12/16 more precisely delineated lesions and 4/16 revealed subclinical

extensions, the HIS has the potential to be a clinical aid in treatment of ill-defined BCCs in the cosmetically sensitive areas of the head and neck region.

**ACKNOWLEDGEMENTS**

This study was funded by research grants from the SILY, Finnish Dermatological Society, the Cancer Foundation Finland, the Foundation for Clinical Chemistry Research, and the Instrumentarium Science Foundation. We want to give our special thanks to dermatopathologist Katriina Lappalainen for her assistance with the histopathological images, and to our irreplaceable assistant, nurse Ulla Oesch-Lääveri.

**REFERENCES**

1 Cakir BO, Adamson P, Cingi C. Epidemiology and economic burden of nonmelanoma skin cancer. *Facial Plastic Surgery Clinics of North America* 2012; **20**:419-22.

2 Kim RH, Armstrong AW. Nonmelanoma skin cancer. *Dermatol Clin* 2012; **30**:125-39.

3 Levell NJ, Igali L, Wright KA, Greenberg DC. Basal cell carcinoma epidemiology in the UK: the elephant in the room. *Clinical & Experimental Dermatology* 2013; **38**:367-9.

4 Holm A, Nissen CV, Wulf HC. Basal Cell Carcinoma is as Common as the Sum of all Other Cancers: Implications for Treatment Capacity. *Acta Derm Venereol* 2016; **96**:505-9.

5 Deady S, Sharp L, Comber H. Increasing skin cancer incidence in young, affluent, urban populations: a challenge for prevention. *Br J Dermatol* 2014; **171**:324-31.

6 Crowson AN. Basal cell carcinoma: biology, morphology and clinical implications. *Modern Pathology* 2006; **19**:127.

7 Cohen PR, Schulze KE, Nelson BR. Basal cell carcinoma with mixed histology: a possible pathogenesis for recurrent skin cancer. *Dermatologic Surgery* 2006; **32**:542-51.

8 Kamyab-Hesari K, Seirafi H, Naraghi ZS, et al. Diagnostic accuracy of punch biopsy in subtyping basal cell carcinoma. *Journal of the European Academy of Dermatology & Venereology* 2014; **28**:250-3.

9 Trakatelli M, Morton C, Nagore E, et al. Update of the European guidelines for basal cell carcinoma management. *European Journal of Dermatology* 2014; **24**:312-29.

10 Burdon-Jones D, Thomas PW. One-fifth of basal cell carcinomas have a morphoeic or partly morphoeic histology: implications for treatment. *Australas J Dermatol* 2006; **47**:102-5.

11 Wolberink EA, Pasch MC, Zeiler M, et al. High discordance between punch biopsy and excision in establishing basal cell carcinoma subtype: analysis of 500 cases. *Journal of the European Academy of Dermatology & Venereology* 2013; **27**:985-9.

12 Richmond-Sinclair NM, Pandeya N, Ware RS, et al. Incidence of basal cell carcinoma multiplicity and detailed anatomic distribution: longitudinal study of an Australian population. *J Invest Dermatol* 2009; **129**:323-8.

13 Betti R, Radaelli G, Mussino F, et al. Anatomic location and histopathologic subtype of basal cell carcinomas in adults younger than 40 or 90 and older: any difference?. *Dermatologic Surgery* 2009; **35**:201-6.

14 Lu G, Fei B. Medical hyperspectral imaging: a review. *J Biomed Opt* 2014; **19**:10901.

15 Neittaanmaki-Perttu N, Gronroos M, Jeskanen L, et al. Delineating margins of lentigo maligna using a hyperspectral imaging system. *Acta Derm Venereol* 2015; **95**:549-52.

16 Neittaanmaki-Perttu N, Gronroos M, Tani T, et al. Detecting field cancerization using a hyperspectral imaging system. *Lasers in Surgery & Medicine* 2013; **45**:410-7.

17 Que SKT. Research Techniques Made Simple: Noninvasive Imaging Technologies for the Delineation of Basal Cell Carcinomas. *J Invest Dermatol* 2016; **136**:33.

18 Larson B, Abeytunge S, Seltzer E, et al. Detection of skin cancer margins in Mohs excisions with high-speed strip mosaicing confocal microscopy: a feasibility study. *Br J Dermatol* 2013; **169**:922-6.

19 Cheng HM, Guitera P. Systematic review of optical coherence tomography usage in the diagnosis and management of basal cell carcinoma. *Br J Dermatol* 2015; **173**:1371-80.

20 Venturini M, Gualdi G, Zanca A, et al. A new approach for presurgical margin assessment by reflectance confocal microscopy of basal cell carcinoma. *Br J Dermatol* 2016; **174**:380-5.

21 Wang KX, Meekings A, Fluhr JW, et al. Optical coherence tomography-based optimization of mohs micrographic surgery of Basal cell carcinoma: a pilot study. *Dermatologic Surgery* 2013; **39**:627-33.

22 Nassiri-Kashani M, Sadr B, Fanian F, et al. Pre-operative assessment of basal cell carcinoma dimensions using high frequency ultrasonography and its correlation with histopathology. *Skin Research & Technology* 2013; **19**:132.

23 Jambusaria-Pahlajani A, Schmults CD, Miller CJ, et al. Test characteristics of high-resolution ultrasound in the preoperative assessment of margins of basal cell and squamous cell carcinoma in patients undergoing Mohs micrographic surgery. *Dermatologic Surgery* 2009; **35**:9-15.

24 Bobadilla F, Wortsman X, Munoz C, et al. Pre-surgical high resolution ultrasound of facial basal cell carcinoma: correlation with histology. *Cancer Imaging* 2008; **8**:163-72.

25 Wetzig T, Kendler M, Maschke J, et al. No clinical benefit of preoperative fluorescence diagnosis of basal cell carcinoma localized in the H-zone of the face. *Br J Dermatol* 2010; **162**:1370-6.

26 Stenquist B, Ericson MB, Strandeberg C, et al. Bispectral fluorescence imaging of aggressive basal cell carcinoma combined with histopathological mapping: a preliminary study indicating a possible adjunct to Mohs micrographic surgery. *Br J Dermatol* 2006; **154**:305-9.

27 van Loo E, Mosterd K, Krekels GA, et al. Surgical excision versus Mohs' micrographic surgery for basal cell carcinoma of the face: A randomised clinical trial with 10 year follow-up. *Eur J Cancer* 2014; **50**:3011-20.

28 Gulleth Y, Goldberg N, Silverman RP, Gastman BR. What is the best surgical margin for a Basal cell carcinoma: a meta-analysis of the literature. *Plastic & Reconstructive Surgery* 2010; **126**:1222-31.

29 Saari H, Aallos V, Holmlund C, et al. Handheld hyperspectral imager. *Next-Generation Spectroscopic Technologies III* 2010/04/28; **7680**:76800D.

30 Jacques SL. Optical properties of biological tissues: a review. *Physics in Medicine & Biology* 2013; **58**:37.

31 Nascimento JMP, Dias JMB. Vertex component analysis: A fast algorithm to unmix hyperspectral data. *IEEE Trans Geosci Remote Sens* 2005; **43**:898-910.

32 Bowles JH, Palmadesso PJ, Antoniades JA, et al. Use of filter vectors in hyperspectral data analysis. *Proceedings of SPIE - The International Society for Optical Engineering* 1995; **2553**:148-157.

33 Barnes RJ, Dhanoa MS, Lister SJ. Standard Normal Variate Transformation and De-Trending of Near-Infrared Diffuse Reflectance Spectra: *Applied Spectroscopy* 1989; **43**:772-7.

**FIGURES AND LEGENDS**

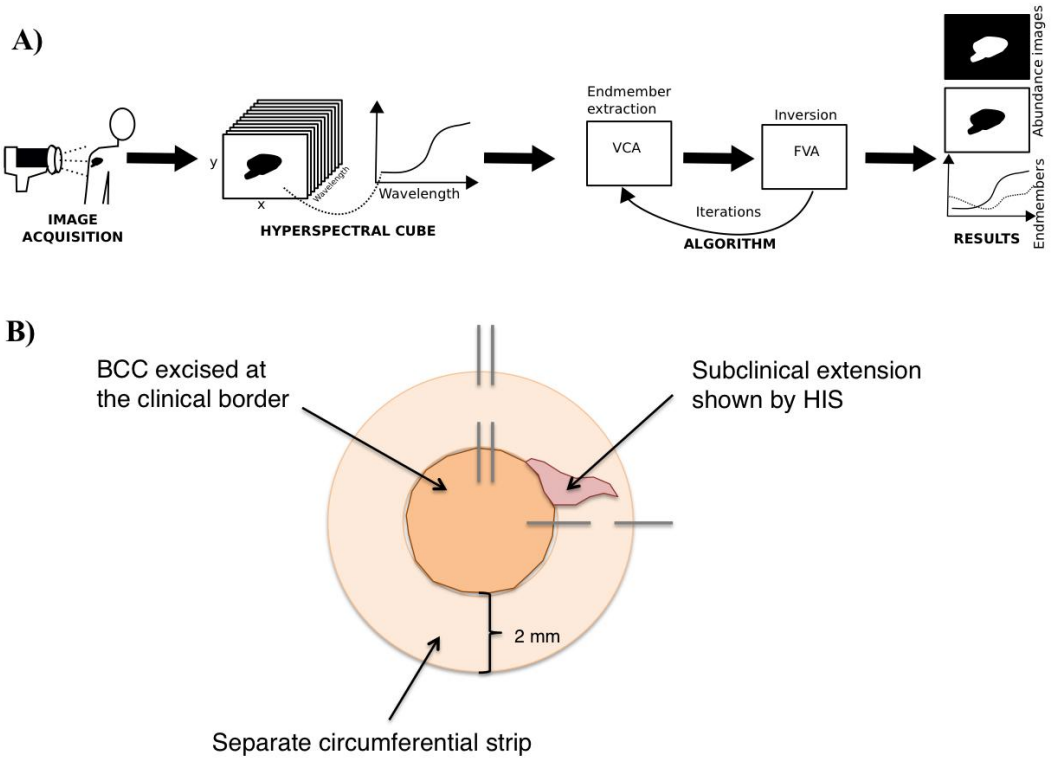


Fig. 1 A) Hyperspectral imaging process and B) operation technique to verify the subclinical extension detected by HIS.

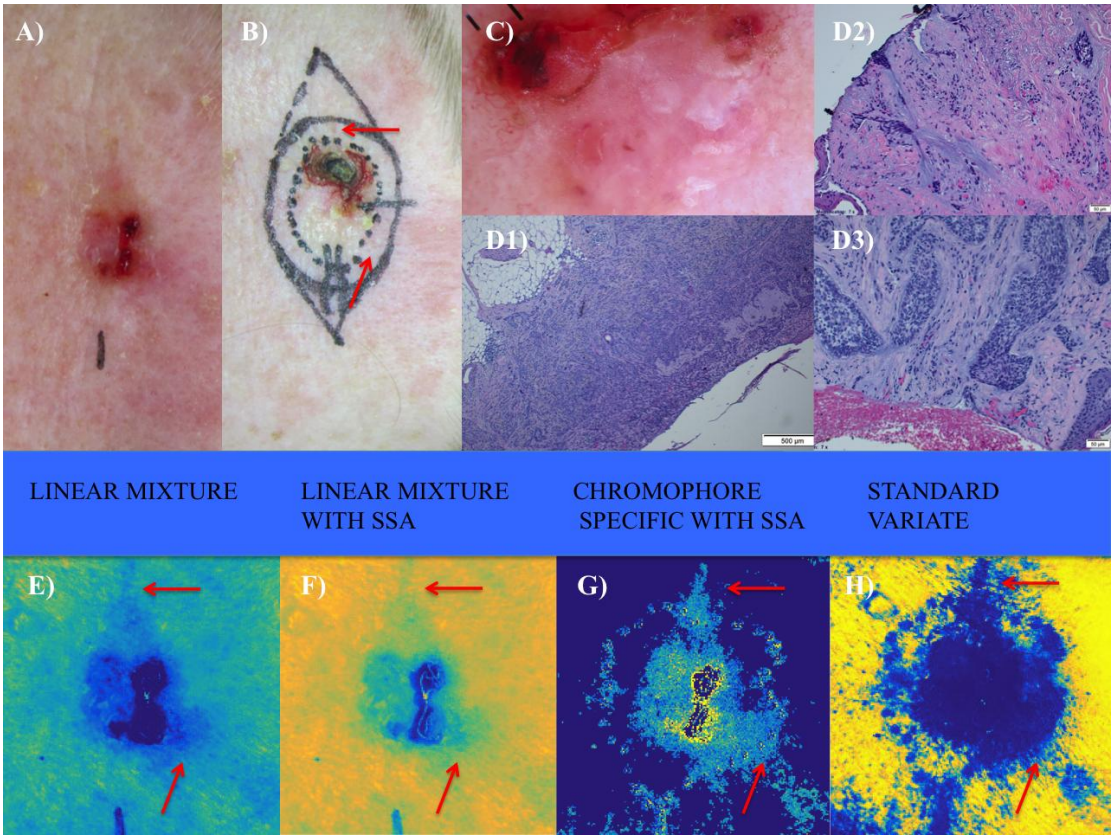


Fig. 2 Example patient with BCC delineated wider by HIS. Histologically, there was a nodular, superficial, micronodular, and infiltrative BCC, with perineural invasion, which showed subclinical micronodular growth in the marginal strip shown by HIS (arrows). A) Clinical picture, B) final excision with our operation technique, C) dermatoscopy image, D1) histological image from the main tumour area with the different aggressive growth patterns D2–D3) histological image, where the subclinical extension of BCC was detected in the separate marginal strip (D2 lower arrow and D3 upper arrow). HIS abundance maps marking the clinically and dermatoscopically assessed tumour border on the skin (arrows pointing the subclinical extension detected by HIS): E) linear mixture F) linear mixture with single scattering albedo (SSA), G) chromophore specific with SSA H) standard variate.

## TABLES

Table 1. Histopathological analyses of the BCCs, anatomic location of the lesion, interpretation of the mathematical models, and the HIS outcome compared to clinical evaluation.

| esion | Anatomic location of the lesion | BCC subtype in the biopsies | BCC subtype in the final excision | BCC subtype in the separate circumferential strip | Additional histopathological findings | Linear mixture model | Enhanced linear mixture model | Chromo-phore specific model | Mean value model | HIS outcome compared to the clinical assessment, and confirmed histologically |
|---|---|---|---|---|---|---|---|---|---|---|
| 1 | right cheek | | superficial, nodular, micronodular | | sun damaged skin | + | + | + | + | false pos.* |
| 2 | tip of nose | | superficial, nodular | | sun damaged skin | - | - | - | 0 | smaller** |
| 3 | preaurically on right cheek | nodulocystic | superficial, nodular, micronodular | superficial | solar lentigo | + | + | + | + | wider*** |
| 4 | tip of nose | | superficial, nodular, micronodular, infiltrative, basosquamous | | sun damaged skin | - | - | - | 0 | smaller |
| 5 | lateral to nasolabial fold on right cheek | nodular | nodular | | sun damaged skin | - | - | - | - | smaller |
| 6 | left cheek | nodular, micronodular | nodular, micronodular | | sun damaged skin | - | - | - | - | smaller |
| 7 | forehead | nodular, micronodular | superficial, nodular, micronodular, infiltrative with perineural invasion | micronodular | actinic keratoses | + | + | + | + | wider |
| 8 | left auricle | superficial, nodular | superficial, nodular | | sun damaged skin | - | - | - | 0 | smaller |
| 9 | right temple | nodular, micronodular, sclerotic | nodular, micronodular, infiltrative with perineural invasion | micronodular | solar lentigo | + | + | + | 0 | wider |
| 10 | left auricle | superficial, nodular | nodular, micronodular, infiltrative | micronodular | sun damaged skin | = | = | = | 0 | false neg. **** |
| 11 | neck, behind left ear | | nodular | | actinic kertoses, solar lentigo | - | - | - | - | smaller |
| 12 | left cheek | nodular | superficial, nodular | | sun damaged skin, solar lentigo | + | + | + | + | false pos. |
| 13 | left cheek | nodular | cicatrix | | eczema | - | - | - | - | smaller |

| | | | | | | | | | | |
|---|---|---|---|---|---|---|---|---|---|---|
| 14 | right ala of nose | nodular | nodular, micronodular | nodular, micronodular | actinic keratoses | = | = | = | = | false neg. |
| 15 | right temple | superficial | superficial, nodular, micronodular, infiltrative with perineural invasion | | sun damaged skin, ulcer | - | - | - | - | smaller |
| 16 | forehead | nodular, infiltrative | nodular, micronodular | nodular, micronodular | sun damaged skin | 0 | + | + | + | wider |

(+) interpret wider in the abundance maps

(-) interpret smaller in the abundance maps

(0) too much of artefact for interpretation

(=) interpreted as same borders as ~~than~~ visually assessed (the margins announced in the tumor specimen were from 0 to 0,9 mm)

* HIS delineated the lesion wider than clinical assessment, but this wasn't supported by histopathology

** HIS delineated the lesion smaller than clinical assessment, and histopathology supported this

*** HIS delineated the lesion wider than the clinical assessment, and the histopathology supported this

**** HIS showed no suspicious for subclinical extension, but in the histopathology there was BCC in the circumferential strip

# PUBLICATION III

**Hexyl aminolevulinate, 5-aminolevulinic acid nanoemulsion, and methyl aminolevulinate in photodynamic therapy of non-aggressive basal cell carcinomas: A non-sponsored, randomized, prospective and double-blinded trial**

Salmivuori M, Grönroos M, Tani T, Pölönen I, Räsänen J, Annala L, Snellman E, Neittaanmäki N.

ACCEPTED MANUSCRIPT: doi:10.1111/jdv.16357

DR. MARI SALMIVUORI (Orcid ID : 0000-0003-0193-0552)
MR. JANNE RÄSÄNEN (Orcid ID : 0000-0003-3809-384X)
DR. NOORA NEITTAANMÄKI (Orcid ID : 0000-0002-8733-5510)

Article type : Original Article

# Hexyl aminolevulinate, 5-aminolevulinic acid nanoemulsion, and methyl aminolevulinate in photodynamic therapy of non-aggressive basal cell carcinomas: A non-sponsored, randomized, prospective and double-blinded trial

M. Salmivuori[1,2,3], M. Grönroos[1,2], T. Tani[1,4], I. Pölönen[5], J. Räsänen[1,2], L. Annala[5], E. Snellman[2,6], N. Neittaanmäki[7]

1) Department of Dermatology and Allergology, Päijät-Häme Social and Health Care Group, Lahti, Finland
2) Department of Dermatology, Tampere University Hospital and Tampere University, Faculty of Medicine and Health Technology, Finland
3) Department of Dermatology and Allergology, Helsinki University Hospital, Finland
4) HUSLAB Laboratory Services, Helsinki University Hospital, Hospital District of Helsinki and Uusimaa, Finland
5) Faculty of Information Technology, University of Jyväskylä, Finland
6) Department of Dermatology, Satasairaala, Pori, Finland
7) Departments of Pathology and Dermatology, Institutes of Biomedicine and Clinical Sciences, Sahlgrenska Academy, University of Gothenburg, Sweden

**Key words:** non-aggressive basal cell carcinoma, photodynamic therapy, methyl aminolevulinate, 5-aminolevulinic acid nanoemulsion, hexyl aminolevulinate

**Short title:** PDT of non-aggressive BCCs with MAL, BF-200 ALA and HAL

**Word count**: Abstract: 248 words; Body text: 2997 words; 1 table; 3 figures

**Corresponding author:** Mari Salmivuori, Department of Dermatology and Allergology, Keskussairaalankatu 7, 15830 Lahti, Finland

Mobile: +358 505 355 616, e-mail: mari.salmivuori@tuni.fi

**Conflict of interest:** The authors declare no conflict of interests.

**Funding:** This clinical trial has been funded by research grants from the Finnish Dermatological Society, the Cancer Foundation Finland, the Foundation for Clinical Chemistry Research, the Instrumentarium Science Foundation, Tampere University, and the Competitive Research Financing of the Expert Responsibility Area of Tampere University Hospital.



**ABSTRACT**

**Background** In the photodynamic therapy (PDT) of non-aggressive basal cell carcinomas (BCCs), 5-aminolevulinic acid nanoemulsion (BF-200ALA) has shown non-inferior efficacy when compared with methyl aminolevulinate (MAL), a widely used photosensitizer. Hexyl aminolevulinate (HAL) is an interesting alternative photosensitizer. To our knowledge, this is the first study using HAL-PDT in the treatment of BCCs.

**Objectives** To compare the histological clearance, tolerability (pain and post-treatment reaction), and cosmetic outcome of MAL, BF-200 ALA, and low-concentration HAL in the PDT of non-aggressive BCCs.

**Methods** Ninety-eight histologically verified non-aggressive BCCs met the inclusion criteria, and 54 patients with 95 lesions completed the study. The lesions were randomized to receive LED-

PDT in two repeated treatments with MAL, BF-200 ALA, or HAL. Efficacy was assessed both clinically and confirmed histologically at three months by blinded observers. Furthermore, cosmetic outcome, pain, post-treatment reactions fluorescence, and photobleaching were evaluated.

**Results** According to intention-to-treat analyses, the histologically confirmed lesion clearance was 93.8% (95% confidence interval [CI] = 79.9–98.3) for MAL, 90.9% (95% CI = 76.4–96.9) for BF-200 ALA, and 87.9% (95% CI = 72.7–95.2) for HAL, with no differences between the arms ($p$=0.84). There were no differences between the arms as regards pain, post-treatment reactions, or cosmetic outcome.

**Conclusions** PDT with low-concentration HAL and BF-200 ALA have a similar efficacy, tolerability, and cosmetic outcome compared to MAL. HAL is an interesting new option in dermatological PDT, since good efficacy is achieved with a low concentration.

Registration numbers: EudraCT with 2014-002746-50 and clinicaltrial.gov with NCT02367547.

## INTRODUCTION

The incidence of basal cell carcinoma (BCC), especially the superficial subtype (sBCC) is rising[1,2]. BCC is as common as all other malignancies combined, and thus causes remarkable health care costs[3,4]. The sBCC and the thin nodular BCC (nBCC) are often classified as low-risk tumours, and they can be treated with non-surgical options[5], i.e. photodynamic therapy (PDT), imiquimod or 5-fluorourasil (5-FU), where imiquimod has superior efficacy [6-7]. The advantages of PDT include a superior cosmetic outcome and short application and down times[8,9].

PDT uses a combination of light, a photosensitizing agent (an exogenous source for photoactive protoporphyrin IX, PpIX), and oxygen to generate a radical oxygen species that cause cell apoptosis and necrosis[10,11]. Of these factors, PpIX production in particular seems to be related to cell death[12]. Thus, changing the prodrug of PpIX could be an effective way to enhance the reaction.

The PpIX produced can be measured as the fluorescence of a photosensitizer[13]. Fluorescence and especially photobleaching (i.e. the difference in fluorescence measured before and after illumination) correlate with the accumulation of PpIX and with efficacy[14,15].

5-aminolevulinic acid (5-ALA) was the first photosensitizer in PDT of skin malignancies with selectivity in the tumour tissue[10]. The esters of 5-ALA like methyl aminolevulinate (MAL) are more lipophilic, and a shorter incubation time is needed, when compared to 5-ALA[11]. With

nanoemulsion of 5-ALA (BF-200 ALA) at a 10% concentration a greater fluorescence was detected after incubation time, when compared to 20% 5-ALA[16]. In addition, BF-200 ALA was shown to penetrate deeper in an *ex vivo* skin model, when compared to MAL[17]. The efficacy of BF-200 ALA is shown to be non-inferior compared to MAL in PDT of non-aggressive BCCs[18]. Hexyl aminolevulinate (HAL) is a long-chain lipophilic 5-ALA ester, capable to produce significantly higher fluorescence intensities in the human epidermis and superficial dermis, when compared to MAL – though in the mid and deep dermis the intensity is only slightly higher[19]. An equal fluorescence intensity is achieved in the rat skin using HAL2% and MAL20%[20]. HAL, BF-200 ALA and MAL seem to be equally tolerated when applied on normal human skin[21].

This prospective trial aims to compare the efficacy and tolerability (i.e. pain and post-treatment-reaction) of MAL, BF-200 ALA, and low-concentration HAL in the PDT of non-aggressive BCCs.

## Materials and methods

The protocol complied with the Declaration of Helsinki and was approved by the Ethics Committee of Tampere University Hospital and by the Finnish Medicines Agency. Written informed consent was obtained from all participants. Patients were recruited from those referred to the Department of Dermatology and Allergology at Päijät-Häme Social and Health Care Group, Lahti, Finland, between March 2015 and September 2018.

The three parallel arms were MAL16% (Metvix®, Galderma Norcid AB), and BF-200 ALA7.8% (Ameluz®, Biofrontera), and HAL2% (mixture of Hexvix® powder, Photocure ASA, and unguentum M cream, Allmirall Hermal GmbH) with allocation ratio of 1:1:1. Of these, MAL and BF-200 ALA are approved for the PDT of non-aggressive BCCs, and HAL is approved for the photodynamic diagnosis of uroepithelial cancer and the treatment of cervical dysplasia by the European Medicines Agency.

### *Inclusion and exclusion criteria*

Patients over 18 years old presenting with a superficial BCC clinically were enrolled. Exclusion criteria included pregnancy, lactation, allergy/intolerance to the photosensitizers used, porphyria, and photosensitivity.

The target lesions had to be located on the trunk or extremities. Lesions located on the face or head were not eligible. In the case of multiple BCCs in the same patient, we included only

lesions located at least 10 cm apart from each other to minimize mixing up the photosensitizers[22]. The target BCCs were included according to clinical inspection with a dermatoscope, and randomized to one of the three arms at the recruitment visit. However, a diagnostic biopsy was taken from all included lesions prior to treatment. Lesions with some other histopathology than BCC were excluded from the analyses. Only lesions confirmed to be non-aggressive, i.e. a superficial or thin nodular – defined as growing into the epidermal-dermal junction or the most upper third of the dermis – could be included for analyses.

*Outcomes*

The primary outcome was histologically verified clearance at three months. The secondary outcomes were pain during the illumination with the use of a long-acting local anaesthetic prior to pre-handling, post-treatment reaction, cosmetic outcome, and fluorescence/photobleaching.

*Power calculations, randomization and treatment allocation*

In the power calculations (alpha=0.05, power=0.85, delta=0.30), it was assumed that BF-200 ALA/HAL would be superior to MAL, as MAL has an efficacy of 72.8% at twelve months[9], although the efficacy might be even lower in a group aged over 60 years[23]. Thus the efficacy of MAL was assumed to be 65%. Same delta-value was used both for BF-200 ALA and HAL. Thus, the needed sample size was 31 lesions/arm. The initial set (93 lesions) was randomized using a web-based validated program, Research randomizer.org®. As the trial proceeded, we noticed of the other histology than BCC being notable, and performed another set of randomization (24 lesions) with closed envelopes (at the moment troubles using Research randomizer®). In total, 117 lesions (39/arm) were randomized, Figure 1.

*Protocol*

Prior to treatment (performed by M.S. and J.R.), the lesions were assessed with a dermatoscope (Dermlite® DL3 or DL3N, 3GenCA, USA, or Heine Delta 20T®). Treatment areas including the lesion, a 5 mm margin, and a biopsy site were marked on plastic sheets with scaling (1x1mm squares). A diagnostic 3 mm punch biopsy was taken prior to curettage at the first session (PDT I), and local anaesthetics (1:1 mixture of lidocaine 10mg/ml cum epinephrine 10 µg/ml to ropivacaine 7.5mg/ml) were infiltrated prior to any procedures at both sessions. Curettage i.e. removing crusts/scabs and handling the whole treatment area was used for all of the lesions. If needed

aluminium chloride was used for haemostasis, and in PDT I the biopsy site was closed with a transparent stitch (Monocryl 4-0). Thereafter a 1 mm thick layer of photosensitizer (treatment area calculated from plastic sheets in $mm^2$, photosensitizer scaled with 1 $mg/mm^2$ dosing) was applied to the treatment area followed by three hours occlusion with a light-impermeable cover before illumination (Aktilite, CL128, Galderma, 37 $J/cm^2$ per session). All lesions were illuminated with the same total time of 7 min and 24 seconds, but recording of pain and illuminating together took approximately 8 minutes of time. The second session (PDT II) followed 8–14 days after PDT I. Figure 2 represents an example case.

*Assessment of efficacy*

At the three-month follow-up visit an experienced dermatologist (M.G.), blinded for treatment, evaluated all lesions with inspection and with a dermatoscope, and took 3 mm control punch biopsies near the diagnostic biopsy site using the marked plastic sheets as guidance. Additional 3 mm punch biopsies were taken from clinically suspicious sites if needed. Non-responsive lesions were completely excised as a second line treatment, which allowed us to evaluate if a mixed histology with aggressive features would exist. An experienced pathologist (T.T.), blinded for treatment, assessed all histopathological specimens.

*Assessment of the treatment tolerability and cosmetic outcome*

Pain was assessed by patients, blinded for photosensitizer, using a visual analogue scale (VAS)[24] at the beginning, in the middle, and in the end of each illumination. No other pain management was used. For our analyses we named the difference of VAS in the middle and at the beginning as 4 min, and the difference of VAS in the end and at the beginning as 8 min. Thus we acknowledged that the pain experienced by the patient at the beginning of the illumination could be something else than zero.

Post-treatment reactions (oedema, erythema, erosion, and crust formation) were photographed 8–14 days after PDT I and assessed afterwards on a five-point scale (none/minimal/mild/moderate/severe) by the blinded observer (M.G.). The cosmetic outcome was assessed on a four-point-scale (excellent/good/fair/poor) at the three-month follow-up visit by the blinded observer (M.G.).

*Fluorescence measurement*

Fluorescence images were taken at the beginning and end of illumination using a digital camera (Canon Ixus 130, 14.1 megapixel with the set-up ISO800, FW 2.8, no zoom), a Wood's light (Philips Burton®, Somerset, USA, kept hand-held at a distance of about 8 cm) and a yellow filter lens (Hoya HMC, yellow-green xo, attached to the top of the Wood's light), as used by Neittaanmäki-Perttu et al.[21] The photosensitizer was removed with saline solution before imaging.

*Statistical analyses and calculations of fluorescence*

Statistical analyses were conducted with a professional statistician using SPSS 23.0 (IBM SPSS Statistics for Windows, Version 23.0. Armonk, NY: IBM Corp.), or a mathematician (I.P.) with Python 3.6 using Numpy and Scipy libraries.

As statistical methods, Fisher's exact test was used to compare the efficacy, post-treatment reactions, and the cosmetic outcome. As regards pain, the comparison between the arms was performed with the Kruskall–Wallis test, and the comparison between the sessions in each arm with the Wilcoxon Signed Rank Test. For fluorescence and photobleaching, the ANOVA test was used to compare the treatment arms, and to calculate the correlation between the histological clearance and the fluorescence/photobleaching, the Chi-squared was used.

Fluorescence images were processed semi-automatically using affine transformation and manually selected matching points by a mathematician (L.A.) with Python 3.6. The intensity was extracted in the red light channel to achieve arbitrary units (A.U.) for fluorescence and photobleaching (as the absolute difference of the mean fluorescence before and after illuminating).

**Results**

Altogether 98 histologically verified non-aggressive BCC (in 57 patients) were included to the study, but there were three dropouts. Thus 54 patients completed the study with 95 non-aggressive BCCs (Figure 1). Table 1 represents the patients and lesion characteristics. In total, six residual lesions were found at three months follow-up (1/31 in MAL, 3/33 in BF-200 ALA, and 2/31 in HAL). In the final excision of non-responsive lesions, there were no aggressive subtypes.

*Lesion clearance with intention-to-treat analyses*

Among the 98 non-aggressive BCCs, i.e. including the dropouts, the histologically verified efficacy was 93.8% (95% CI = 79.9–98.3) for MAL, 90.9% (95% CI = 76.4–96.9) for BF-200

ALA, and 87.9% (95% CI = 72.7–95.2) for HAL (in the comparison of the arms; $p$=0.84). Thus, there were no differences between the arms in terms of efficacy.

*Tolerability and cosmetic outcome*

Pain results for the 95 BCCs of the 54 patients who completed the study are reported in Figure 3A. No differences were found in pain between the arms during illumination (MAL vs BF-200 ALA vs HAL; PDT I 4 min $p$=0.21, 8 min $p$=0.18; PDT II 4 min $p$=0.47, 8 min $p$=0.87). In the HAL group, the second session was more painful than the first session (PDT I vs PDT II; 4 min $p$=0.006, 8 min $p$=0.005). There was no difference in pain between the sessions in the other arms (PDT I vs PDT II; MAL 4 min $p$=0.17, 8 min $p$=0.79; BF-200 ALA 4 min $p$=0.45, 8 min $p$=0.43).

Among the 95 BCCs, no differences were either found in the post-treatment reactions ($p$=0.49; Figure 3B, and Figure 2E). There was one treatment-related withdrawal from the trial, as one patient from the MAL group experienced remarkable swelling, oedema, erythema, and haematoma in the treatment area after PDT I, and refused to attend PDT II.

Among the 95 BCCs, the cosmetic outcome was regarded as good/excellent in 77.4% of the lesions in the MAL group, 75.7% in the BF-200 ALA group, and 61.3% in the HAL group, with no differences between the arms ($p$=0.61; Figure 3C, and Figure 2F).

*Fluorescence and photobleaching*

In total, fluorescence images were available from 84 lesions in 49 patients from PDT I, and respectively from 91 lesions in 51 patients from PDT II. At the beginning of the illumination, fluorescence was lower in HAL2% compared to MAL16% and BF-200 ALA7.8% (PDT I $p$=0.043 and PDT II $p$=0.043). However, there was no statistical significant difference in photobleaching between the arms (PDT I $p$=0.09 and PDT II $p$=0.42). We found no correlation between the histological clearance and the photobleaching (PDT I $p$=0.40, PDT II $p$=0.77) or fluorescence (PDT I $p$=0.77, PDT II $p$=0.55). Fluorescence and photobleaching showed a wide variation.

**Discussion**

To our knowledge, this is the first trial using HAL-PDT for non-aggressive BCCs. Morrow et al. have earlier suggested that HAL is more effective in equimolar doses compared to MAL and 5-ALA[25]. Dögnitz et al. reported that HAL could be used in smaller concentrations to achieve a similar distribution of PpIX in the BCC tissue compared to 5-ALA[26]. Our results support the idea.

Kiesslich et al. demonstrated for 5-ALA, MAL, and HAL *in vitro* that after a certain threshold limit, the intracellular PpIX concentration doesn't rise by increasing the concentration of the prodrug, but under this threshold the concentration matters, also the incubation time of the prodrug[27]. There are many variables in PDT, and thus the protocol used can affect the efficacy[28,29]. Consequently, the optimal concentration and protocol for HAL-PDT of non-aggressive BCCs is still unexplored.

In a recent multi-centre trial, Morton et al. reported a three-month clinical clearance of 91.8% for MAL and 93.4% for BF-200 ALA in the PDT of non-aggressive BCCs[18]. In another multi-centre trial, Arits et al. reported clinical clearance of 84.2% at three months for MAL-PDT[9]. We and Morton et al. used curettage, but Arits et al. reported 'a non-traumatic surface preparation'. In our experience, some small trauma can occur in curettage, and physical pre-treatment in PDT enhances the PpIX uptake[30,31].

Morton et al. have shown the similar tolerability of BF-200 ALA and MAL[18]. Interestingly, HAL seems to have a more precise effect on the site of application compared to 5-ALA on mice skin, and this could be beneficial in terms of post-treatment reactions[32]. Neittaanmäki-Perttu et al. reported that on healthy human skin, HAL2% caused a similar erythema as BF-200 ALA7.8% and MAL16%, and in terms of pain, there was a significant difference in the respective comparison[21]. In our results, for BCC we did not found any differences between the arms in terms of adverse events.

As regarding pain, Lindeburg et al. have reported that PDT II is more painful than PDT I when treating actinic keratosis and sBCC with MAL-PDT[33]. Perhaps due to the small sample size, this difference was found only for HAL in our results. Our mean and median VAS score was 2.3 at its highest. Interestingly, Morton et al. had a highest mean pain score (on a 1–10 scale) of 4.5 without analgesia, despite the use of a BF-RhodoLED (Biofrontera) light source with reduced pain levels compared to Aklite (Galderma)[34]. Thus, it seems that a long-acting local anaesthetics prior to pre-handling could be effective in pain management – though this differs from the European PDT guidelines[35]. Previously, nerve blocking has been shown to be an effective option, whereas topical analgesia has not[36]. Our method should be studied more closely in a prospective and randomized setting, including in carcinomas in situ and head locations, where pain can be a major obstacle[37].

In PDT, the use of local analgesia can have a potential impact on efficacy through vasoconstriction, pH, and oxygen availability[37]. The use of epinephrine in particular could lead to

this. Infiltration of local anaesthetics has earlier been used during illumination with lidocaine/prilocaine cum ropivacaine, and also cum epinephrine, with good treatment success[38,39]. However, our pain management protocol didn't affect the results.

We found a good/excellent cosmetic outcome in 71.6% of all the lesions at three months. We did not achieve the results of Jansen et al.[8] (the same trial as by Arits et al.), who reported a good/excellent cosmetic outcome in MAL-PDT for 89.5% of patients at five years. However, the cosmetic outcome tends to improve over time[18].

Non-surgical options provide a cost-effective alternative to surgery in the treatment of non-aggressive BCCs[40], and patients with multiple lesions or facial lesions are willing to risk the recurrence rate for a better cosmetic outcome[41]. The advantages of PDT include the cosmetic outcome[8], the shorter application and down times, and the mode of delivery[9], but the major disadvantage is the lower efficacy compared to imiquimod[6]. However, the topical creams demand good patient compliance and correct patient selections, as the creams are applied by the patient at home for a number of weeks. Regarding the economic aspect of low-concentration HAL, there could be benefits in the manufacture of the cream, as only a low concentration is demanded. Interestingly in the daylight PDT of thin actinic keratosis, a similar efficacy was achieved with HAL0.2% as compared to MAL16%[42].

The strengths of our study are the investigator-initiated double-blinded design, histopathological confirmation in addition to the clinical evaluation, and the complete excision of the non-responsive lesions to examine the possible underlying mixed histologies as the cause for treatment failure. We assumed our patients would be over 60 years, and this corresponded to our material quite accurately; only 6/54 of the analysed patients were under 60 years.

The limitations of our study design are a limited sample size and optimistic assumptions in the power calculations. The taking of diagnostic biopsies at the first treatment session should also be considered a limitation, since these could potentially lead to lesion resolution due to inflammation induced by the biopsy. A limitation of the pain analyses was the absence of a control group for local anaesthetics. Furthermore, the summation of pain may have occurred in patients with multiple lesions, but in our protocol lesions (not patients) were randomized, and thus the possible effect should be quite equal for all arms. A major limitation in the fluorescence/photobleaching analyses was the lack of a validated imaging system.

In conclusion, HAL is an interesting new option for dermatological PDT. The efficacy and tolerability of low-concentration HAL was comparable with BF-200 ALA and MAL. Dose-finding studies and larger trials are warranted in the future for HAL.

**Acknowledgments**

We want to thank Marc Bauman and Teija Inkinen at Biomedicum, Helsinki University, for the HAL analyses, Maarit Bäckman from the YA pharmacy for manufacturing the HAL cream, Mika Helminen from Tampere University Hospital for the statistical analyses, Ulla Tuovinen and the staff of Päijät-Häme Dermatology clinic for recruiting the patients, and our assisting nurse Ulla Oesch-Lääveri for everything.

**References**

1 Lomas A, Leonardi-Bee J, Bath-Hextall F. A systematic review of worldwide incidence of nonmelanoma skin cancer. *Br J Dermatol* 2012; **166**:1069-80.

2 Arits, A H M M., Schlangen MHJ, Nelemans PJ, Kelleners-Smeets NWJ. Trends in the incidence of basal cell carcinoma by histopathological subtype. *Journal of the European Academy of Dermatology & Venereology* 2011; **25**:565-9.

3 Holm A, Nissen CV, Wulf HC. Basal Cell Carcinoma is as Common as the Sum of all Other Cancers: Implications for Treatment Capacity. *Acta Derm Venereol* 2016; **96**:505-9.

4 Bentzen J, Kjellberg J, Thorgaard C, et al. Costs of illness for melanoma and nonmelanoma skin cancer in Denmark. *European Journal of Cancer Prevention* 2013; **22**:569-76.

5 Trakatelli M, Morton C, Nagore E, et al. Update of the European guidelines for basal cell carcinoma management. *European Journal of Dermatology* 2014; **24**:312-29.

6 Jansen MHE, Mosterd K, Arits, Aimee H M M, et al. Five-Year Results of a Randomized Controlled Trial Comparing Effectiveness of Photodynamic Therapy, Topical Imiquimod, and Topical 5-Fluorouracil in Patients with Superficial Basal Cell Carcinoma. *J Invest Dermatol* 2018; **138**:527-33.

7 Roozeboom MH, Arits, Aimee H M M., Mosterd K, et al. Three-Year Follow-Up Results of Photodynamic Therapy vs. Imiquimod vs. Fluorouracil for Treatment of Superficial Basal Cell Carcinoma: A Single-Blind, Noninferiority, Randomized Controlled Trial. *J Invest Dermatol* 2016; **136**:1568-74.

8 Jansen MHE, Koekelkoren FHJ, Nelemans PJ, et al. Comparison of long-term cosmetic outcomes for different treatments of superficial basal cell carcinoma. *J Am Acad Dermatol* 2018; **79**:961-4.

9 Arits, Aimee H M M, Mosterd K, Essers BA, et al. Photodynamic therapy versus topical imiquimod versus topical fluorouracil for treatment of superficial basal-cell carcinoma: a single blind, non-inferiority, randomised controlled trial. *Lancet Oncology* 2013; **14**:647-54.

10 Kennedy JC, Pottier RH, Pross DC. Photodynamic therapy with endogenous protoporphyrin IX: basic principles and present clinical experience. *Journal of Photochemistry & Photobiology.B - Biology* 1990; **6**:143-8.

11 Ozog DM, Rkein AM, Fabi SG, et al. Photodynamic Therapy: A Clinical Consensus Guide. *Dermatologic Surgery* 2016; **42**:804-27.

12 Lee JB, Choi JY, Chun JS, et al. Relationship of protoporphyrin IX synthesis to photodynamic effects by 5-aminolaevulinic acid and its esters on various cell lines derived from the skin. *Br J Dermatol* 2008; **159**:61-7.

13 Tyrrell J, Campbell S, Curnow A. Validation of a non-invasive fluorescence imaging system to monitor dermatological PDT. *Photodiagnosis & Photodynamic Therapy* 2010; **7**:86-97.

14 Tyrrell JS, Campbell SM, Curnow A. The relationship between protoporphyrin IX photobleaching during real-time dermatological methyl-aminolevulinate photodynamic therapy (MAL-PDT) and subsequent clinical outcome. *Lasers in Surgery & Medicine* 2010; **42**:613-9.

15 Tyrrell J, Paterson C, Curnow A. Regression Analysis of Protoporphyrin IX Measurements Obtained During Dermatological Photodynamic Therapy. *Cancers* 2019; **11**.

16 Schmitz L, Novak B, Hoeh A, et al. Epidermal penetration and protoporphyrin IX formation of two different 5-aminolevulinic acid formulations in ex vivo human skin. *Photodiagnosis & Photodynamic Therapy* 2016; **14**:40-6.

17 Maisch T, Santarelli F, Schreml S, et al. Fluorescence induction of protoporphyrin IX by a new 5-aminolevulinic acid nanoemulsion used for photodynamic therapy in a full-thickness ex vivo skin model. *Exp Dermatol* 2010; **19**:302.

18 Morton CA, Dominicus R, Radny P, et al. A randomized, multi-national, non-inferiority, phase III trial to evaluate the safety and efficacy of BF-200 ALA gel versus MAL cream in the treatment of non-aggressive basal cell carcinoma with photodynamic therapy (PDT).. *Br J Dermatol* 2018; **179**;309–319.

19 Togsverd-Bo K, Idorn LW, Philipsen PA, et al. Protoporphyrin IX formation and photobleaching in different layers of normal human skin: methyl- and hexylaminolevulinate and different light sources. *Exp Dermatol* 2012; **21**:745-50.

20 Togsverd-Bo K, Lerche CM, Philipsen PA, et al. Porphyrin biodistribution in UV-exposed murine skin after methyl- and hexyl-aminolevulinate incubation. *Exp Dermatol* 2012; **21**:260-4.

21 Neittaanmaki-Perttu N, Neittaanmaki E, Polonen I, et al. Safety of Novel Amino-5-laevulinate Photosensitizer Precursors in Photodynamic Therapy for Healthy Human Skin. *Acta Derm Venereol* 2016; **96**:108-10.

22 Palsson S, Gustafsson L, Bendsoe N, et al. Kinetics of the superficial perfusion and temperature in connection with photodynamic therapy of basal cell carcinomas using esterified and non-esterified 5-aminolaevulinic acid. *Br J Dermatol* 2003; **148**:1179-88.

23 Lindberg-Larsen R, Solvsten H, Kragballe K. Evaluation of recurrence after photodynamic therapy with topical methylaminolaevulinate for 157 basal cell carcinomas in 90 patients. *Acta Derm Venereol* 2012; **92**:144-7.

24 Hawker GA, Mian S, Kendzerska T, French M. Measures of adult pain: Visual Analog Scale for Pain (VAS Pain), Numeric Rating Scale for Pain (NRS Pain), McGill Pain Questionnaire

(MPQ), Short-Form McGill Pain Questionnaire (SF-MPQ), Chronic Pain Grade Scale (CPGS), Short Form-36 Bodily Pain Scale (SF-36 BPS), and Measure of Intermittent and Constant Osteoarthritis Pain (ICOAP). *Arthritis care & research* 2011; **63**:240.

25 Morrow DIJ, McCarron PA, Woolfson AD, et al. Hexyl aminolaevulinate is a more effective topical photosensitiser precursor than methyl aminolaevulinate and 5-aminolaevulinic acids when applied in equimolar doses. *J Pharm Sci* 2010; **99**:3486-98.

26 Dognitz N, Salomon D, Zellweger M, et al. Comparison of ALA- and ALA hexyl-ester-induced PpIX depth distribution in human skin carcinoma. *Journal of Photochemistry & Photobiology.B - Biology* 2008; **93**:140-8.

27 Kiesslich T, Helander L, Illig R, et al. Real-time analysis of endogenous protoporphyrin IX fluorescence from delta-aminolevulinic acid and its derivatives reveals distinct time- and dose-dependent characteristics in vitro. *J Biomed Opt* 2014; **19**:085007.

28 Wang H, Xu Y, Shi J, et al. Photodynamic therapy in the treatment of basal cell carcinoma: a systematic review and meta-analysis. *Photodermatol Photoimmunol Photomed* 2015; **31**:44-53.

29 Roozeboom MH, Arits, A H H M., Nelemans PJ, Kelleners-Smeets NWJ. Overall treatment success after treatment of primary superficial basal cell carcinoma: a systematic review and meta-analysis of randomized and nonrandomized trials. *Br J Dermatol* 2012; **167**:733-56.

30 Bay C, Lerche CM, Ferrick B, et al. Comparison of Physical Pretreatment Regimens to Enhance Protoporphyrin IX Uptake in Photodynamic Therapy: A Randomized Clinical Trial. *JAMA Dermatology* 2017; **153**:270-8.

31 Nissen CV, Wiegell SR, Philipsen PA, Wulf HC. Short-term chemical pretreatment cannot replace curettage in photodynamic therapy. *Photodermatol Photoimmunol Photomed* 2016; **32**:146-52.

32 Casas A, Perotti C, Fukuda H, et al. ALA and ALA hexyl ester-induced porphyrin synthesis in chemically induced skin tumours: the role of different vehicles on improving photosensitization. *Br J Cancer* 2001; **85**:1794-800.

33 Lindeburg KEK, Brogaard HMV, Jemec GBE. Pain and photodynamic therapy. *Dermatology* 2007; **215**:206-8.

34 Zaar O, Sjoholm Hylen A, Gillstedt M, Paoli J. A prospective, randomized, within-subject study of ALA-PDT for actinic keratoses using different irradiation regimes. *Photodermatol Photoimmunol Photomed* 2018; **34**:338-42.

35 Morton CA, Szeimies R, Sidoroff A, Braathen LR. European guidelines for topical photodynamic therapy part 1: treatment delivery and current indications - actinic keratoses, Bowen's disease, basal cell carcinoma. *Journal of the European Academy of Dermatology & Venereology* 2013; **27**:536-44.

36 Ang JM, Riaz IB, Kamal MU, et al. Photodynamic therapy and pain: A systematic review. *Photodiagnosis & Photodynamic Therapy* 2017; **19**:308-44.

37 Wang B, Shi L, Zhang YF, et al. Gain with no pain? Pain management in dermatological photodynamic therapy. *Br J Dermatol* 2017; **177**:656-65.

38 Borelli C, Herzinger T, Merk K, et al. Effect of subcutaneous infiltration anesthesia on pain in photodynamic therapy: a controlled open pilot trial. *Dermatologic Surgery* 2007; **33**:314-8.

39 Debu A, Sleth J, Girard C, et al. The use of subcutaneous infusion tumescent anesthesia in photodynamic therapy pain control. *Paediatr Anaesth* 2012; **22**:600-1.

40 Aguilar M, de Troya M, Martin L, et al. A cost analysis of photodynamic therapy with methyl aminolevulinate and imiquimod compared with conventional surgery for the treatment of superficial basal cell carcinoma and Bowen's disease of the lower extremities. *Journal of the European Academy of Dermatology & Venereology* 2010; **24**:1431-6.

41 Martin I, Schaarschmidt M, Glocker A, et al. Patient Preferences for Treatment of Basal Cell Carcinoma: Importance of Cure and Cosmetic Outcome. *Acta Derm Venereol* 2016; **96**:355-60.

42 Neittaanmaki-Perttu N, Karppinen TT, Tani T, et al. Long-term Outcome of Low-concentration Hexyl-5-aminolaevulinate Daylight Photodynamic Therapy for Treatment of Actinic Keratoses. *Acta Derm Venereol* 2017; **97**:120-1.

**Figure legends**

Figure 1. Flow-chart of the trial.

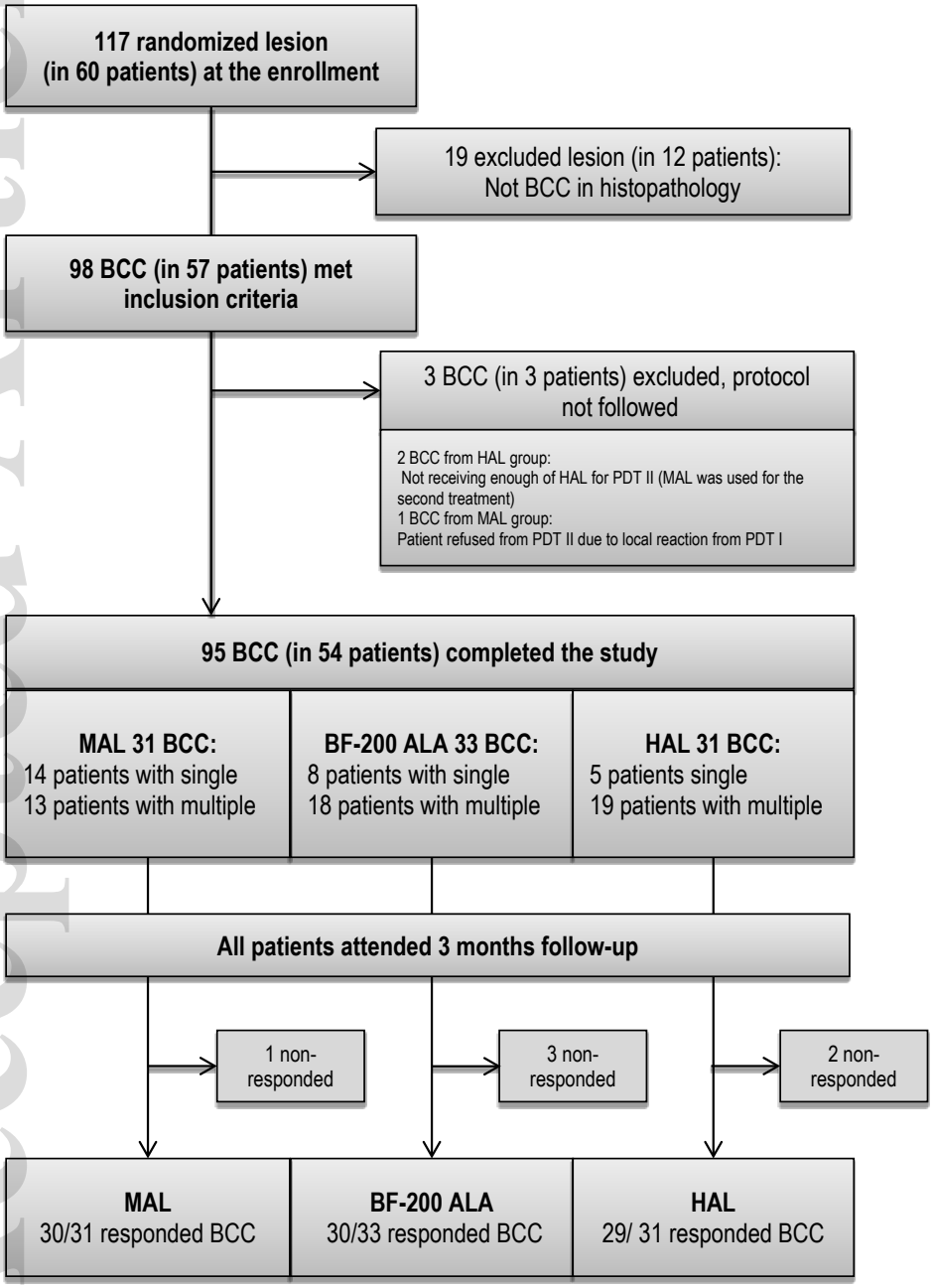

Figure 2. Example lesion with images from all phases of the protocol. The example lesion was randomized to the HAL group: A) Clinical image of an sBCC; B) Dermatoscopic image at baseline; C) Marking the lesion, treatment area, and diagnostic biopsy site (copied on plastic sheets with scaling); D) Histology presenting an sBCC in the diagnostic biopsy; E) Post-treatment reaction after PDT I, assessed as strong; F) Clinical image at thee months' follow-up; cosmetic outcome assessed as fair; G) Dermatoscopic image at three months; H) Biopsy site of the control biopsy at three months; and I) Histology of the responsive lesion with reactive changes at three months.

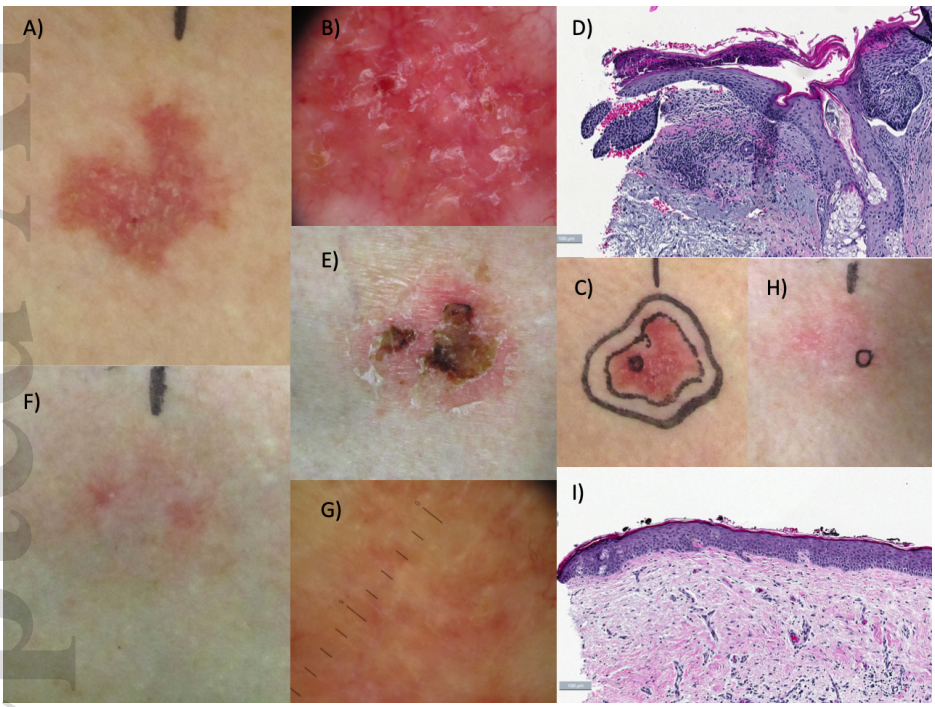


Figure 3. A) Results for pain during the illumination of the PDT for different photosensitizers. In the analyses we named the difference of the recorded VAS in the middle and at the beginning as 4 min (4 min= VAS of the middle – VAS at the beginning), and the difference of recorded VAS in the end and at the beginning was named as 8 min (8 min= VAS of the end – VAS at the beginning); B) severity of post-treatment reactions (visually assessed on scale

none/minimal/mild/moderate/severe); and C) cosmetic outcomes (visually assessed on scale excellent/good/fair/poor).

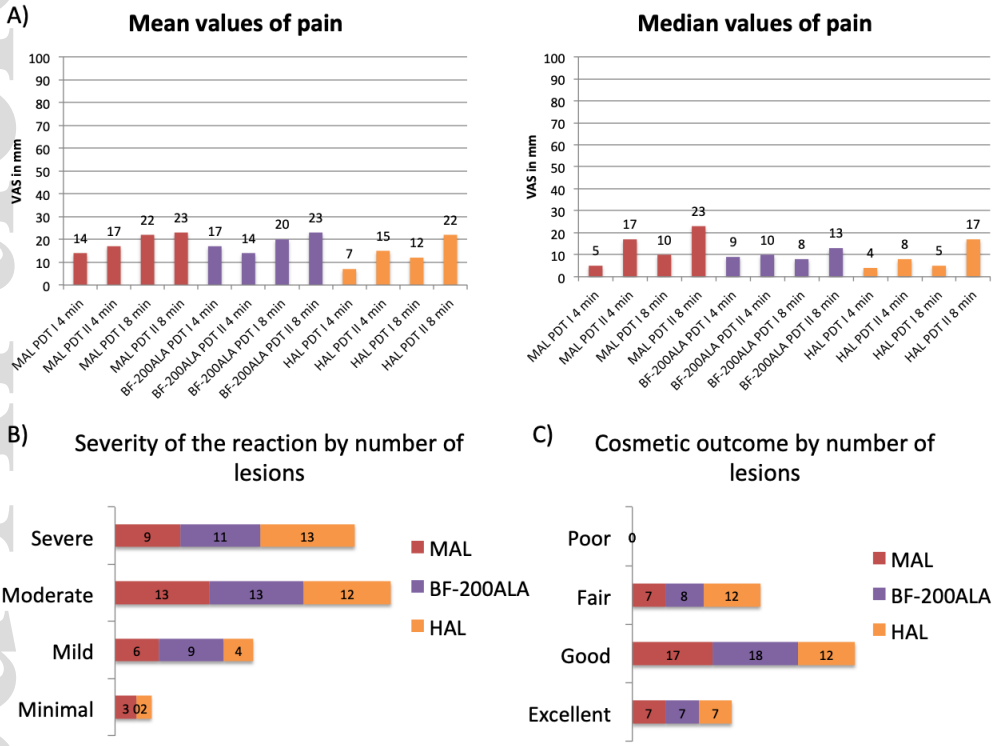

**Tables**

Table 1. Patient and lesion characteristics.

| | MAL | BF-200 ALA | HAL |
|---|---|---|---|
| **Patient Characteristics** | | | |
| Patients | 27 | 26 | 24 |
| with single lesion | 14 | 8 | 5 |
| with multiple lesions | 13 | 18 | 19 |
| Female | 10 | 5 | 12 |
| Male | 17 | 21 | 12 |
| Average age in years (range) | 71 (47–91) | 74 (51–91) | 74 (57–91) |
| Anamnestic skin phototype | | | |
| Phototype I | 6 | 4 | 7 |
| Phototype II | 10 | 13 | 8 |
| Phototype III | 11 | 9 | 9 |
| Phototype IV | 0 | 0 | 0 |
| Immunosuppression or previous radiotherapy | 2 | 1 | 2 |
| Previous history of skin cancer (AK, MB, MM, SCC, BCC) | 19 | 20 | 19 |
| Previous history of BCC | 13 | 19 | 16 |
| **Lesion characteristics** | | | |
| Lesions | 31 | 33 | 31 |
| Location on trunk | 25 | 26 | 25 |
| Location on extremities | 6 | 7 | 6 |
| Average treatment area in $mm^2$ (range) | 439 (150–1100) | 377 (130–850) | 376 (160–750) |
| New | 30 | 30 | 29 |
| Recurrent | 1 | 3 | 2 |